Molecular characterization and *in vivo* functional analysis of putative immunoprotective molecules in the soft tick, *Ornithodoros savignyi*

Venisha Raghoonanan

Submitted in partial fulfillment of the requirements for the degree

Magister Scientiae

In the Faculty of Natural and Agricultural Sciences

University of Pretoria

Pretoria

2010, July 12

UNIVERSITY OF PRETORIA

FACULTY OF NATURAL AND AGRICULTURAL SCIENCES

DEPARTMENT OF BIOCHEMISTRY

<u>Full name:</u> Venisha Raghoonanan   <u>Student number:</u> 23322757

<u>Title of the work:</u> Molecular Characterization and *in vitro* Functional Analysis of Putative

Immunoprotective Molecules in the Soft Tick, *Ornithodoros savignyi*

(Acari: Argasidae)

Declaration

1. I declare that the dissertation, which is herewith submitted for the degree *Magister Scientiae* at the University of Pretoria, is my own work and has not previously been submitted for a degree at this or any other tertiary institution.

2. I understand what plagiarism entails and am aware of the University's policy in this regard.

3. I declare that this dissertation is my own, original work. Where someone else's work was used (whether from a printed source, the internet or any other source) due acknowledgement was given and reference was made according to departmental requirements.

4. I did not make use of another student's previous work and use it as my own.

5. I did not allow and will not allow anyone to copy my work with the intention of presenting it as his/her own work.

Signature: _____   Date: _____

Acknowledgements

Table of Contents

Chapter 1: Literature overview

Chapter 2: Molecular identification of microplusin homologs in the argasid tick, *O. savignyi*

Chapter 3: The identification and molecular characterization of lysozyme from the argasid tick, *O. savignyi*

Chapter 4: *In* vivo functional analysis of lysozyme and defensin in the argasid tick, *O. savignyi*

List of Figures

Chapter 3

Chapter 4

List of tables

Abbreviations

A

AMP   antimicrobial peptides (AMPs: antimicrobial peptides)

B

BLAST   basic local alignment search tool

C

cDNA   complementary DNA

D

DEPC   diethyl pyrocarbonate
Dif   Dorsal-related immune factor
DNA   deoxyribonucleic acid
DNase   deoxyribonuclease
dNTP   deoxyribonucleotide triphosphate
dsRNA   double stranded RNA
DTT   dithiothreitol

E

EST   expressed sequence tag
EtBr   ethidium bromide

G

GFP   green fluorescent protein

H

HEWL   hen egg white lysozyme

I

IL-1R	interleukin-1 receptor
Imd	immunodeficient

L

LB	Luria-Berthani
LD PCR	long distance PCR
LPS	lipopolysaccharide
LRR	leucine rich repeat
LTA	lipotechoic acid

M

MCS	multiple cloning site
miRNA	micro RNA
MM	molecular weight marker
mRNA	messenger ribonucleic acid

N

NAG	N-acetyl glucosamine
NAM	N-acetyl muramic acid
NEMO	$NF_\kappa B$-essential modulator

O

ORF	open reading frame

P

PAMP	pathogen associated molecular pattern
PBS	phosphate buffered saline
PCR	polymerase chain reaction
PPAE	prophenoloxidase activating enzyme
PRR	pattern recognition receptor

R

RACE	rapid amplification of cDNA ends

Rel	response element
RISC	RNA induced silencing complex
RNA	ribonucleic acid
RNase	ribonuclease
rNTP	ribonucleotide triphosphate

S

| siRNA | small interfering RNA |
| ssRNA | single stranded RNA |

T

TIGR	The Institute of Genomics Research
TIR	Toll interleukin-1 receptor
tRNA	transfer RNA
TSGPs	tick salivary gland proteins

U

| UTR | untranslated region |

Since ticks are classified as hematophagous ectoparasites, the primary feeding event involves a bloodmeal on a vertebrate host. Such activities facilitate the ingestion of microorganisms which may be detrimental to the survival of a tick. It is observed, however, that ticks are able to survive such invasion by microorganisms and in several cases, facilitate the transmission of pathogens, while themselves remaining unaffected. This phenomenon is attributed to the innate immune system of ticks. The focus of this project is on stimulus-induced immunoreactive peptides known as antimicrobial peptides.

In chapter 2, an attempt was made to identify a homolog of the anti Gram-positive and bacteriostatic peptide microplusin, in the salivary glands of the argasid tick *Ornithodoros savignyi*. It was reported previously that tissue and life stage specific expression of this transcript occurs in the fat body of adult, fully fed, female *Rhipicephalus (Boophilus) microplus* ticks. The positive control used for this study was unsuccessful due to the incorrect tissue and life stage of *R. (B.) microplus* ticks. No significant homolog was identified due to the possible existence of stringent regulation of expression as well as differences in the induction stimuli between argasid and ixodid ticks.

Lysozyme catalyzes the cleavage of the β-1,4 glycosidic bond between *N*-acetyl muramic acid and *N*-acetyl glucosamine of the peptidoglycan layer of bacterial cell walls affording the molecule antibacterial activity. In argasid ticks, lysozyme was observed to be induced by feeding. In chapter 3, an attempt was made to elucidate the *O. savignyi* homolog of the *O. moubata* lysozyme molecule. The partial sequence obtained revealed the presence of a lysozyme homolog in *O. savignyi*. The tissue expression profile revealed constitutive expression in the midgut and ovaries and induction of transcription in the hemolymph upon feeding. In salivary glands, upregulation was observed following ingestion of Gram-positive bacteria.

In chapter 4, the tissue expression profile of *O. savignyi* defensin was investigated. It was found that transcription is induced following the ingestion of Gram-positive bacteria, while in the hemolymph upregulation was observed upon feeding. Furthermore, chapter 4 saw the attempts made at the RNAi mediated silencing of the lysozyme and defensin transcripts. Silencing, analysed by real time PCR, was not efficient as no statistically significant silencing was observed. Observation of the phenotype revealed mortality. However, statistical analysis of silencing revealed that the mortality observed was not due to silencing, but non-specific and possibly the result of injury during injection.

Overall, the abovementioned experiments revealed the tissue specificity of expression of ixodid microplusin and that a more strategic approach is required for the elucidation of the argasid homolog. The partial *O. savignyi* lysozyme sequence was elucidated together with the tissue expression profile of this molecule and *O. savignyi* defensin. The RNAi experiments require optimization for future studies.

Chapter 1:

Literature overview

1.1 Ticks: Classification, lifecycle and disease transmission

Ticks are obligate hematophagous ectoparasites that primarily feed on animals and man, and serve as vectors transmitting diseases caused by protozoa, viruses, bacteria and rickettsiae (Vredevoe, 2006). Economically, tick bites are detrimental to the quality of hides produced from infested animals as well as the loss of cattle due to tick-borne diseases (Rajput *et al.*, 2006). These arthropods are divided into two major families: Ixodidae (hard ticks) and Argasidae (soft ticks) (Sonenshine, 1993). Figure 1.1 represents a graphical view of the differences between the argasid and ixodid families. The major differences between these families are summarized in Table 1.1.
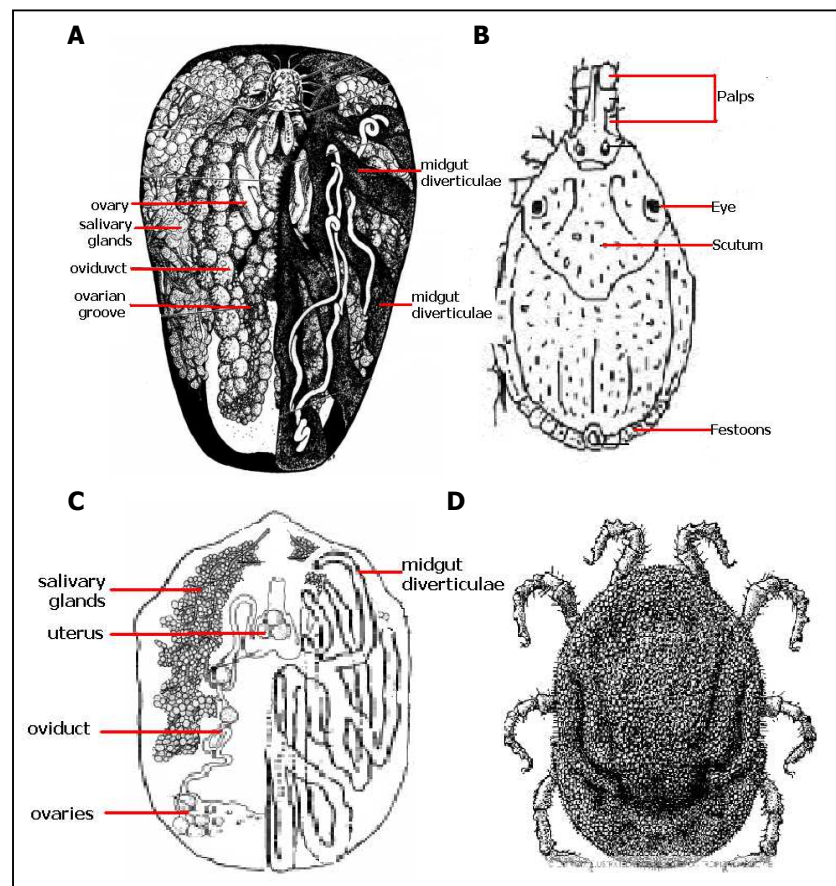
Figure 1.1: **Diagrammatic representation of the differences between Ixodidae and Argasidae** where (A) represents the internal anatomy of an ixodid female (adapted from Sonenshine, 1991) and (B) represents the external morphology of the ixodid tick (Ruedisueli *et al.*, 2006). (C) represents the internal anatomy of the argasid female (adapted from Sonenshine, 1991) and (D) shows the general morphology of the argasid tick (http://pathmicro.med.sc.edu, 2007)

Table 1.1: Basic differences between the families Ixodidae and Argasidae (Nuttall, 1908 and Ruedisueli *et al.*, 2006)

Characteristic	Ixodidae (hard tick)	Argasidae (soft tick)
Morphology	Dorsally visible capitulum (mouth parts)	Capitulum visible ventrally
	Scutum and festoons present	Scutum and festoons absent
	Eyes present dorsally on scutum sides	Eyes present on lateral surface of supra coxal folds
Feeding time	Long: days to weeks	Short: hours to days
Host species and mode of dwelling	Non-nidicolous: finds host and remains attached throughout life stage	Nidicolous: inhabits the nest/burrow of host
	May target new host in each life stage	Adult and nymphal stages feed on same host
	Targets small rodents, larger mammals and man	Usually targets birds, bats and in some cases cattle and man
Lifespan	Short (~ 1 month)	Long (exceeding two years)
Life cycle	Three basic stages: Larvae hatch from eggs and give rise to nymphs and adults respectively through feeding and moulting	Up to as many as 11 stages: where nymphal stages may be characterized by 2-8 distinct cycles
	A single bloodmeal and moult between stages	Multiple bloodmeals between stages
Mating and oviposition	Mating occurs and female feeds prior to laying ~23 000 eggs. Following this oviposition event the female dies.	Female undergoes numerous oviposition events in the adult stage and lays several batches of eggs throughout her lifespan

The lifespan of an argasid tick is constituted by three basic stages (Figure 1.2). The first involves the hatching of eggs into larvae which feed on the first host and subsequently moults through several nymphal stages during feeding on subsequent hosts. Adults mate following feeding and the cycle repeats itself. A single adult may progress through multiple gonotrophic cycles, which includes feeding and mating, within a complete life cycle.
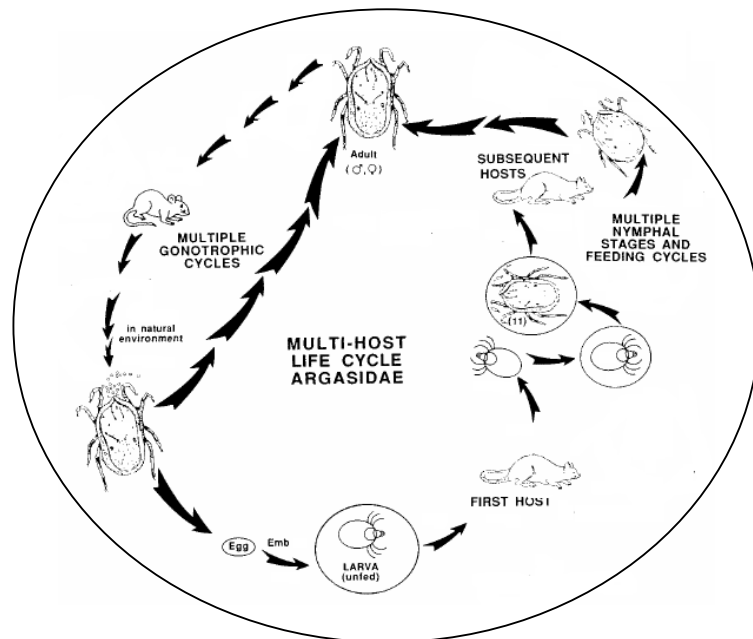
Figure 1.2: The typical multiple host life cycle of an argasid tick (adapted from Sonenshine, 1991)

In general, ixodid ticks are arthropod vectors of various diseases. A tick attaches to a host infected with a pathogen. During the bloodmeal the tick ingests the pathogen circulating in the blood of the infected host. Once ingested this pathogen may reproduce within the tick. When the tick feeds on the next vertebrate host, the pathogen is re-transmitted to the new host leading to infection. This mode of transmission is known as vertical transmission. Other modes of transmission include trans-stadial referring to pathogen transmission from one life stage to the next while transovarian transmission involves the transmission of pathogens to larvae in the first and second gonotrophic cycles. (Sonenshine, 1993).

In the case of the argasid tick, *Ornithodoros savignyi*, Charrel *et al.*, found in 1995 that this tick species was able to successfully transmit Alkhurma Haemorrhagic Fever Virus from camels to humans. This allowed for the serological and genetic characterization of the family of tickborne flaviviruses transmitted by *O. savignyi*.

The work of Shanbaky and Helmy in 2000, investigated the transmission of *Borrelia* sp. by *O. savignyi* in Egypt. It was found that nymphs acquire the spirochete during the bloodmeal and are able to transmit this pathogen to the subsequent hosts. Furthermore, trans-stadial transmission to the adult stage was observed in addition to transovarian transmission.

Bloodfeeding in ticks is a non-sterile process and during this process, hematophagous ectoparasites are exposed to various microorganisms of bacterial and fungal origin. These microorganisms are ingested; however no adverse effect is seen in terms of tick survival (DeMar, 2006). This phenomenon can be attributed to the tick immune defense system, specifically, innate immunity.

1.2 Immune defense systems

The ability of living organisms to defend against invading biotic or abiotic entities is referred to as immunity (Figure 1.3). An invading entity is initially confronted by physical barriers such as the skin of mammals or the integument (cuticle) of insects. Penetration of these initial barriers leads to exposure of the invading entity to components of the innate immune system. The cellular components include phagocytic cells which function in ingestion and destruction of the invader. Furthermore, cells participating in opsonization, encapsulation or nodulation of the invader are recruited to the site of infection. The humoral component of this system involves release of molecules exhibiting cytotoxicity towards the invader (Lavine & Strand, 2002). These responses are coupled to represent the innate immune system of an

organism which may be described as the initial, rapid, non-specific response against foreign invaders, mediated by germ-line encoded factors (Lavine & Strand, 2002).

Acquired immunity, the second line of defense, arises primarily through the engagement of receptors produced by the somatic rearrangement of genes. A defining characteristic of acquired immunity is the ability of an organism to develop and maintain immune memory against invading organisms (Lavine & Strand, 2002). Characteristically, vertebrates are able to elicit an innate immune response upon initial infection followed by elicitation of an adaptive immune response in the case of continual stimulation by the invading microorganism. In invertebrates, the sole response to invading microorganisms is an innate immune response, the focus from this point onward.
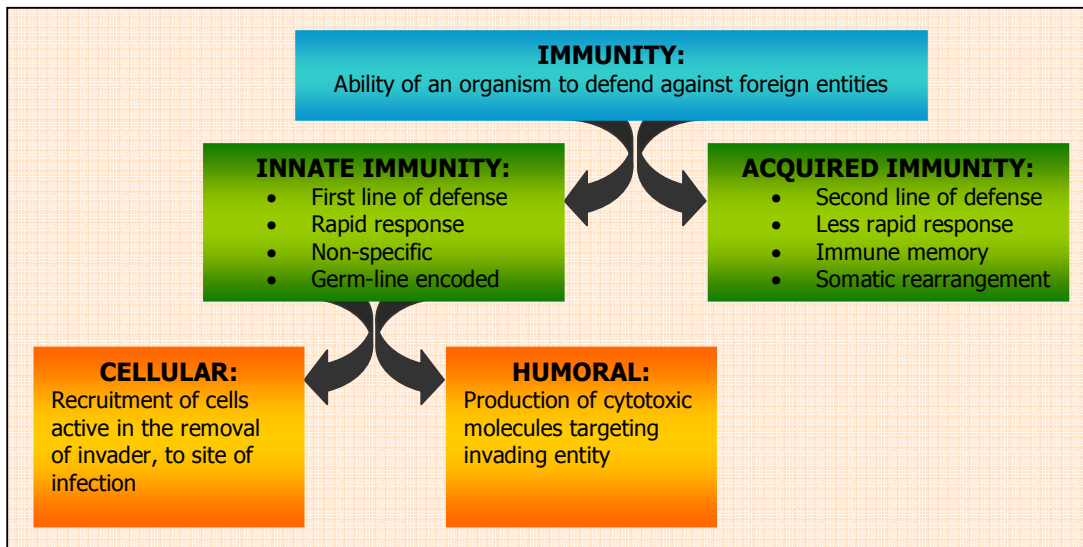
Figure 1.3: Division of immune defense systems into the acquired and innate immune responses

1.3 Immune response of arthropods

The majority of literature available on the immune responses in invertebrates implicates the absence of an adaptive immune response (Jiggins & Kim, 2005). This therefore implies that the invertebrate innate immune response relies upon a limited number of receptors, which are encoded by germ-line factors on the surface of immune cells (cellular immunity) as well as effector molecules that exhibit cytotoxicity towards invaders (humoral immunity) (Jiggins & Kim, 2005).

1.3.1 Cellular immunity mediated by hemocytes

An invading microorganism encounters the integument, gut, clotting mechanisms of hemolymph and several cytotoxic molecules at the site of entrance (Figure 1.4). If the microorganism is able to successfully traverse these barriers, the hemocoel (internal body cavity of the insect) is encountered where additional cytotoxic molecules and hemocytes are encountered which serve characteristic functions culminating in elimination of the invading microorganism (Lavine & Strand, 2002).

The basic process of hemocyte-mediated innate immunity involves, first, recognition of the invading microorganism and second, initiation of a hemocyte-mediated defense which includes intracellular signaling, chemotaxis and release of effector molecules. The overall outcome thereafter involves hemocyte adhesion to and cytotoxicity towards the invading microorganism (Jiravanichpaisal *et al.*, 2006).

Granular hemocytes are a rich source of stored antimicrobial peptides (AMPs) (Lavine & Strand, 2002). Upon immune stimulation, these specialized hemocytes release these AMPs, through the process of degranulation, which then exhibit cytotoxicity to the invader (Figure 1.4) (Jiravanichpaisal *et al.,* 2006).
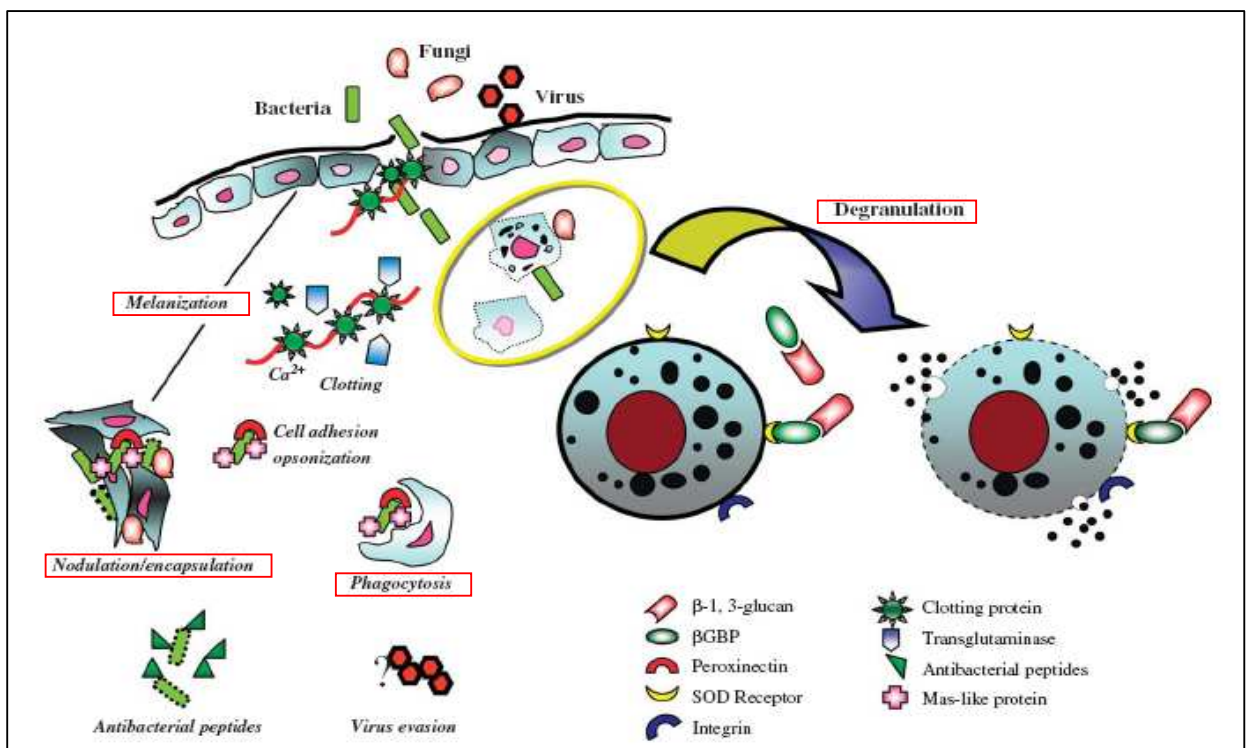
Figure 1.4: Hemocyte mediated defense processes in invertebrates (Jiravanichpaisal *et al.*, 2006)

As seen in Figure 1.4, penetration of the first line of defense (such as the integument of insects by bacteria, viruses or fungi leads to the induction of several hemocyte mediated responses, which includes nodulation or encapsulation as well as adhesion of opsonins to the surface which facilitates ingestion by phagocytosis. Further immune stimulation leads to the induction of synthesis and release of antimicrobial peptides (AMPs) by immune related tissues. The major roles of hemocytes are indicated by the process headings in red squares (Figure 1.4).

1.3.1.1 Phagocytosis, nodulation, encapsulation and melanization

Phagocytosis involves extension of pseudopodia of phagocytic cells around the invading entity ultimately leading to engulfment, internalization and "digestion" of the invading entity (Figure 1.5). Hemocytes are capable of engulfing and digesting abiotic and biotic entities as well as apoptotic bodies, through the process of apoptosis (Lavine & Strand, 2002). Nodulation involves binding of hemocytes to bacterial aggregations while encapsulation involves binding of hemocytes to parasitic invaders, nematodes as well as abiotic targets such as chromatography beads (Lavine & Strand, 2002) (Figure 1.5).
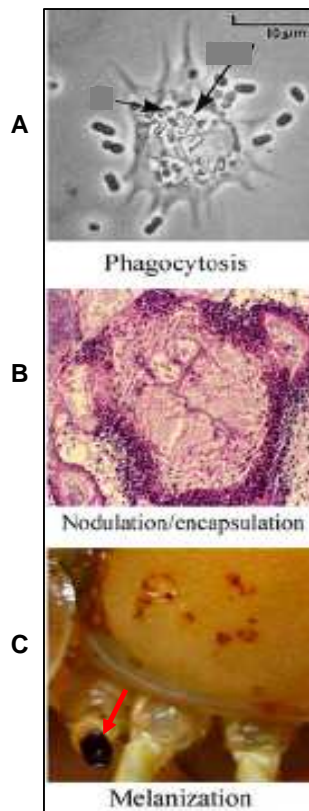
Figure 1.5: Phagocytosis (A), nodulation/encapsulation (B) and melanization (C) in Drosophila melanogaster (Jiravanichpaisal *et al.*, 2006). (A) extended pseudopodia of phagocytes engulf bacteria with bacterial digestion (indicated by the black arrows). (B) dark purple masses indicate aggregation of hemocytes around bacteria (in the case of nodulation) or larger pathogens (in the case of encapsulation). (C) shows a melanotic spot arising (indicated by the red arrow) through the process of melanization (external response) mediated by the prophenoloxidase cascade.

The prophenoloxidase cascade leading to melanization is a common mechanism of cellular innate immunity in organisms including arthropods, mollusks, ascidians, echinoderms, millipedes, bivalves and brachiopods.   This pathway is activated by the presence of lipopolysaccharide (LPS), peptidoglycan or β–1,3 glucan (Jiravanichpaisal *et al.*, 2006) (Figure 1.6). Prophenoloxidase enzymes are synthesized as inactive precursor enzymes or zymogens.   Recognition of the abovementioned bacterial or fungal components leads to cleavage of the zymogen by serine proteases. The active enzyme elicits monophenol mono-oxygenase activity which allows for the conversion of tyrosine to melanin via an enzyme catalyzed oxidation of phenols to quinones which ultimately leads to the formation of melanin at the site of infection or wounding in the organism (Leclerc & Reichart, 2004).
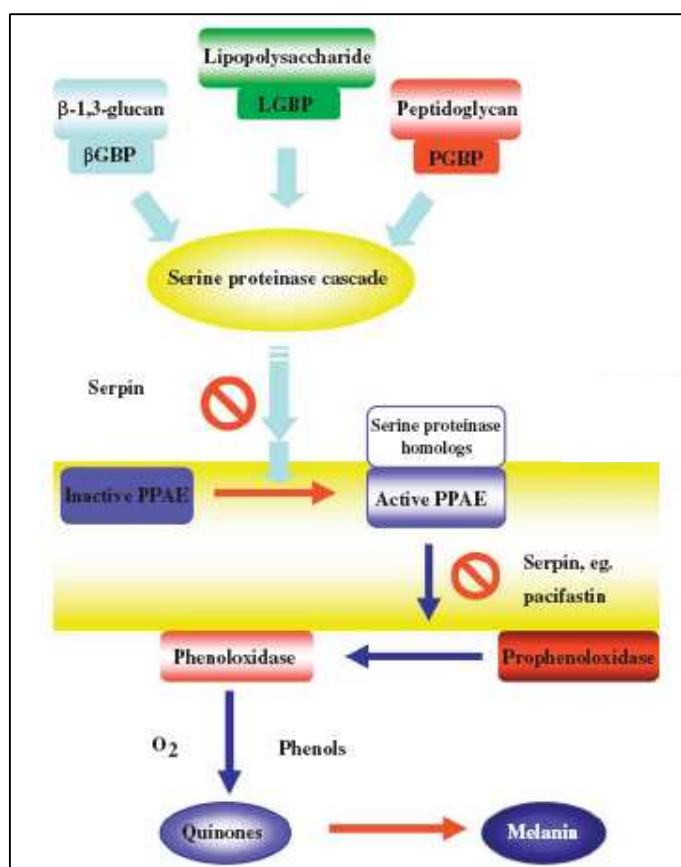
Figure 1.6: The activation of prophenoloxidase and processes of the prophenoloxidase cascade leading to melanization (Jiravanichpaisal *et al.,* 2006): Binding of β-1,3-glucan, LPS or peptidoglycan to the associated protein binding partners leads to the induction of a serine protease cascade which culminates in the activation of the prophenoloxidase activating enzyme (PPAE). This enzyme then catalyzes the activation of prophenoloxidase to phenoloxidase which converts quinones to melanin. The prophenoloxidase enzyme possesses a single disulfide bridged structure known as the clip domain. In addition to the catalytic activity of prophenoloxidase in innate immunity, it has been observed that upon cleavage at the clip domain (leading to zymogen activation) of recombinant prophenoloxidase, the fragment released showed antimicrobial activity *(*Jiravanichpaisal *et al., 2006).*

1.3.2 Humoral immunity

Despite the fact that innate immunity is divided into the cellular (as discussed above) and humoral branches, a clear distinction of these branches is difficult since several attributes of the humoral innate immune response are linked with the elicitation of the cellular innate immune response (Hoffmann & Reichart, 2002). For example, the recognition and binding of cellular components leads to the induction of several humoral cascades facilitated by the Toll and Imd pathways culminating in induction of synthesis of cytotoxic molecules which may in the case of phagocytes assist in intracellular destruction of the phagocytozed invader (Hoffmann & Reichart, 2002).

The mechanisms of recognition by humoral and cellular components of the innate immune system will be discussed using the humoral immune response of *Drosophila melanogaster*. This organism serves as the ideal model organism for the study of the invertebrate immune response for several reasons including the fact that no adaptive immune response is present and a high resistance to microorganisms is prevalent in this species (Hoffmann & Reichart, 2002). This situation is similar to that observed in ticks, however, no correlation between the immune responses of *D. melanogaster* and *O.savignyi* have been established.

Since microorganisms represent the oldest basic life forms, the emergence of metazoans required that these organisms develop defense mechanisms against the threat of an invading microorganism. These mechanisms typically include the ability to recognize an invader and specifically target a response focused at the specific elimination of the invader without cytotoxicity and cross reactivity to self cells.

1.3.2.1 Innate immune response of *D. melanogaster*

The epithelial surfaces of *D. melanogaster*, cells of the genital and digestive tracts, trachea and Malpighian tubules are seen to be the first line of defense to invading microorganisms. These cells produce and secrete antimicrobial peptides which target the microorganism of interest and lead to destruction of these invaders prior to further penetration into the hemocoel (Figure 1.6) (Hoffmann & Reichart, 2002).

In the case of survival and subsequent penetration of epidermal barriers, cellular responses such as phagocytosis, nodulation and/or encapsulation serve to destroy the microorganism (Hoffmann & Reichart, 2002).
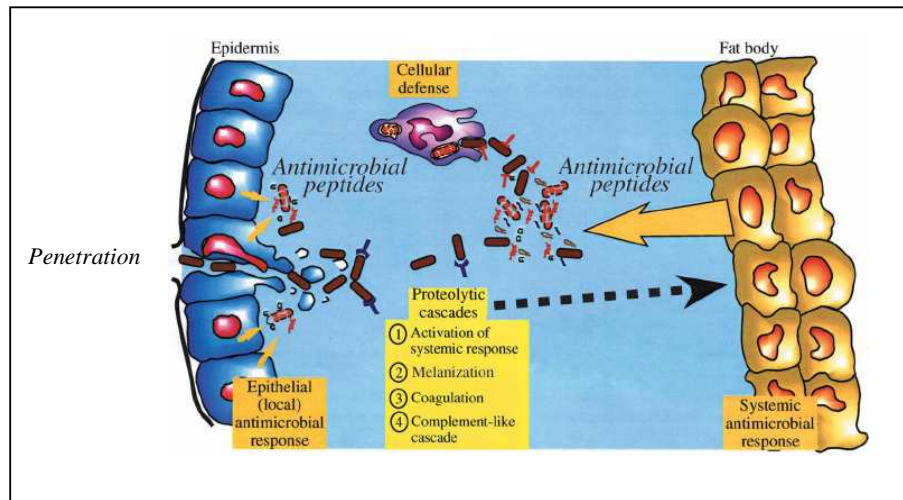
Figure 1.7: Schematic representation of humoral immune responses elicited against microorganisms by *D. melanogaster* (Hoffmann & Reichart, 2002)

As observed in Figure 1.7, penetration of the epithelial surface (first line of defense) leads to activation of a cellular immune response. Further stimulation by the invading microorganism leads to induction of a systemic antimicrobial response which is characterized by induction of synthesis of AMPs by hemocytes and/or the fat body, melanization, coagulation of hemolymph or a putative complement-like cascade.

The major features of the humoral response to such microbial invasion are induction of synthesis of AMPs. In *D. melanogaster* the major organ of synthesis of AMPs is the fat body, similar to the situation in ticks (Leclerc & Reichart, 2004). This tissue develops from the mesoderm during embryogenesis and shows immune defensive activity from the larval life stage (Tzou *et al.*, 2002). Depending on specific characteristics of the invading microorganism, different signaling pathways are activated with the end result of induction of synthesis of AMPs with specific cytotoxicity to the microorganism recognized (Table 1.2) (Hoffmann & Reichart, 2002).

Table 1.2: AMPs *induced* in *D. melanogaster* following invasion by indicated microorganisms (Hoffmann and Reichart, 2002)

Antimicrobial peptide family	Main biological activities at physiological concentrations	Number of genes		Post-translational modifications	Concentration in the blood (systemic response)	Epithelia expressing various antimicrobial peptides
		Per genome	Expressed			
Diptericin	Antibacterial, Gram-negative	2	2	Two O-glycosylations, COOH-terminal amidation	0.5 μM	Midgut
Attacin	Antibacterial, Gram-negative	4	4			Midgut
Drosocin	Antibacterial, Gram-negative	1	1	O-glycosylation	40 μM	Calyx, oviduct, tracheae
Cecropin	Antibacterial, Gram-negative	4	4	COOH-terminal amidation	50 μM	Calyx, oviduct, seminal receptacle, spermathecae
Defensin	Antibacterial, Gram-positive	1	1		1 μM	Seminal receptacle, spermathecae, labellar glands
Metchnikowin	Antifungal	1	1		40 μM	Labellar glands
Drosomycin	Antifungal	7	2		100 μM	Labellar glands, seminal receptacle, spermathecae, tracheae, salivary glands

Recognition and response to Gram-positive bacteria and fungi

The activity of the Toll receptor in the induction of synthesis of AMPs was first elucidated in 1981 by Boman and his colleagues during an investigation into AMPs of the moth *Hyalophora cecropia* (Hoffmann, 1995). This receptor is a transmembrane protein with an extracellular domain composed of leucine-rich repeats (LRRs). The intra-cytoplasmic domain shows significant homology to the interleukin 1 receptor (IL-1R) and this domain is referred to as the Toll-IL-1R (TIR) domain (Hoffmann & Reichart, 2002).

Recognition of a Gram-positive bacterium or fungus leads, by means of detection of lipotechoic acid (LTA) and peptidoglycan, to initiation of an as yet undeciphered cascade of a series of four serine proteases (Hoffmann & Reichart, 2002). This cascade culminates in cleavage of a member of the cystine-knot family of growth factor like- and cytokine like-proteins namely Spaetzle (Hoffmann *et al.,* 1999). Cleaved Spaetzle binds to LRRs of the extracellular domain of the Toll protein leading to activation of the Toll receptor. The intracellular domain of the Toll receptor then interacts with several adaptor proteins namely Tube and Pelle. Pelle is a member of the serine-threonine kinase family of proteins and possesses a death domain. Upon activation of these kinases Cactus protein pre-bound to Dorsal is phosphorylated leading to dissociation of the Cactus-Dorsal complex (Hoffmann *et al.,* 1999). Dorsal, a response element (Rel) binding protein, is active during dorsoventral patterning processes in embryogenesis of *D. melanogaster,* however, a related homolog namely Dorsal-related immune factor (Dif) is as the name states active in the cascade response of the immune system (Hoffmann & Reichart, 2002). This protein possesses Rel homology domain which consists of an ankyrin repeat.

Once Dif has been released from the Cactus-Dif complex, it undergoes translocation to the nucleus where upon dimerization binds directly to the $NF_\kappa B$ *cis*-regulatory response element upstream of the AMP gene promoter. This binding leads to the activation of transcription of the AMP gene. As seen in Table 1.2, drosomycin (antifungal), metchnikowin (antifungal) and defensins (anti Gram-positive bacteria) undergo induction for synthesis using the cascade described above namely the Toll pathway (Figure 1.7). Toll mutants were seen to show a highly decreased resistance to fungi. However, the ability to survive a Gram-positive bacterial challenge was attributed to the presence of an alternate pathway (Kimbrell & Beutler, 2001).
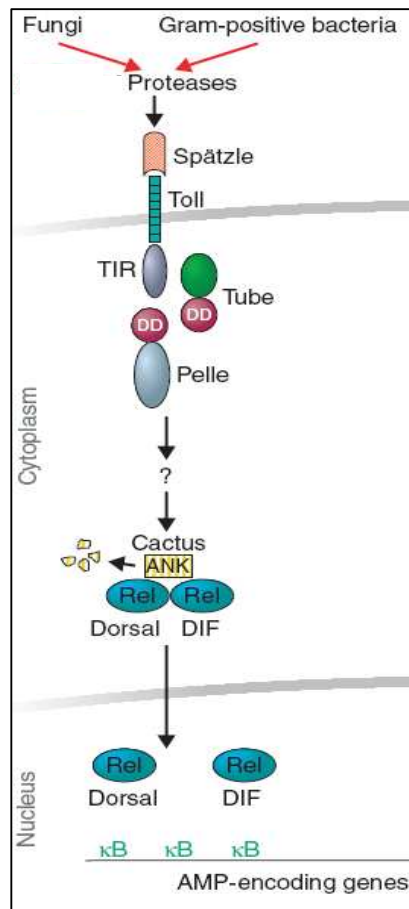
Figure 1.8: Diagrammatic representation of the Toll pathway in *D. melanogaster* (Tzou *et al.,* 2002).

Recognition and response to Gram-negative bacteria

D. melanogaster mutants deficient in the *Imd* gene were seen to be immunodeficient when exposed to both Gram-positive and Gram-negative bacteria, however exposure to fungi showed no adverse effect (Kimbrell & Beutler*.,* 2001). The suggestion that the Imd pathway serves as an alternative pathway for induction of synthesis of AMPs was supported by the discovery of the induction of diptericin by the action of the Imd pathway in the respiratory tract of *D. melanogaster* (Kimbrell & Beutler*,* 2001). As indicated in Figure 1.9, the initiation or activation of the Imd pathway is dependent upon the recognition of bacterial LPS. This recognition leads to the activation of the equivalent of a signalosome named NEMO (NF$_\kappa$B-essential modulator), consisting of homologs of the mammalian I$_\kappa$B kinase$_\beta$ (IKK$_\beta$) and a structural component (IKK$_\gamma$). NEMO is involved in the activation of Relish (a Rel binding protein) (Tzou *et al.,* 2002). Relish is activated by an endoproteolytic cleavage of the Rel homology domain from the ankyrin repeat region bearing the terminal COOH moeity involved in maintaining Relish in an inactivated state. Activated Relish is translocated to the nucleus and is directly involved in upregulation of synthesis of AMPs facilitating an antibacterial response. The major AMP produced in response to Gram-positive and Gram-negative bacteria via induction of the Imd pathway is diptericin (Hoffmann & Reichart*,* 2002).
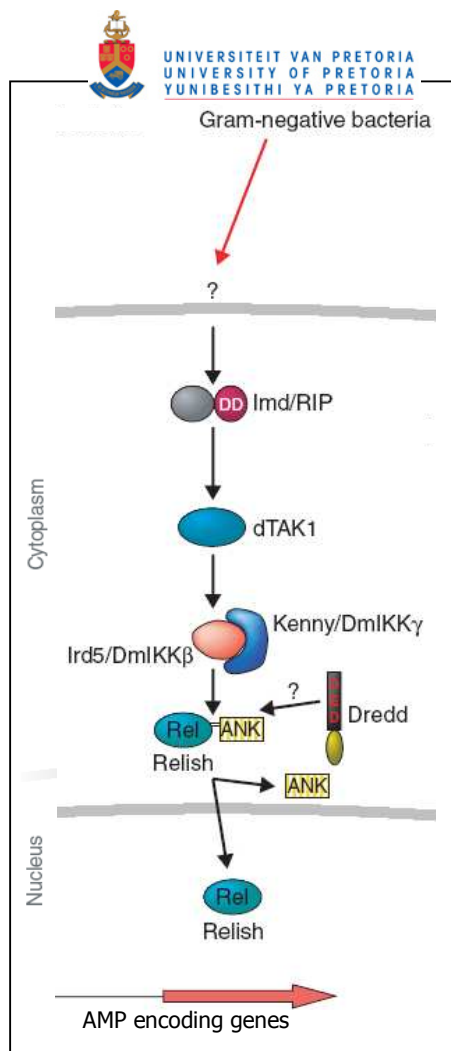
Figure 1.9: Diagrammatic representation of the Imd pathway in *D. melanogaster* (Tzou *et al.,* 2002).

The Toll and Imd pathways are initiated by the recognition of Gram-positive bacteria, fungi and Gram-negative bacteria. The recognition of bacterial components such as LTA, LPS and peptidoglycan by hemocytes are facilitated by pattern recognition receptors (PRRs) on the surface of hemocytes (Hoffmann & Reichart, 2002). These PRRs recognize pathogen associated molecular patterns PAMPs such as the aforementioned components and leads to initiation of the abovementioned responses which ultimately culminate in induction of synthesis of AMPs (Kurata *et al.,* 2006).

AMPs: Activity and characteristics

Once upregulated via recognition of Gram-positive or Gram-negative bacteria or fungi, AMPs are effective in elimination of a foreign invader. Table 1.3 shows the overall effectivity of several AMPs from different species.

Table 1.3: Summary of the major characteristics of AMPs: Homologues between plants and *D. melanogaster* are indicated in yellow for Drosomycin and in blue for defensins

Class	Organism	Antimicrobial peptide	Characteristic	Reference
Arachnida (Phylum: Arthropoda)	*D.melanogaster*	Drosomycin	Antifungal	Hoffmann, 1995
		Defensin	Anti Gram-positive	Hoffmann *et al.*, 2002
		Cecropin	Anti Gram-negative	Hoffmann *et al.*, 2002
		Metchnikowin	Antifungal	Hoffmann *et al.*, 2002
	Tachypleus tridentatus	Big defensin	Anti Gram-positive, Anti Gram-negative and antifungal	Iwanaga, 2002
		Tachystatin	Anti Gram-positive, Anti Gram-negative and antifungal	Iwanaga, 2002
		Tachycitin	Anti Gram-negative and synergistic enhancement of activity of Big defensin	Iwanaga, 2002
	Rhipicephalus (Boophilus) microplus	Microplusin	Cysteine-rich Anti Gram-positive and bacteriostatic	Fogaca *et al.*, 2004
		Defensin	Anti Gram-positive	Fogaca *et al.*, 2004
	Ornithodoros moubata	Defensin	Anti Gram-positive	Nakajima *et al.*, 2001
	Haemaphysallis longicornis	Longicin	Anti Gram-positive, Anti Gram-negative and parasiticidal	Tsuji & Fujisoki, 2007
	Aedes aegypti	3 defensin isoforms	Anti Gram-positive	Lowenberger, 2001
		Cecropin	Anti Gram-negative	Lowenberger, 2001
		Transferrins	Bactericidal-(iron sequestering activity)	Lowenberger, 2001
Nematodes	*Caenorhabditis elegans*	Putative AMP	Anti Gram-positive, Anti Gram-negative and parasiticidal	Kim *et al.*, 2005
Annelids	*Eisenia foetida*	Fetidins	Bactericidal-(cytolytic activity)	Cooper *et al.*,2002
		Coelomic cytolytic factor 1 (CCF-1)	Glucanase activity and activation of prophenoloxidase cascade. Specific to yeast and gram negative bacterial cell wall components	Cooper *et al.*,2002
		Lysenin	Hemolytic peptide specifically binding to sphingomyelin	Cooper *et al.*,2002
		Eiseniapore	Membrane pore/channel formation	Cooper *et al.*,2002
		Lumbricin 1	Proline rich AMP active against Gram-positive and Gram-negative bacteria	Cooper *et al.*,2002
Vertebrates	Mammals	α-defensin	Antimicrobial and antiviral activity	Oppenheim *et al.*, 2003
		β-defensin	Antimicrobial	Oppenheim *et al.*, 2003
Plants	*Brassicaceae*	Drosomycin homolog	Antifungal	Hoffmann, 1995

AMPs include a class of peptides or polypeptides with less than 50-100 amino acids and are either constitutively expressed in secretory cells or induced upon infection. AMPs adopt an amphipathic structure and the majority are cationic in nature due to a larger percentage of arginine and lysine residues as well as C-terminal amidation which has been hypothesized to stabilize the peptide against *in vivo* protease activity (Bulet *et* al., 2004). In general, it is

expected that cationic AMPs are able to interfere with membrane permeability (Table 1.4). Association of the AMP with the membrane is mediated by electrostatic interactions between the positively charged peptide and the negatively charged polar head groups in the membrane. Additionally, these cationic peptides are able to form pores in the membrane of target cells and subsequently be internalized. AMPs are thereafter able to bind to intracellular targets, for example the DNA of microorganism and prevent successful transcription (Bulet *et* al., 2004).

There are three basic models stipulating the mechanism of membrane permeation by AMPs (Table 1.4). The barrel-stave mechanism (Figure 1.10) involves electrostatic or hydrophilic interactions of the peptide with the polar head groups of the phospholipid bilayer leading to the formation of pores through which cytoplasm and ions may leak culminating in cellular disintegration (Shai & Jelinek, 2002).
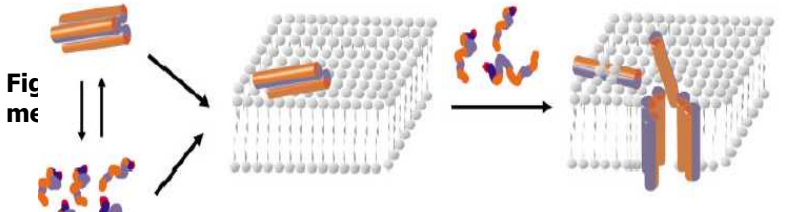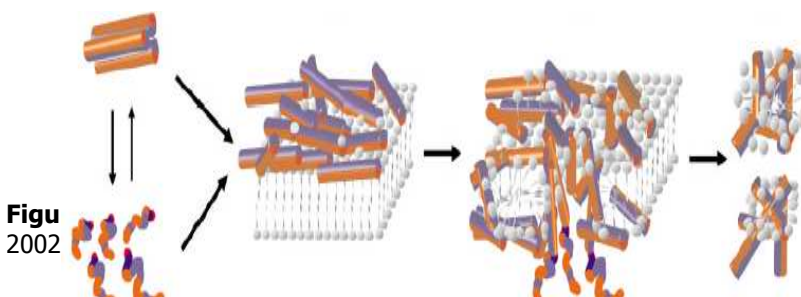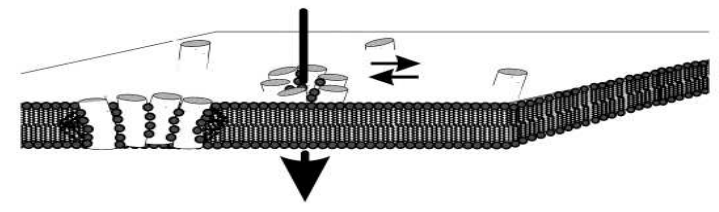
The carpet model (Figure 1.11) is characterized by hydrophobic interactions between the cell membrane and the AMP. This interaction leads to the formation of transient pores and cellular disintegration (as in the barrel-stave mechanism) (Shai & Jelinek, 2002).

The toroidal pore mechanism (Figure 1.12) involves individual interactions of the AMP with lipids in the cell membrane leading to a change in orientation of the lipid relative to the peptide and so formation of membrane pores and ultimately cellular disintegration (Matsuzaki K., 2002).

Hancock & Chapple, (1999) have also described the detergent-like model (aggregate pore model) where self associating AMPs form a micelle. Upon collision of these micelles with the membrane, membrane lipids are absorbed. This then leads to pore formation.

The overall cellular events following pore formation involve the collapse of the transmembrane electrochemical gradient, cessation of cellular respiration, the depletion of ATP and cell death (Shai *et al.,* 2002).

Table 1.4: Table summarizing the three basic models of action of antimicrobial peptides

Model of action	Mechanism	Graphical representation
Barrel stave mechanism	Peptides bind to cell membrane through electrostatic or hydrophilic interactions with phospholipid polar head groups. Further AMPs may be recruited to this site. Peptides insert into the membrane forming pores through which cellular components/ions may enter/exit leading to cellular disintegration.	Fig me
Carpet model	Peptide binding is facilitated by interaction of the hydrophobic surface of the peptide with the cell membrane. Once a threshold concentration of the peptide has been reached, the peptides insert themselves into the membrane and form transient pores which lead to eventual cellular disintegration as mentioned for the barrel stave mechanism above.	Figu 2002
Toroidal pore mechanism	Peptide binding is the same as described for the carpet model. Peptide insertion leads to a change in the orientation of the phospholipid relative to the peptide forming transient pores which lead to membrane disintegration in the same manner as described above.	**Figure 1.12: Schematic representation of the toroidal pore model** (Bechinger, 2004)

16

1.3.2.2 Immune response of ticks

Since ticks are classified as obligate hematophagous ectoparasites, the primary feeding event involves a bloodmeal on a vertebrate host. During this non-sterile feeding process various Gram-positive, Gram-negative or fungal microorganisms may be ingested. For this reason, an effective immune response is essential to ensure tick survival following a bloodmeal. Table 1.5 shows the functional importance of tick hemocytes in the elicitation of a cellular innate immune response.

Table 1.5: Table summarizing tick hemocytes and functional importance in the elicitation of a cellular innate immune response (adapted from the text of DeMar, 2006)

Family	Species	Hemocyte	Function
Ixodidae	*B. microplus*	Plasmatocytes	Most abundant cell involved in phagocytosis
		Granulocytes	Specifically phagocytic towards *Borrelia burgdorferi*
Argasidae	*O. moubata*	Granulated plasmatocytes	Phagocytosis
		Granulocytes	
		Lepidopteran spherulocyte homolog	Function unidentified

Major responses of the humoral innate immune response include humoral factor mediated nodulation or encapsulation as well as phagocytosis. Recognition of invading pathogens may lead to recognition of PAMPs by PRRs on tick hemocytes. This has been proposed to lead to induction of synthesis of antimicrobial peptides by means of stimulation of homologous Toll- or Imd-like pathways as seen in *D. melanogaster* (DeMar, 2006). Antimicrobial peptides, with specific focus on those characterized from ticks will be discussed in Chapter 2.

Gram-positive and Gram-negative bacteria as well as fungi and nematodes trigger release of melanotic material via activation of the prophenoloxidase cascade. This melanotic material initially accumulates around the invader and as the response continues, the density of aggregate formation increases until the invader is completely entrapped. This encapsulation may lead to recruitment of cytotoxic or phagocytic cells to the site of infection and so destruction of the invading microorganism (DeMar, 2006).

Prophenoloxidase activity was not detected in the hard tick species (*Amblyomma americanum, Dermacentor variabilis* and *Ixodes scapularis*) studied by Zhioua *et al.*, (1997). However, significant activity was detected in the Greater Wax moth, *Galleria mellonella*,

implicating that the prophenoloxidase cascade is indeed present in other invertebrate species. In 2002, the results of Kadota *et al.*, implicated that prophenoloxidase activity is essential during the moulting of 4th instar nymphs of *O. moubata.* Furthermore, experimental evidence of Simser *et al.,* (2004), denied the absence of the prophenoloxidase cascade in ticks as several invertebrate serine protease homologs involved in the initiation of the prophenoloxidase cascade, were identified in the ixodid tick, *D. variabilis.*

1.4 *O. savignyi* as a model

The argasid tick, *O. savignyi*, is present mainly in arid or semi arid areas of continental Africa (Theiler & Hoogstraal , 1955). This nocturnal tick species may feed on several hosts (Charrel *et al.*, 2007) and has been implicated in animal toxicoses following a tick bite due to the presence of a unique family of lipocalins, the tick salivary gland proteins (TSGPs) (Mans *et al.,* 2003).

A defensin peptide was characterized from the hemolymph of this tick species (Olivier N.A., MSc thesis, University of Pretoria, Biochemistry). Subsequently two defensin isoforms were cloned and sequenced (Botha M.E., 2007, Hons. Project, University of Pretoria, Biochemistry). Since little further knowledge is available on this tick, exploration of the innate immune mechanisms of this tick will provide a greater knowledgebase to the academic sector of tick research. The findings in the prominent representative of the argasid tick species *O. moubata* may be compared to significant findings in the closely related *O. savignyi* argasid tick in order to attempt presentation of comparison of possible conservation of immune mechanisms within this genus.

1.5 Aims of this study

Since ticks are classified as obligate hematophagous ectoparasites of the phylum arthropoda conservation within the innate immune system may be seen as a result of proteins or peptides of homologous functions due to the fact that effector molecules are significantly conserved across species. Furthermore, *in vivo* functional analysis will allow the elucidation of the possible functional roles of putative immunoprotective molecules.

Chapter 2 aims identify and characterize microplusin homologs in ticks of the Argasidae family. Identification of such homologs across tick species would represent conservation in

the immune response in terms of the function elicited by the peptide, thereby providing a clearer understanding of humoral innate immunity in ticks.

Lysozyme is involved in enzymatic cleavage of the 1,4-β-glycosidic bond linking N-acetylglucosamine (NAG) and N-acetylmuramic acid (NAM) in the peptidoglycan cell walls of Gram-positive bacteria (Kopacek *et al., 1999).* Since lysozyme is implicated in immunoprotective and/or digestive roles in several arthropod species, specifically ixodid *Dermacentor andersoni* and *D. variabilis* and argasid *O. moubata* ticks. The aim in chapter 3 is the identification and molecular characterization of a homologous lysozyme molecule in the gut of the argasid tick, *O. savignyi.*

Furthermore, it is clear that defensins are molecules of common existence across species. Additionally, in the case of AMPs, such as defensins, a synergistic effect of one peptide may be elicited on a second peptide, such as lysozyme. To investigate the functional roles of these putative immunoprotective molecules and evaluate possible synergism between them on an mRNA level, chapter 4 focuses on the the tissue expression profile of defensins as well as the RNAi mediated silencing of the defensin gene together with that of lysozyme. The idea of synergism between defensins and lysozyme was suggested by Sonenshine in 2008 where it is hypothesized that the knockdown of the defensin mRNA transcript may induce upregulation of transcription of the lysozyme transcript as a protective mechanism of tick immunity.

Chapter 2:

Molecular identification of microplusin homologs in the argasid tick, *Ornithodoros savignyi*

2.1 Introduction

Antimicrobial peptides (AMPs) are stimulus-induced peptides found in organisms ranging from plants, invertebrates and vertebrates including large mammals as well as man. A common feature of these peptides is their cationic nature (Table 2.1) and inherent low molecular weight (Marshall & Arenas, 2003). However, AMPs lacking the characteristic cationic nature have also been described for all kingdoms (Table 2.2). These include anionic peptides; aromatic peptides as well as peptides derived from oxygen-binding proteins, for example the bovine haemoglobin fragment showing antifungal activity in the midgut of *Rhipicephalus (Boophilus) microplus* (Vizioli & Salzet, 2002).

In general, cationic AMPs may be divided into three major classes namely linear α-helical peptides lacking cysteine residues, cyclic peptides rich in cysteine and peptides containing high concentrations of a particular amino acid, commonly glycine, histidine or proline (Bulet *et al.,* 1999).

Table 2.1: Cationic AMPs as well as model organism and range of antimicrobial activity
(Vizioli & Salzet, 2002)

Structure and representative peptides	Organism	Antimicrobial activity
Linear α-helix peptides		
Cecropins	Insects, pig	Bacteria, fungi, virus, protozoa, metazoa
Clavanin, styelin	Tunicates	Bacteria
Magainin, dermaseptin	Amphibians	Bacteria, protozoa
Buforins	Amphibians	Bacteria, fungi
Linear peptides rich in certain amino acids		
Pro-rich:		
drosocin, metchnikowins,	Fruit fly	Bacteria
pyrrhocoricin,	Hemipteran	Bacteria, fungi
metalnikowin		
Gly-rich:		
diptericins, attacins	Dipterans	Bacteria
His-rich:		
histatin	Human	Bacteria, fungi
Try-rich:		
indolicidin	Cattle	Bacteria
Single disulfide bridge		
Thanatin	Hemipteran	Bacteria, fungi
Brevinins	Frog	Bacteria
Two disulfide bridges		
Tachyplesin II	Horseshoe crab	Bacteria, fungi, virus
Androctonin	Scorpion	Bacteria, fungi
Protegrin I	Pig	Bacteria, fungi, virus
Three disulfide bridges		
α-Defensins	Mammals	Bacteria, fungi
β-Defensins	Mammals	Bacteria, fungi
Defensins	Insects	Bacteria, fungi, protozoa
Penaeidins	Shrimp	Bacteria, fungi
More than three disulfide bridges		
Tachycitin	Horseshoe crab	Bacteria, fungi
Drosomycin	Fruit fly	Fungi
Gambicin	Mosquito	Bacteria, fungi, protozoa
Heliomicin	Lepidopteran	Bacteria, fungi
Defensins	Plants	Fungi

21

Table 2.2: Non-cationic AMPs as well as model organism and range of antimicrobial activity (Vizioli & Salzet, 2002)

Structure and representative peptides	Organism	Antimicrobial activity
Anionic peptides		
Neuropeptide derived:		
Enkelytin	Bovine, human,	Bacteria
Peptide B	Bovine, human, leech, mussel	Bacteria
Aspartic acid rich:		
H-GDDDDDD-OH	Ovine	Bacteria
Dermcidin	Human	Bacteria
Aromatic dipeptides		
N-β-alanyl-5-S-glutathionyl-3,4-dihydroxyphenylalanine	Flesh fly	Bacteria, fungi
p-Hydroxycinnamaldehyde	Saw fly	Bacteria, fungi
Peptides derived from oxygen-binding proteins		
Hemocyanin derived	Shrimp	Bacteria
Hemoglobin derived	Tick	Bacteria
Lactoferrin	Human	Bacteria, virus

2.1.1 Linear α–helical peptides

These peptides (Figure 2.1) include cecropins and defensins of the genus Lepidoptera and Diptera, respectively (Hoffmann, 1995). Such peptides are produced primarily in the fat body of insects and may be secreted into the hemolymph. Alternatively, these peptides may be synthesized by the blood- or epithelial cells in mammalian organisms (Bulet *et al.,* 2004). The range of activity includes Gram-positive and -negative bacteria as well as anti-fungal and anti-protozoan activity. Furthermore, these peptides are potent activators of hemolysis and are approximately 30-40 amino acid residues in length and usually show C-terminal amidation (Bulet *et al.,* 2004).
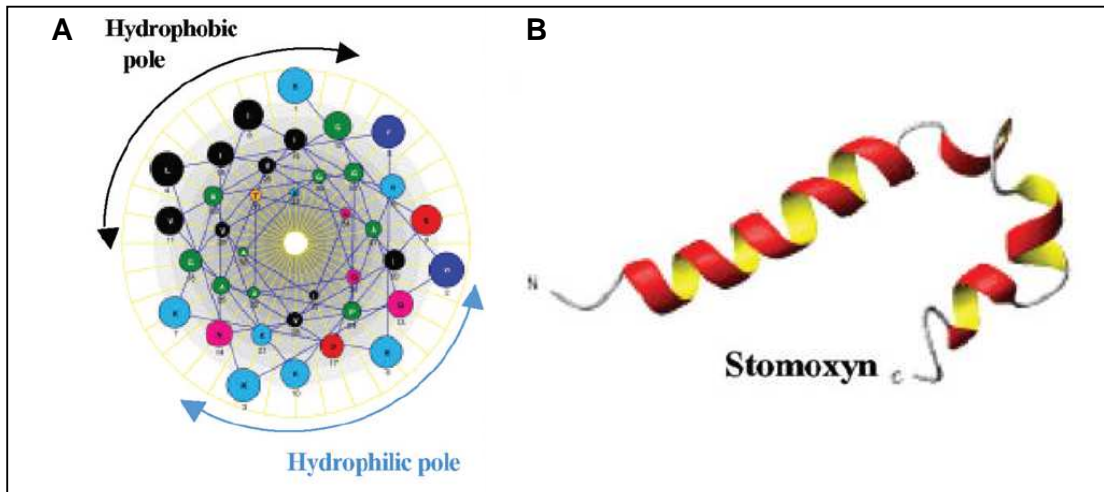
Figure 2.1: **The structure of an typical α–helical AMP (A) and ribbon structure of stomoxyn (B) (Bulet *et al.*, 2004):** In (A) the typical amphipathic structure afforded by an α-helix is shown. This amphipathicity (blue indicates hydrophilic while black indicates hydrophobic amino acids) allows insertion of the α-helix into the cell membrane of bacterial cells. In (B) the three dimensional structure of stomoxyn is shown with α-helices (red and yellow bands) linked together via loops (black lines).

2.1.2 Cyclic peptides containing cysteine

The prototype of this group is Drosomycin, a 44 residue peptide, isolated from *D. melanogaster* (Fehlbaum *et al.*, 1994). Typically, these peptides are rich in cysteine residues which promote the formation of disulphide bonds and ultimately a cyclic structure. Those peptides possessing only a single disulphide bond are able to form β-hairpin like structures (Figure 2.2A) while those with several disulphide bonds form complex folded structures (Figure 2.2B) (Bulet *et al.*, 2004).
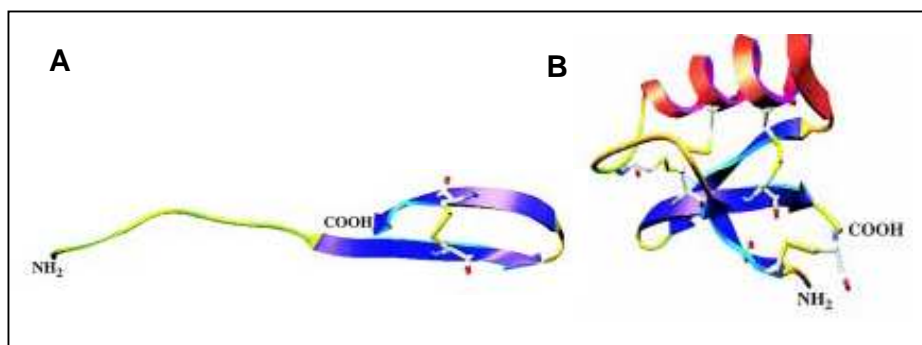
Figure 2.2: (A) Arthropod β-hairpin defensin, thanatin, from *Pidisus maculiventris* (Bulet *et al.*, 1999) and (B) the three dimensional structure of Drosomycin (Bulet *et al.*, 2004): A single disulphide bridge may stabilize two individual β–sheets (blue) forming a β–hairpin structure as seen in the case of thanatin (A). Cysteine-rich peptides such as drosomycin may consist of α-helices (red) as well as β-sheets (blue) linked together by loops (yellow). The entire structure may then be stabilized by disulfide bridges occurring between predetermined cysteine residues (indicated as red dots on Figure B).

2.1.3 Proline and Glycine rich peptides

Proline rich peptides may be divided into unsubstituted and *O*-glycosylated peptides (Bulet *et al.*, 1999). Unsubstituted peptides are divided into short and a long chain groups, respectively. The short chain group refers to those isolated from Hemipteran species and possess, on average, 15 to 17 amino acids, of which some 4-5 residues are proline. The prototype of this group is the metalnikowins from arthropods *Podisus prasin and P. maculiventris* (Levashina *et al.,* 1995). A 34 amino acid residue peptide, abaecin from *Apis mellifera* serves as the prototype for the long chain group. These proteins possess a characteristic Pro-Arg-Pro repetitive motif which is common to all unsubstituted proline rich long chain peptides, except abaecin of *A. mellifera* (Rees *et al.*, 1997).

O-glycosylated peptides are represented by the prototype drosocin from *D. melanogaster,* which is a 19 amino acid peptide containing six proline residues. *O*-glycosylation occurs through post-translational modification of a single threonine residue (Thr-11) and is essential for activity. Related peptides have been isolated from *D. melanogaster* (drosocin), hemipteran pyrrhocoricin from *P. apterus*, lepidopteran lebocin from *Bombyx mori* and hymenopteran formaecins from *Myrmecia gulosa* (Hara & Yamakawa, 1995). The major differences between these molecules are sugar moieties attached during post-translational modification of the threonine residue. The glycine rich polypeptides comprise a family known as gloverins. These peptides are, as the name states, rich in glycine residues and are primarily active against *Candida sp.* (Bulet *et al.*, 1999).

2.1.4 Tick AMPs

Various tick AMPs have been discovered in recent years and it is evident that differences between species, tissue, organ of synthesis, localization and differences in the required induction stimuli exist. In some cases it is necessary for the tick to feed in order to allow for induction while in other cases septic injury alone mounts a potent immune response culminating in nduction, synthesis and release of AMPs (Sonenshine, 1993).

In 2002, four defensin isoforms were discovered to be constitutively expressed in the midgut of the argasid tick *Ornithodoros moubata* (Nakajima *et al.,* 2002)*.* It was found that expression of these defensin isoforms was upregulated in the tick midgut following a bloodmeal. In general, these defensins showed anti-*Staphylococcus aureus* activity. Investigation into tissue specific expression revealed that constitutive expression of defensin

isoforms occurs in the midgut, fat body and reproductive tract of adult female ticks. The eggs of *O. moubata* however, showed no antibacterial activity (Nakajima *et al.,* 2002).

A histidine rich AMP called hebraein, was isolated from the egg wax extract of the ixodid tick *Amblyomma hebreaum* (Lai *et al.,* 2004a). This AMP showed antimicrobial activity against *S. aureus, Candida albicans, C. glabrato* as well as *Escherichia coli.* Studies of mutants using low histidine content and antimicrobial assays at differing pH showed that the peptide is optimally functional at a pH between 6.2 and 6.4. Additionally, peptide mutants lacking a high histidine content were unable to elicit an efficient antimicrobial response as compared to the wild type. In this case, it is evident that enrichment of a particular amino acid as well as induced physiological pH (as seen in the tick midgut following a bloodmeal) is essential for optimal antimicrobial response by an AMP (Lai *et al.*, 2004a).

Peptide defensins (Peptide 1 and Peptide 2) were isolated and characterized from the hemolymph of *A. hebraeum* (Lai *et al.,* 2004b). Both peptides were isolated from hemolymph of blood fed females and were found to have both anti Gram-positive and negative activity. No antifungal activity was observed.

The argasid, *O. moubata* defensin was shown to posess anti *B. burgdorferi* activity (Johns *et al.,* 2001). Bulet *et al.,* showed in 2004 that the mode of action of defensins differs from traditional antibiotics. Membrane depolarization afforded by defensins allows for collapse of the transmembrane electrochemical gradient, cessation of cellular respiration, depletion of ATP and cell death. This mode of action allows AMPs the ability to target several multi drug resistant microorganisms.

An AMP, ixodidin, isolated from the cattle tick (*R. (B.) microplus*) showed novel potent serine protease inhibitory activity along with antimicrobial activity towards *Micrococcus luteus* and *E. coli* (Fogaca *et al.,* 2006). The precise mode of action of ixodidin has not yet been established, however, it is hypothesized that either activity is directed against the bacterial membrane or that inhibition of serine proteases leads to inability of invading pathogens to infest host tissue (Fogaca *et al.,* 2006). Additionally in 2005, Yu *et al.,* discovered another AMP, ixosin, in the salivary glands of *Ixodes sinensis*. This AMP showed activity against *E. coli, S. aureus* as well as *C. albicans*. Ixosin is synthesized as a precursor polypeptide constituted of 79 amino acids, after which the signal peptide is cleaved producing a mature AMP of 23 amino acids (Yu *et al.,* 2006).

Antibacterial activity was found in the egg wax of *A. hebraeum* (Arrieta *et al.,* 2006). In this study, it was shown that organic and aqueous extract of eggs was able to elicit a potent anti Gram-negative response, while anti Gram-positive activity was marginal. Furthermore, the denuded egg (egg with egg wax extracted), was unable to elicit any antimicrobial activity. Transmission electron microscopy of *S. epidermidis* cells treated with the AMP revealed thickened bacterial cell walls as well as electron lucent zones in the cytoplasm of bacteria (Figure 2.3). The investigators interpreted these observations to be due to leakage of cytoplasmic contents in areas of membrane perforation by the AMP.
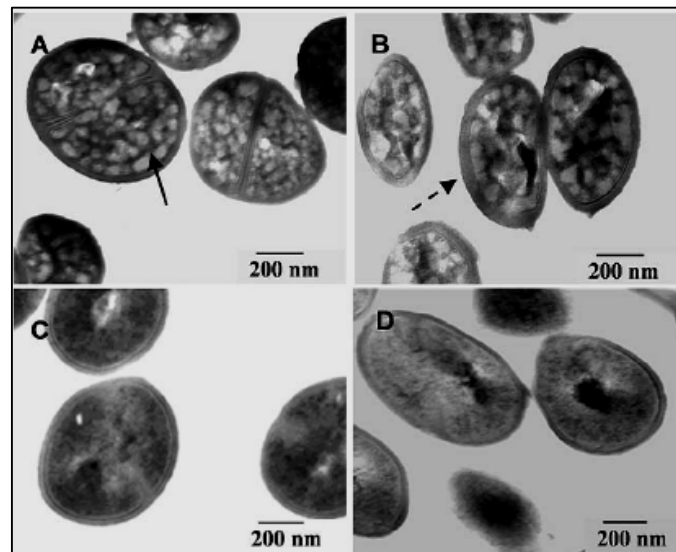
Figure 2.3: *S. epidermidis* cells treated with egg wax extract of *A. hebreaum* (Arrieta *et al.,* 2006)**:** Solid arrow indicates electron lucent zones assumed to arise due to the leakage of cytoplasmic contents from pores formed in the membrane by AMPs. The dashed arrow indicates thickened cell wall, C and D represent untreated cells

The basis of this study follows the discovery of the cysteine-rich AMP, microplusin, from *R. (B.) microplus* (Fogaca *et al.,* 2004). This 10 kDa polypeptide is synthesized as a 110 amino acid precursor protein. Cleavage of the 20 amino acid signal peptide yields a mature AMP of 90 amino acids containing six cysteine residues implicating formation of three disulphide bonds and production of an AMP with a cyclic structure. Microplusin was selectively isolated from cell free hemolymph of the ixodid tick using high performance liquid chromatography (HPLC). Purified protein was used in antimicrobial assays against *M. luteus, E.coli* as well as *S.aureus.* Microplusin showed significant antimicrobial activity against Gram-positive bacteria and was furthermore bacteriostatic in action towards *M. luteus.* Analysis of tissue specific expression of microplusin using real time PCR, showed high levels of expression within the fat body, hemocytes as well as the ovaries (Fogaca et al., 2004).

Ingestion of blood by a tick leads to a change in the internal physiological environment such as an increase in core temperature as well as a decrease in internal pH (Arrieta *et al.,* 2006). These changes are accompanied by induction of synthesis of AMPs which specifically target various different microorganisms that may be ingested. Over the past couple of years numerous tick AMPs have been discovered. A common feature of these tick AMPs is the requirement for induction via a bloodmeal, septic injury or induced immune challenge. A further common feature of tick AMPs is their specificity towards Gram-positive and Gram-negative bacteria, as well as fungi. This is an inherent capability of the immune system of invertebrates. For this reason, an investigation into AMPs may provide a clearer insight into the innate immune system of ticks. Since most of these AMPs show a potent response towards microorganisms, leading to an almost immediate eradication, these molecules may prove to be efficient natural antibiotics (Bulet *et al.,* 1999).

2.1.5 Identification of microplusin homologs in *O. savignyi*

The focus of this chapter is the identification of microplusin homologs in the argasid tick *O. savignyi.* Microplusin is found in the ixodid tick species, *R. (B.) microplus,* which was used as a positive control. It was proposed that a microplusin homolog may be found in the salivary glands of the argasid tick species *O. savignyi* based on BLAST searches of the available microplusin sequence (GeneBank Accesion number AY 233212) that show an approximate 37% identity to a novel salivary gland AMP found in the salivary glands of the argasid tick, *Argas monolakensis*.

An investigation into the mode of action of the homolog may provide insight into the mechanism of survival of a tick when challenged by microorganisms and so facilitate an understanding of the immune processes in ticks.

2.2 Hypothesis

An argasid microplusin homolog is expressed in salivary glands of *O savignyi.*

2.3 Aim

To identify microplusin homologs in the argasid tick, *O. savignyi,* by means of PCR and amplification of cDNA ends (5'- and 3'- RACE).

2.4 Materials and Methods

2.4.1 Ticks and hemolymph collection

Ticks were purchased from farmers in the Northern Cape (Upington) who collected them by the sifting of sand. Ticks were stored in the sand at room temperature. Hemolymph collection was facilitated by immobilization of ticks on double-sided tape, with the ventral surface exposed. A 30 gauge needle was used to puncture the first pair of coxae at the base of the trochanter. Application of moderate pressure on the ventral surface of the tick allowed for leakage of hemolymph, which was collected and immediately placed into TRI-Reagent (Sigma-Aldrich).

2.4.2 Tick dissections

In order to obtain specific tissue samples for RNA isolation, ticks were dissected by means of modifications of the protocol developed by Ribeiro, 1988. This method was developed for the dissection of ixodid tick species and involved the submergence of fed or unfed ticks in sterile phosphate buffered saline (PBS) (10 mM H_2PO_4, 5 mM KH_2PO_4, 140mM NaCl). An incision was made in the dorsal cuticle facilitating the protrusion of the midgut diverticulae which were removed with forceps. Modifications made involved the immobilization of argasid ticks in paraffin wax. An incision was inflicted around the cuticle along the dorso-ventral axis, the dorsal cuticle completely removed with forceps and the internal cavity washed with sterile PBS. Salivary glands were removed and washed in PBS. Following washing, all tissues were placed into 1 ml of TRI-Reagent and stored at -20°C for long term storage.

2.4.3 RNA isolation

Total RNA was isolated from mixed life stages of *R. (B.) microplus*, as well as salivary glands and gut of fed and unfed *O. savignyi* females using the manufacturer's protocol (TRI-Reagent, Sigma). RNA isolated from partially fed adult females was obtained from A. Nijhof, University of Utrecht. TRI-Reagent (proprietary composition) is an RNA isolation reagent supplied as a monophasic solution composed of phenol and guanidine thiocyanate which allow for denaturation of membrane components. Guanidine thiocyanate is an RNase inhibitor due to its inherent protein denaturation ability. Furthermore, guanidine thiocyanate is a chaotropic reagent facilitating the disruption of non-covalent interactions thereby additionally contributing to the lysis of cells during the homogenization of tissues in

TRI-Reagent. Dissected salivary glands and midgut of *O. savignyi* as well as eggs and mixed life stages and adults of *R. (B). microplus* submerged in TRI-Reagent were homogenized using a 1 ml syringe and needles of decreasing size in the range of 23 gauge to 30 gauge. Once homogenized, solutions were centrifuged at 12000 X g, tissue debris pelleted and supernatants collected.

Chloroform (200 μl) was added to supernatants, followed by vigorous mixing which allowed for extraction of excess phenols and development of an aqueous phase (in which nucleic acids are dissolved), an interface (constituted by proteins) and a lower organic phase (containing lipids). The upper aqueous phase was transferred into a new tube and 500 μl of isopropanol was added which facilitates the dehydration and subsequent precipitation of nucleic acids. The solution was incubated for 10 minutes at room temperature and subsequently centrifuged at 12000 X g for 15 minutes at 4°C. Washing of the pellets with 1 ml of 75% ethanol by means of centrifugation for 5 minutes allowed for removal of contaminating salts. Evaporation of residual alcohol was facilitated by drying the pellet on a vacuum concentrator (Bachoffer, Germany). Final pellets were reconstituted in 25 μl diethyl pyrocarbonate (DEPC) treated H$_2$O. Spectrophotometric measurements at 260 nm allowed for determination of concentration and a ratio of the absorbance at 260 and 280 nm of 1.8-2.0 was used as a measure of purity. Samples were thereafter stored at -70°C.

2.4.4 cDNA (complementary DNA) synthesis

cDNA synthesis using a polyT primer allows conversion of poly-A tailed mRNA to single stranded complementary DNA. cDNA was purified in order to remove excess enzyme and dNTPs (deoxyribonucleotide triphosphates) and converted to double stranded cDNA using long distance (LD) PCR where the amplification with the terminal anchor primers facilitated the production of full length double stranded (ds) cDNA. The protocol followed for successive steps is based upon a modification of the Super SMART PCR cDNA synthesis kit (BD Biosciences Clontech, Alameda, CA). Modifications involved the replacement of the PowerScript Reverse Transcriptase with Superscript III (Invitrogen, Carlsbad, CA) .

The principle of this cDNA synthesis method (Figure 2.4) involves binding of the unique poly T anchor primer to the poly A tail of mRNA. First strand cDNA synthesis is performed by the reverse transcriptase activity of SuperScript III which catalyzes addition of dNTPs onto the available poly T anchor primer. An inherent property of reverse transcriptase enzymes derived from Moloney Murine Leukemia Virus (in this case SuperScript III) is the addition of

3-5 cytosine residues to the 3'-end of newly generated first strand cDNA. The subsequent step involved the binding of a dG-tailed SMART II A oligonucleotide to this dC tailed first strand by conventional Watson-Crick base pairing. Template switching activity was then stimulated and the strand extended to incorporate the 5' anchor sequence. This double-anchor-bearing first strand cDNA may then be amplified using primers specific to unique anchor sequences, ultimately producing amplified ds cDNA.
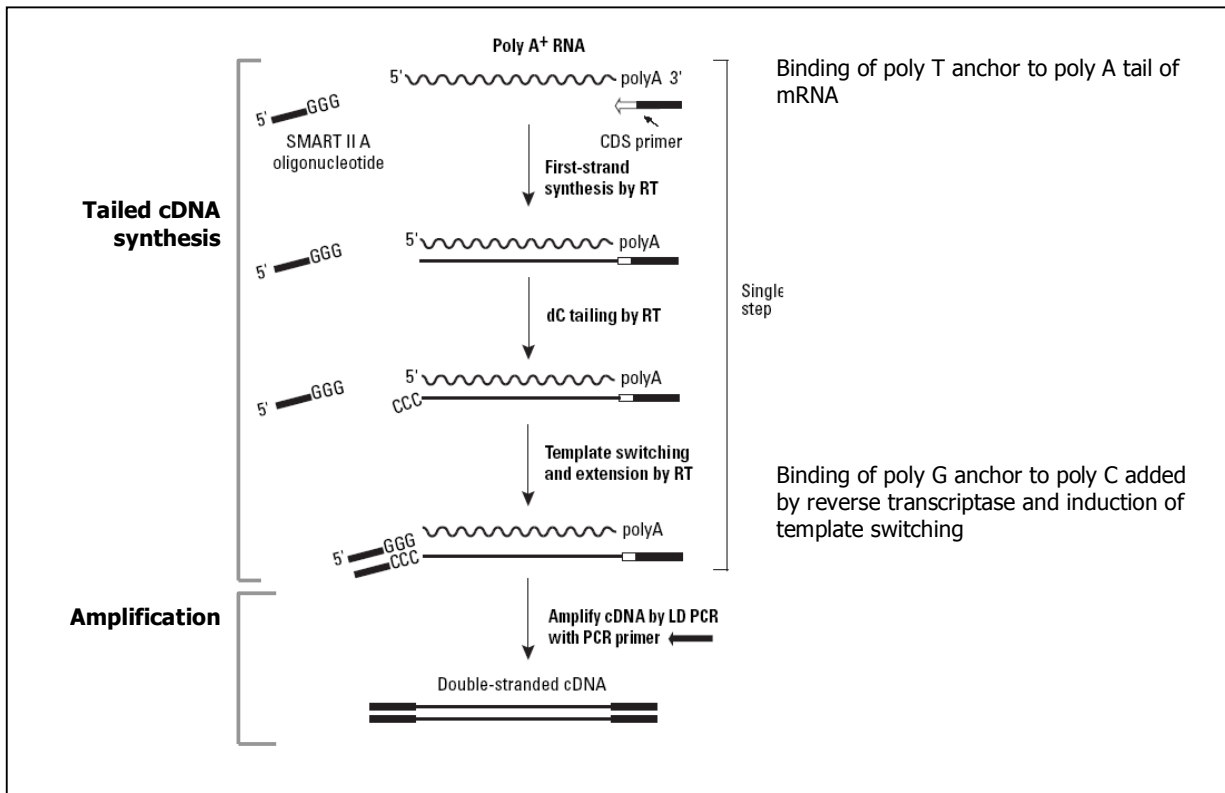
Figure 2.4: The principle of cDNA synthesis adapted from the Clontech Super SMART PCR cDNA Synthesis Kit User Manual, 2002.

As starting material, 500 ng of RNA isolated from salivary glands was used. To this 12 pmoles/μl (10mM stock) of poly T anchor primer (AAG CAG TGG TAT CAA CGC AG AGT AC(T)$_{30}$ VN) and 12 pmoles/μl (10 mM stock) of SMART IIA oligonucleotide (AAG CAG TGG TAT CAA CGC AGA GTA CTC GGG) was added. DEPC-H$_2$O was added to a final volume of 64 μl. The 64 μl reaction mixtures were centrifuged and incubated at 65°C for 2 minutes in a thermal cycler allowing for denaturation of secondary structures. Following incubation, samples were placed on ice immediately for 5 minutes to prevent reformation of RNA secondary structures. To each reaction tube, 20 μl 5X First strand buffer, 2 μl 100 mM dithiothreitol (DTT), 10 μl 50 X dNTPs (10 mM each) (Roche Diagnostics, USA), 100 U RNase inhibitor (Promega, USA), 500 U Superscript III reverse transcriptase (Invitrogen, USA) and

5 μl DEPC-H_2O were added. Samples were mixed by gentle pipetting and spun down in a microcentrifuge. This was followed by incubation at 42°C for 90 minutes in a Perkin Elmer Gene Amp PCR system 2400. Finally, 2 μl (0.5 M) EDTA (ethylene diamine tetra-acetate) was added to terminate the reaction. Samples were stored at -20°C.

2.4.5 Amplification of first strand cDNA

Single stranded cDNA was amplified as follows: 5 μl (50ng) of first strand cDNA sample was constituted with double distilled deionized water to a final volume of 80 μl. To this 4 μl of H_2O, 10 μl 10 X ExTaq buffer, 2 μl 50 x dNTPs (10 mM each), 12 μM 5' PCR IIA (AAG CAG TGG TAT CAA CGC AGA GTA CT) (with 5' anchor) primer, 12 μM poly T anchor (with 5' anchor) primer and 10 U ExTaq DNA polymerase (Takara, Japan) were added. The abovementioned anchor sequences are complementary allowing for suppression PCR. Reaction mixtures were mixed by gentle vortexing and subsequently spun down in a microcentrifuge. Samples were placed in a preheated thermal cycler and cycled as follows: initial 95°C incubation for 1 minute (denaturation), and 15 cycles (95°C for 15 seconds, 65°C for 30 seconds, and 72°C for 3 minutes). For optimization of cycle number, the procedure was followed is shown in Table 2.3.

Table 2.3: Procedure followed for the optimization of cycle number

Cycles	Volume	Action
15	70 μl	Stored at 4°C
	30 μl	Amplified for 3 additional cycles
18	5 μl	Stored at 4°C to run on gel
	25 μl	Amplified for 3 additional cycles
21	5 μl	Stored at 4°C to run on gel
	20 μl	Amplified for 3 additional cycles
24	5 μl	Stored at 4°C to run on gel
	15 μl	Amplified for 3 additional cycles
27	5 μl	Stored at 4°C to run on gel
	10 μl	Amplified for 3 additional cycles
30	5 μl	Stored at 4°C to run on gel
	5 μl	Stored at 4°C to run on gel

The 5 µl samples which were stored at 4°C were analysed on a 1.2% agarose-ethidium bromide (EtBr) gel and the optimum number of cycles was determined as the cycle number at which reactions were still in the linear amplification phase, minus one. Once the optimum cycle number was determined, the initial 70 µl sample that was stored at 4°C was amplified in the thermal cycler for the additional cycles required.

Purification of amplified DNA was facilitated by use of the Nucleospin Extract II PCR clean-up and Gel extraction kit (Macherey-Nagel, Duren, Germany). Addition of 300 µl of buffer NT (proprietory specifications) to each sample provided the chaotropic environment necessary for binding of cDNA to the silica membrane of columns provided. Samples were loaded onto columns and centrifuged at 11000 X g for 1minute. Wash buffer (500 µl) was used to wash columns 3 times via centrifugation at 11000 X g for 1 minute. Finally, columns were centrifuged for an additional minute in order to facilitate complete drying of the silica membrane. Elution was performed by addition of 50 µl buffer NE (5 mM Tris-HCl, pH 8.5) to membranes which were allowed to soak for 2 minutes with lids open and centrifuged at 11000 X g for 1 minute. Concentration of purified DNA was determined using the Gene Quant spectrophotometer. The remaining sample was stored in a low adhesion siliconized tube at -20°C.

2.4.6 Primer design

Primers were designed and validated using the Oligo Primer Analysis Software (Version 6.71).

To date, expressed sequence tags (ESTs) of four ixodid tick species (*R. (B.) microplus, A. variegatum, I. scapularis* and *R. appendiculatus*) are available online at the TIGR database at http://compbio.dfci.harvard.edu/tgi/tgipage.html. These databases allowed the use of Basic local alignment search tool (BLAST) to identify possible homologs in species available, using the microplusin sequence (GeneBank AY233212) as the query sequence. Protein BLAST was performed using EST translated sequences (ExPasy Translate Tool, http://ca.expasy.org/tools/dna.html). In each instance, the correct reading frame was selected and amino acid sequences were aligned against microplusin using Clustal W (http://www.ebi.ac.uk/clustalw/). This alignment (Figure. 2.5) was then analyzed for similarity and identity using GeneDoc (Version 2.6.003) allowing for identification of high similarity regions in tick species which were used to design a degenerate primer.

2.4.6.1 Degenerate primer design

The sequence of the mRNA transcript was deduced from the amino acid sequence and since more than one codon can code for a single amino acid (principle of degeneracy), the codon redundancy table was used in order to incorporate all possible codon combinations producing a degenerate primer. A degenerate primer (MP_forw_deg) was designed for the first 8 amino acids (excluding the starting methionine) on the N-terminal of the immature (bearing the signal sequence) microplusin sequence (Figure 2.5).

According to Fogaca *et al.*, (2004), a degenerate primer designed based on the first seven amino acids of the mature microplusin peptide was able to facilitate the identification of microplusin via PCR mediated screening. This primer named Primer 1, was used as an additional primer to facilitate the identification of microplusin in the ixodid tick, *R. (B.) microplus* (Figure 2.6).
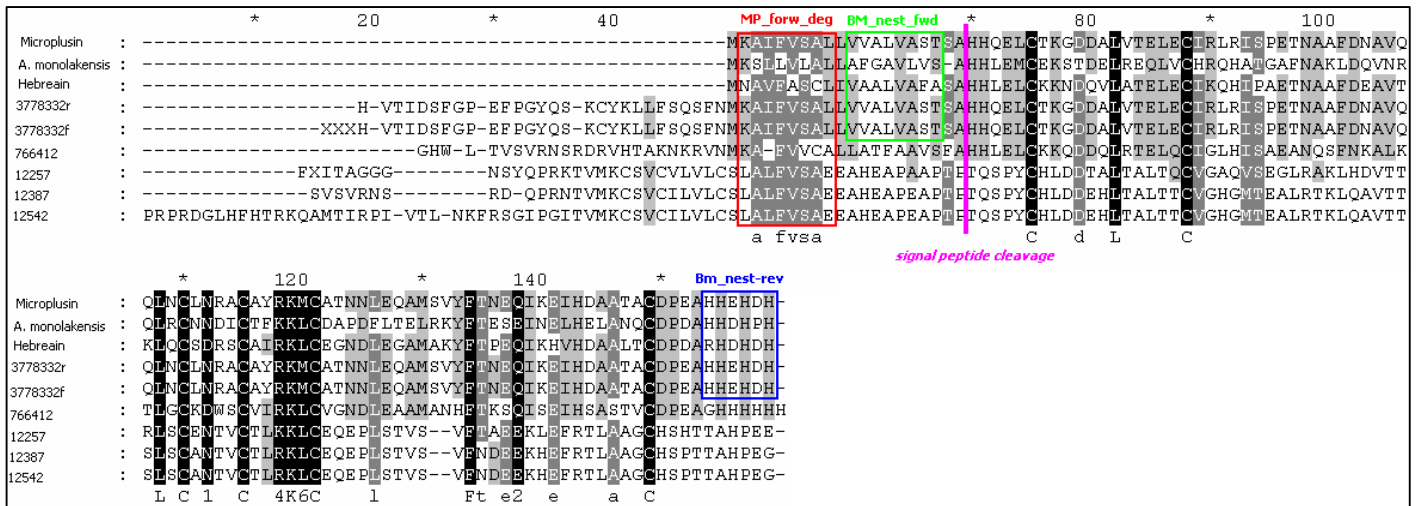
Figure 2.5: Alignment of amino acid sequences of possible microplusin homologs obtained from EST libraries available at the TIGR database: Microplusin represents the full length amino acid sequence, i.e., including the signal peptide. Cleavage of the signal peptide is indicated in pink while ESTs of high similarities are given by their respective numbers. Hebraein (from *A. hebreaum* and peptides similar to microplusin in *Argas monolakensis* are indicated. The region indicated in red was used for the design of the degenerate primer MP_forw_deg. The pair of gene specific nested primers is indicated in bright green (Bm_nest_fwd) and dark blue (Bm_nest-rev).

2.4.6.2 Gene specific primer design

As a positive control to be used on *R. (B.) microplus* tissue, a forward gene specific primer, Bm_nest_fwd, was designed from amino acids 11-18. Additionally, a reverse gene specific primer, Bm_nest_rev (amino acids 105-110 (6 amino acids) of the microplusin peptide, including signal peptide), was designed. These primers were used in a nested PCR.

A second pair of gene specific primers were designed based upon the sequence of the salivary gland microplusin-like antimicrobial peptide of the argasid tick, *A. monolakensis.* These primers included MonoF and MonoR.

An additional pair of gene specific primers was designed in an attempt to amplify out a full length microplusin transcript from *R. (B.) microplus.*. This primer pair consisted of MicroF as the forward primer and MicroR as the reverse primer (Figure 2.6).

The abovementioned primers are listed in Table 2.4.

Table 2.4: Primers designed for amplification of microplusin and possible homologs
* where H represents A, C or T, Y represents C or T, I represents inosine, W represents A or T, S represents G or C, B represents G,C or T, R represents A or G and N represents any nucleotide.

Primer name	Nature	Sequence (5' --> 3")	Melting temperature (°C)
MP_forw_deg	Degenerate	GCT **H**TT TT**Y** GTT **WSI** GC**I BW**	54.7
Bm_nest-fwd	Gene specific to *R. (B.) microplus*	GTG GTC GCC CTT GTG GC	53.9
Bm_nest_rev	Gene specific to *R. (B.) microplus*	TTA ATG GTC GTG CTC ATG GTG	54.7
Primer 1	Degenerate (Fogaca *et al*, 2004)	CA**Y** CA**Y** CA**R** GA**R** Y**T**N TG**Y** AC	52.3
MicroF	Gene specific to *R. (B.) microplus*	GCC TTC GCA TCA G	52.0
MicroR	Gene specific to *R. (B.) microplus*	TTA ATG GTC GTG CTC ATG GTG GGC	66.0
MonoF	Gene specific to *A. monolakensis*	ATG AAA TCC CTC CTG GTC CTC G	65.0
MonoR	Gene specific to *A. monolakensis*	AAT CAC CCC TAC TCT CAC CC	62.0
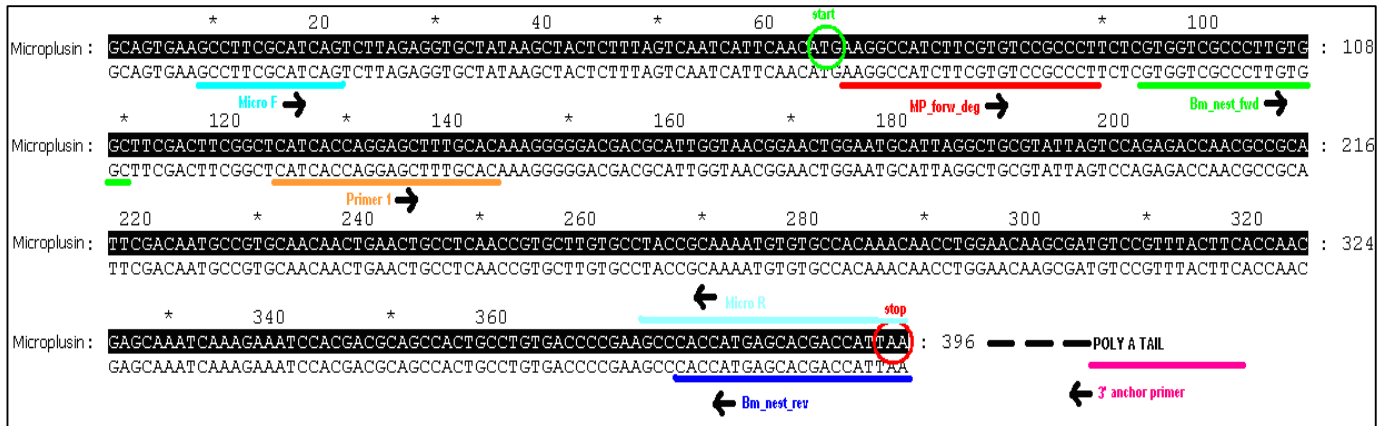
Figure 2.6: Nucleotide sequence of the microplusin transcript from _R. (B.) microplus_ showing regions used in primer design and annotation of primer directions: The start codon is encircled in green, while the stop codon is encircled in red. The forward degenerate primer, MP_forw_deg which when used in conjunction with the 3' anchor primer (indicated in pink) may yield the microplusin transcript from the first amino acid of the peptide. Bm_nest_fwd (indicated in green) and Bm_nest_rev (indicated in dark blue) are the gene specific primer pair designed for use in nested PCR. Primer 1 (indicated in orange) represents the primer of Fogaca _et al._, 2004 while the second pair of gene specific primers designed in an attempt to amplify the full length microplusin transcript, is indicated in bright blue.

2.4.7 3'-RACE

This method of PCR utilizes the 3' anchor primer and an internal primer in order to amplify the 3' terminal of a transcript. Since microplusin was first isolated in the hard tick _R.(B.) microplus_, cDNA synthesized from RNA isolated was used as the positive control. It was expected that a band of approximately 330 bp would represent the sequence of the microplusin preprotein. Similarly sized bands were expected in the species to be screened. In general, in PCR reactions performed the positive control was tick β-actin amplified using a β-actin forward (CAG ATC ATG TTT GAG ACC TTC AAC) and reverse (GSC CAT CTC YTG CTC GAA RTC) primer pair. Negative controls included reactions containing only either the forward or reverse primer. Polymerases used included ExTaq (Takara Bio Inc., Japan), rTaq (Takara Bio Inc., Japan) and GoTaq (Promega, USA). Reactions were performed on the MJC Research PTC 100 Programmable Thermal Cycler. Figure 2.7 below presents a schematic representation of the 3'-RACE attempts made.
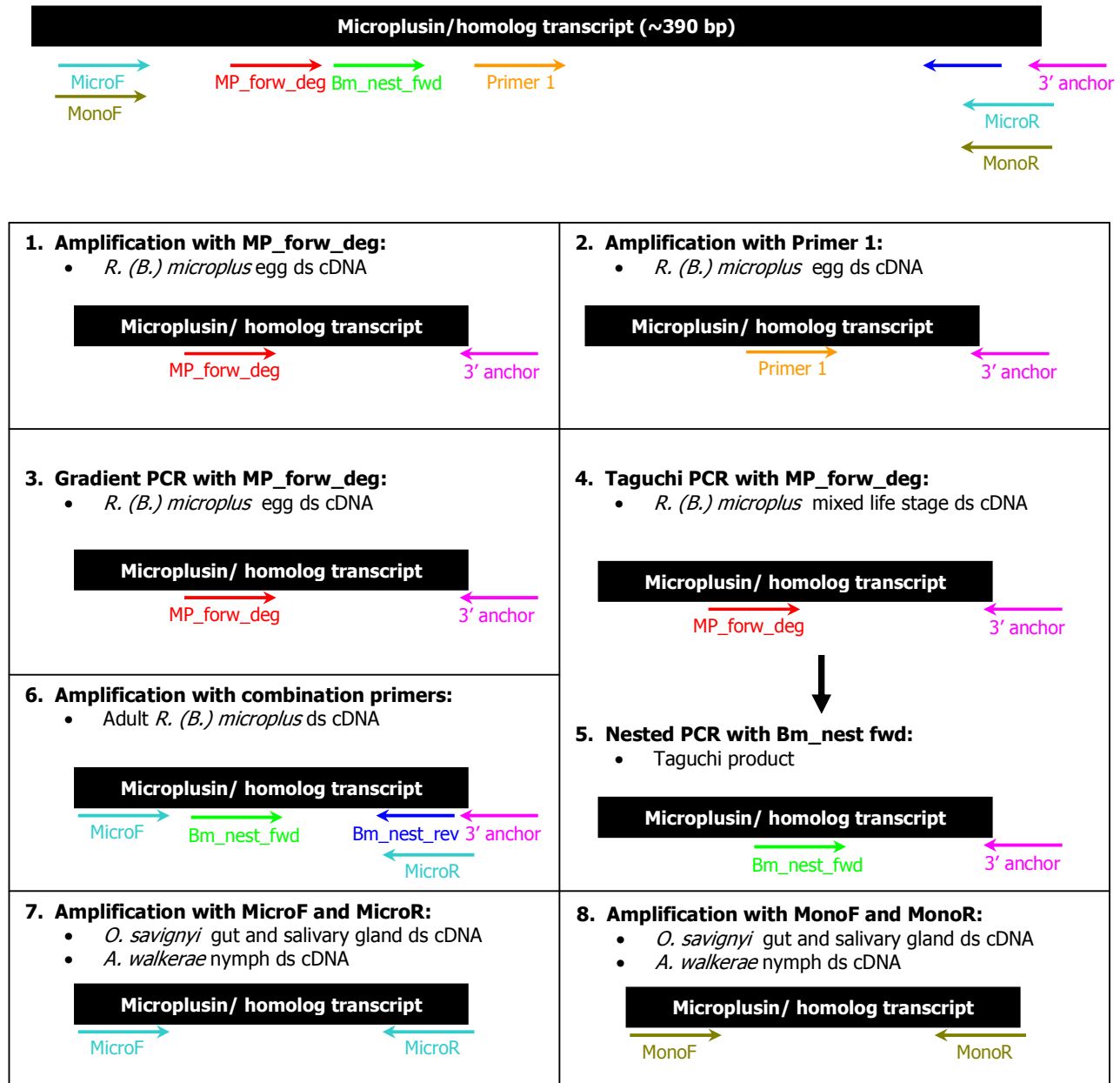
Figure 2.7: Schematic representation of 3'-RACE attempts: The estimated position and direction of the primer pairs used in addition to the species and tissue used as template are indicated

2.4.7.1 Amplification with MP_forw_deg primer

An initial attempt to amplify the microplusin transcript was made via 3' RACE using the MP-forw_deg primer and the 3' anchor primer. The reaction involved 1 μl (100-200 ng) amplified cDNA, from *R. (Boophilus) microplus,* to which 2 μl of rTaq buffer (Mg^{2+} free), 2 μl dNTPs (2.5 mM each), 1.5 μl MgCl$_2$ (25 mM), 50 pmoles MP_forw_deg and 10 pmoles of the 3' anchor primer (AAG CAG TGG TAT CAA CGC AGA GTA CTC) was added. The final reaction volume was constituted to 20 μl by addition of H$_2$O. Initial denaturation at 94°C was allowed for 7 minutes followed by incubation at 80°C for 30 seconds. At this point 1.25 U of rTaq diluted in rTaq 10 X buffer was added to each tube. The reaction was allowed to proceed for 30 cycles at 94°C for 30 seconds (denaturation), 50°C for 30 seconds (annealing) and 72°C for 2 minutes (extension). A final extension step at 72°C for 7 minutes was included.

2.4.7.2 Amplification with Primer 1

According to Fogaca *et al.* (2004)*,* a degenerate primer designed based on the first seven *N*-terminal amino acids of mature microplusin from *R. (B.) microplus,* was able to facilitate identification of microplusin via PCR mediated screening together with the 3' anchor primer. Initial denaturation at 94°C was allowed for 5 minutes followed by incubation at 80°C for 30 seconds. At this point 1.25 U of ExTaq diluted in ExTaq 10 X buffer was added to each tube. The reaction was allowed to proceed for 30 cycles at 94°C for 30 seconds (denaturation), 54°C for 30 seconds (annealing) and 72°C for 30 seconds (extension). A final extension step at 72°C for 7 minutes was included.

2.4.7.3 Gradient PCR

A gradient PCR was performed using 75 pmoles of the MP_forw_deg primer and 10 pmoles of the 3' anchor primer. Initial denaturation at 94°C was allowed for 7 minutes followed by incubation at 80°C for 30 seconds. At this point 1.25 U of rTaq in the corresponding buffer was added to each reaction tube. The reaction was allowed to proceed for 10 cycles at 94°C for 30 seconds, 50°C for 30 seconds and 72°C for 2 minutes. A second set of 28 cycles were allowed at 94°C for 30 seconds, 55°C for 30 seconds and 72°C for 2 minutes A final extension at 72°C was allowed to proceed for 7 minutes after which reactions were maintained at 4°C. The product of this reaction was analysed on a 2.0% agarose-ethidium bromide gel.

2.4.7.4 Taguchi PCR

Taguchi optimization is a systematic approach to evaluate numerous PCR parameters such as template concentration, primer concentration and $MgCl_2$ concentration (Cobb and Clarkson, 1994). The template used was *R. (B.)* microplus egg ds cDNA and the primer to be optimized was the degenerate primer MP_forw_deg while the 3' anchor primer was maintained at 10 pmoles. Parameters tested are shown in Table 2.5 while reaction combinations tested are shown in Table 2.6.

Table 2.5: Concentration of reaction components compared

Reaction set	Template (*R. (B.) microplus* suppression PCR amplified cDNA) (ng)	MP_forw_deg (pmoles)	$MgCl_2$ (mM)
A	100	50	1.5
B	150	100	2.0
C	200	200	2.5

Table 2.6: Reaction combinations investigated

Reaction	Template	MP_forw_deg	$MgCl_2$
1	A	A	B
2	A	B	C
3	A	C	A
4	B	A	C
5	B	B	A
6	B	C	B
7	C	A	A
8	C	B	B
9	C	C	C

Reactions were setup in combinations shown above and subjected to 35 cycles: 94^oC for 3 min, 80^oC for 30 seconds, 94^oC for 30 seconds, 50^oC for 30 seconds, 72^oC for 2 min and a single final extension step of 72^oC for 7 min and thereafter stored at 4^oC.

2.4.7.5 Nested PCR

Nested PCR is based on the use of internal gene specific primers on a template derived from a previous PCR reaction. In this case the use of the gene specific primers on the product produced by the reaction primed by MP_forw_deg, was expected to generate a more specific product representative of microplusin. The reaction was set up using 1 μl of template (the product of the Taguchi PCR combination 9) to which 2 μl of the 10 X ExTaq buffer (Mg^{2+} included), 2 μl of dNTPs (2.5 mM each), 10 pmoles of the gene specific forward primer (Bm_nest_fwd) and 10 pmoles of the gene specific reverse primers (Bm_nest_rev) were added. The final reaction volume was constituted to 20 μl by means of addition of H$_2$O. Initial denaturation at 94°C was allowed for 7 minutes followed by incubation at 80°C for 30 seconds. At this point 1.25 U of ExTaq in the corresponding buffer was added to each reaction tube. The reaction was allowed to proceed for 35 cycles at 94°C for 30 seconds, 50°C for 30 seconds and 72°C for 2 minutes. A final extension at 72°C was allowed to proceed for 7 minutes after which reactions were maintained at 4°C. The product of this reaction was analysed on a 2.0% agarose-ethidium bromide (EtBr) gel.

2.4.7.6 PCR using combinations of the gene specific, degenerate and anchor primers

A PCR protocol was set up in all possible combinations of abovementioned primer pairs and on cDNA synthesized from *R. (B.) microplus* mixed life stages and adults and *O. savignyi* gut and salivary gland cDNA (as described previously in section 2.4.4 - 2.4.5). The reaction utilized 1 μl of cDNA as template to which 2 μl of 10 X ExTaq buffer (25 mM Mg^{2+} included), 2 μl of dNTPs (2.5 mM each), 10 pmoles of the gene specific forward primer (Bm_nest_fwd) or 50 pmoles of the degenerate primer (MP_forw_deg) and 10 pmoles of the gene specific reverse primer (Bm_nest_rev) or the 3' anchor primer was added. The final reaction volume was constituted to 20 μl by means of addition of H$_2$O. Initial denaturation at 94°C was allowed for 7 minutes followed by incubation at 80°C for 30 seconds. At this point 1.25 U of ExTaq in the corresponding buffer was added to each reaction tube. The reaction was allowed to proceed for 35 cycles at 94°C for 30 seconds, 54°C for 30 seconds and 72°C for 2 minutes. A final extension at 72°C was allowed to proceed for 7 minutes following which reactions were maintained at 4°C. The product of this reaction was analysed on a 2.0% agarose-ethidium bromide (EtBr) gel.

Two pairs of gene specific primers, MicroF and MicroR as well as MonoF and MonoR, were used in a reaction involving the use of 1 μl of template *(R. (B.) microplus* adult total cDNA and *O. savignyi gut* and salivary gland cDNA where the cDNA synthesis protocol was modified. Modifications involved the replacement of the specified 3' anchor primer with a modified poly T anchor primer (GCT ATC ATT ACC ACA ACA CTC (T)$_{18}$ VN, with a melting temperature of 58.3^{o}C). Synthesis of cDNA followed the method presented in section 2.4.4 - 2.4.5. Double stranded cDNA was used as template for subsequent PCR reactions, to which 2 μl of the 10 X ExTaq buffer (Mg^{2+} included), 2 μl of dNTPs (2.5mM each), 10 pmoles of gene specific forward primer (MicroF or MonoF) and 10 pmoles of gene specific reverse primer (MicroR or MonoR) were added. The final reaction volume was constituted to 20 μl by means of addition of water. Initial denaturation at 94°C was allowed for 7 minutes followed by incubation at 80°C for 30 seconds. At this point 1.25 U of ExTaq in the corresponding buffer was added to each reaction tube. The reaction was allowed to proceed for 35 cycles at 94°C for 30 seconds, 50°C for 30 seconds and 72°C for 2 minutes. A final extension at 72°C was allowed to proceed for 7 minutes following which reactions were maintained at 4°C. The product of this reaction was analysed on a 2.0% agarose-ethidium bromide (EtBr) gel.

Additionally, the PCR using the MicroF/MicroR primer pair was repeated by A. Nijhof (University of Utrecht) on individual tissues of adult female *R. (B.) microplus* ticks. These tissues included eggs, larvae and nymphs as well as unfed and fed midgut, ovaries and fat body of adult females.

2.4.8 Precipitation of PCR products using NaOAc/EtOH precipitation

PCR products were precipitated by addition of a tenth of the volume of 3M NaOAc (pH 5) to the PCR product in addition to 3 volumes of 100% EtOH. The solution was mixed, briefly centrifuged and incubated at -70°C overnight. Samples were subsequently centrifuged at 16000 X g for 45 minutes at 4°C. Supernatants were discarded and the pellets washed with 70% EtOH and again centrifuged at 16000 X g for 15 minutes at 4°C. After discarding the final supernatants, the products were dried *in vacuo* and redissolved in 10 μl water. Concentrations were determined using the Gene Quant and remaining template DNA stored at -20°C.

2.4.9 Ligation of precipitated PCR products into pGEM T Easy

Amplification with a Taq DNA polymerase allows for incorporation of a single adenine residue on the 3' end of the amplified strand. For this reason, opposite ends of the PCR product may be described as A-tailed. The pGEM T Easy Vector system (Promega, USA) possesses a single T overhang at the site of insert ligation. Hydrogen bonding between vector and insert allows for ligation of the insert into the vector via A-T cloning. T4 DNA ligase then seals the nick that was present and the final product is the pGEM T Easy vector with insert ligated. The reaction that was performed in order to ligate fragments of interest into the pGEM T Easy Vector system is shown in Table 2.7.

Table 2.7: Procedure followed for ligation of purified 350 bp band into the pGEM T Easy Vector system

Reagent	Volume
2 X T4 DNA ligase buffer	5 μl
pGEM T Easy Vector (50 ng/μl)	1 μl
PCR product	**x μl**
T4 DNA ligase (3 U/μl)	1 μl
Water	to a final volume of 10μl

where x refers to ng of insert required, calculated as follows;

$$\frac{\text{ng of vector} \times \text{kb size of insert}}{\text{kb size of vector}} \times \text{insert:vector molar ratio} = \textbf{ng of insert}$$

These reactions were incubated at 4°C overnight and ligation reactions were precipitated by addition of 2 μl transfer RNA (tRNA) (10 mg/ml), 2 μl sodium acetate (pH 5.0) and 30 μl 100% ethanol to ligation reactions. tRNA was added as a modification to the standard protocol in order to increase transformation efficiency during electroporation. Solutions were centrifuged for 45 minutes at 16000 X g at 4°C. Once supernatant was removed, samples were dried *in vacuo* (Bachoffer, Germany) and redissolved in 20 μl PCR water.

2.4.10 Preparation of electrocompetent cells

Glycerol cell stocks of *E. coli* DH5α (F⁻ endA1 glnV44 thi-1 recA1 relA1 gyrA96 deoR hupG Φ80d/acZΔM15 (lacZYA-argF) U169, hsdR17 (r_k^- m_k^+) λ−) was inoculated into 2 X 15 ml Luria Bertani (LB) broth (0.01% (w/v) tryptone, 0.01% (w/v) sodium chloride and 0.005% (w/v) yeast extract) and incubated at 37°C overnight with shaking at 250 rpm. Two of these 15 ml overnight cultures were inoculated into 2 x 500 ml pre-warmed (37°C) LB broth and grown until an OD_{600nm} of between 0.5 and 0.6 was reached. Cultures were poured into pre-chilled centrifuge bottles and cooled on ice for 20 minutes. All subsequent steps were performed on ice. Cells were pelleted by centrifugation at 2000 X g for 15 minutes at 4°C. Supernatant was removed and the cell pellet resuspended in 10 ml ice cold H_2O by swirling before addition of 240 ml of ice cold water. Cells were washed by centrifugation at 2000 X g for 15 minutes at 4°C. Again, supernatant was removed and the wash step repeated. Washed cells were resuspended in 10 ml of 10% glycerol and pooled into two sterile 50 ml tubes. These were then incubated for 60 minutes on ice, cells pelleted by centrifugation at 2000 X g for 15 minutes at 4°C, and supernatants removed. Final pellets were resuspended in 0.5 ml of 10% glycerol. Pellets were pooled producing a final volume of 1 ml. Cells were aliquoted (90 μl per tube) and stored immediately at -70°C.

2.4.11 Transformation by electroporation

In order to facilitate selection and amplification of recombinant plasmids, precipitated and redissolved ligation product was electroporated into electrocompetent *E. coli* DH5α cells. Cuvettes (0.1cm; Bio-Rad) were placed at -20°C, 1 hour prior to use. DH5α cells were allowed to thaw on ice before 20 μl of the ligation reaction was added and mixed by gentle swirling. This solution was then pipetted into the cuvette and inserted into the Electroporator 2510 (Eppendorf Germany) and pulsed at 2000 V for 3-5 milli seconds. Electroporated cells were added to 100 μl LB broth and incubated at 37°C for 45 minutes with shaking at 200 rpm. Cells (10 μl) were plated onto LB-ampicillin plates (1% (w/v) agar in LB broth, 1 : 500 (50 mg/ml) ampicillin) and incubated upside down at 37°C for 12 hours. Remaining cells were stored at 4°C.

2.4.12 Colony PCR

In order to identify clones carrying recombinant plasmids, colony PCR was performed using the SP6 (CATACGATTTAGGTGACACTATAG) and T7 (TAATACGACTCACTATAGGG) primers which are specific to respective regions bordering the multiple cloning site (MCS) of the pGEM T Easy Vector.

PCR grade H_2O (10.5 μl) was added to PCR tubes and random colonies were picked with a pipette tip and pipetted into PCR tubes containing PCR grade water and subsequently placed into 5 ml LB-ampicillin (LB broth containing 1000 times dilution of 50mg/ml ampicillin) to allow colony growth. To each PCR tube, 12.5 μl Kapa Ready Mix, 5 pmoles of T7 primer and 5 pmoles of SP6 primer was added. Initial denaturation at 94°C was allowed for 7 minutes. The reaction was then allowed to proceed for 30 cycles at 94°C for 30 seconds, 50°C for 20 seconds and 72°C for 2 minutes. A final extension at 72°C was allowed to proceed for 7 minutes after which the reactions were maintained at 4°C. Positive colonies were identified by agarose-EtBr electrophoresis and regrown overnight at 37°C with shaking at 200 rpm.

2.4.13 Plasmid isolation

Plasmid isolation was performed using the Nucleospin Plasmid Isolation kit (Macherey-Nagel, Duren, Germany). Once overnight cultures reached an OD_{600nm} of approximately 2, 2.5 ml of each culture was centrifuged for 10 minutes at 5000 X g to collect cells. Supernatants were then aspirated and 250 μl of resuspension buffer (buffer A1 containing RNase enzymes) was used to resuspend the cell pellet by vortexing. Buffer A2 (250 μl) was added and mixed by gentle inversion of the tubes 6 times. This solution was incubated at room temperature for 5 minutes. Buffer A2 (proprietary composition) contains sodium dodecyl sulfate (SDS) which leads to lysis of bacterial membranes and liberation of nucleic acids. Furthermore, this buffer is alkaline in pH facilitating denaturation of all DNA within the sample. Buffer A3 (300 μl) was added and solutions mixed by gentle inversion of the tubes 6 times. Solutions were then centrifuged at 16000 X g for 10 minutes at room temperature to remove the insoluble SDS precipitate, genomic DNA and dissociated protein complexes. The supernatant was loaded onto columns and centrifuged at 16000 X g for 1 minute after which 600 μl of buffer A4 was added and centrifuged at 16000 X g for 1 minute. This step facilitated washing of the silica membrane with ethanolic buffer. An additional centrifugation step of 16000 X g for 1 minute allowed removal of excess ethanol and drying of the silica membrane. Due to the fact that the isolated plasmid was to be used in downstream sequencing reactions, the final product was eluted by centrifugation for 1 minute at 16000 X g after a 1 minute incubation period with 50 μl PCR

water applied to the membrane. The 5 mM Tris-Cl (pH8.5) supplied by the kit was not used as salts would decrease the efficiency of downstream sequencing reactions. The concentration of a 10 times dilution of   purified plasmid was determined using the Gene Quant spectrophotometer.

2.4.14 Sequencing of recombinant plasmids

Directional sequencing was performed with either the T7 or SP6 primers. To 500 ng of plasmid DNA, 3 μl of sequencing buffer, 1 μl (5 μM) of either the SP6 or T7 primer was added and constituted to a final volume of 18 μl with H$_2$O. Reaction mixtures were spun down briefly in a microcentrifuge and incubated at 94°C for 2 minutes to allow denaturation of plasmid DNA. ABI Big Dye solution (2 μl) was added in a hot start addition at 80°C after 1 minute. Reactions were cycled: 96°C for 20 seconds, 50°C for 30 seconds and 60°C for 3 minutes for a total of 26 cycles. Sequencing reactions were precipitated by addition of 10 μl of sodium acetate (pH 5.0) and 60 μl of 100% ethanol followed by centrifugation for 40 minutes at 4°C to allow precipitation of the sequencing product. The supernatant was gently aspirated and pellet washed with 250 μl of freshly prepared 70% ethanol and centrifuged for 5 minutes following which the supernatant was gently aspirated.   This wash step was repeated.   The final precipitated product was dried *in vacuo* and sent to the sequencing facility (University of Pretoria) where automated nucleotide sequencing was performed.

2.4.15 Analysis of sequences

Sequences and chromatograms obtained were corrected for clarity of ambiguous nucleotides with the use of the BioEdit Sequence Alignment Editor (Version 7.0.5.3) (Hall, 1999). Corrected chromatograms were analysed for removal of plasmid sequence and for identification of the forward and reverse primers. Remaining insert-specific sequences were translated using the ExPasy translate tool (http://ca.expasy.org/tools/dna.html) and compared to that of the known microplusin sequence by means of the Clustal X program (Gibson *et al.,* 1994). Alignments were visualized and analyzed for similarity and identity using GeneDoc (Version 2.6.003).

2.5 Results and discussion

2.5.1 Optimization of cycle number during ds cDNA synthesis

In order to provide a template for PCR mediated screening of the species, isolated RNA was converted to cDNA. The method of choice for cDNA synthesis involved the use of suppression PCR (complementary 5' and 3' anchor sequences which form panhandle structures at high concentrations of PCR product) which would ensure equalization of transcript levels within the sample. This would prevent the masking of low abundance transcripts by the presence of high abundance transcripts. Additionally, amplification of cDNA would increase quantities of template available due to limited ticks and hence RNA samples. cDNA synthesis involved initial conversion of the RNA to first strand cDNA which upon purification was used as template for long distance amplification (LD) PCR reaction producing ds cDNA. Concentration was determined, following purification, to be 55 ng/ul for *R.(B.) microplus*. First strand cDNA was then amplified by LD PCR using the universal primer and aliquots were taken at different cycle numbers in order to determine the optimal cycle number. These aliquots were analysed on a 1.2% agarose-EtBr gel (Figure 2.8).
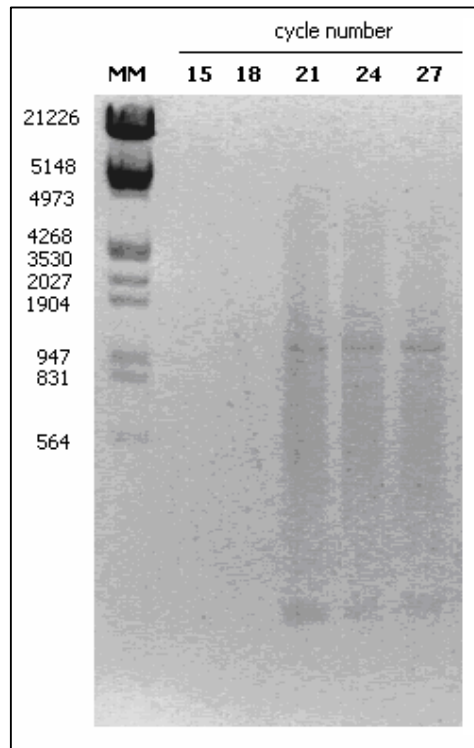
Figure 2.8: Agarose-EtBr (1.2%) gel analysis of aliquots taken during the optimization of cycle number during ds cDNA synthesis: MM represents λ–phage DNA (EcoRI + HindIII digested) marker; Lane 2 -6 represents 15 -27 cycles in increments of 3.

Since the product at 21 and 24 cycles remained constant, this means that this product represents the plateau phase of amplification. For this reason the optimal number of cycles for *R.(B.) microplus* was determined to be 20 cycles (optimal number of cycles minus one).

2.5.2 3' RACE

This method of PCR utilized the 3' anchor primer and an internal primer in order to amplify the 3' terminal of the transcript. In general, in the PCR reactions performed the positive control was tick β-actin amplified using a β-actin forward and reverse primer pair. Negative controls included reactions containing only either forward or reverse primer.

2.5.2.1 Amplification with MP_forw_deg

R. (B.) microplus egg amplified ds cDNA was screened with the degenerate primer MP_forw_deg and the 3' anchor primer. In this initial reaction 100 ng and 200 ng of template was compared. Products of this reaction are shown in Figure 2.9.
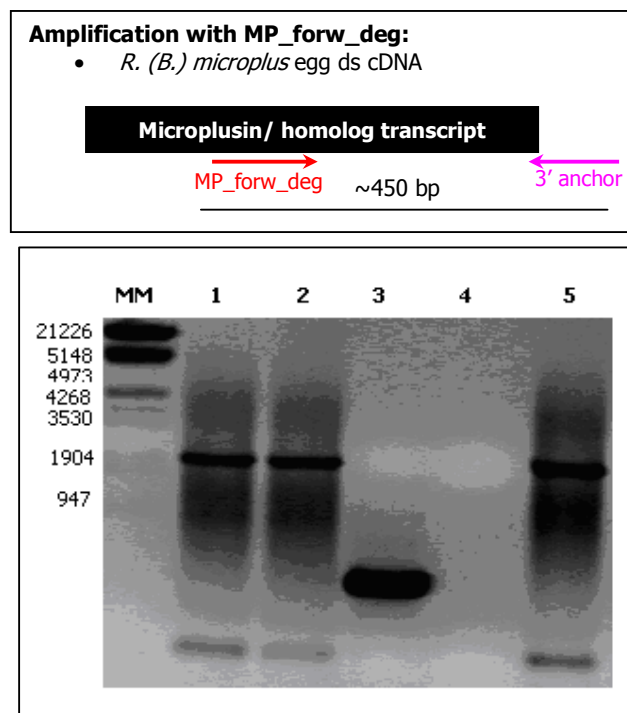
Figure 2.9: Agarose-EtBr (1.5%) gel analysis of 3'-RACE product of screening of *R. (B.) microplus* egg ds cDNA with the degenerate primer: MM represents λ-phage DNA (EcoRI + HindIII digested) marker; Lane 1: 100 ng template; Lane 2: 200 ng template; Lane 3: positive control (actin); Lane 4: negative control (MP_forw_deg) and Lane 5: negative control (5' PCR IIA only).

The presence of the same bands (~1900bp) in the experimental sample and the negative control (lane 6) should be noted. This represents non-specific binding and amplification by the

3′ anchor primer and raises the implication that the bands visible in the experimental samples (lanes 2 and 3) are simply non-specific products amplified by the reverse primer. Smears below 2000 bp are present indicating severe non-specific binding by the primer pair and overamplification is also evident (> 2000 bp). Lane 4 represents the β-actin DNA positive control. The single band of the expected size indicates that PCR components were successful in facilitating amplification. Sequence analysis of the abovementioned bands confirmed no significant similarity or identity to microplusin (data not shown).

2.5.2.2 Gradient PCR

Since the abovementioned 3′-RACE reaction was unsuccessful in producing the desired product, it was reasoned that increasing specificity of binding of the 3′ anchor primer would be an alternate solution to the problem of non-specific binding and amplification by this primer. This was done through the use of step (gradient) PCR. Attempts at optimization of this reaction involved increasing the concentration of the degenerate primer to 75 μM and decreasing the reverse (3′ anchor) primer concentration to 5 μM. Additionally, an attempt was made to optimize the cycle number. Furthermore the annealing temperature and time was decreased to increase specificity of binding of the primers. Figure 2.10 shows the results of the gradient PCR.

Gradient PCR with MP_forw_deg:
- *R. (B.) microplus* egg ds cDNA

Microplusin/ homolog transcript

MP_forw_deg   ~450 bp   3' anchor
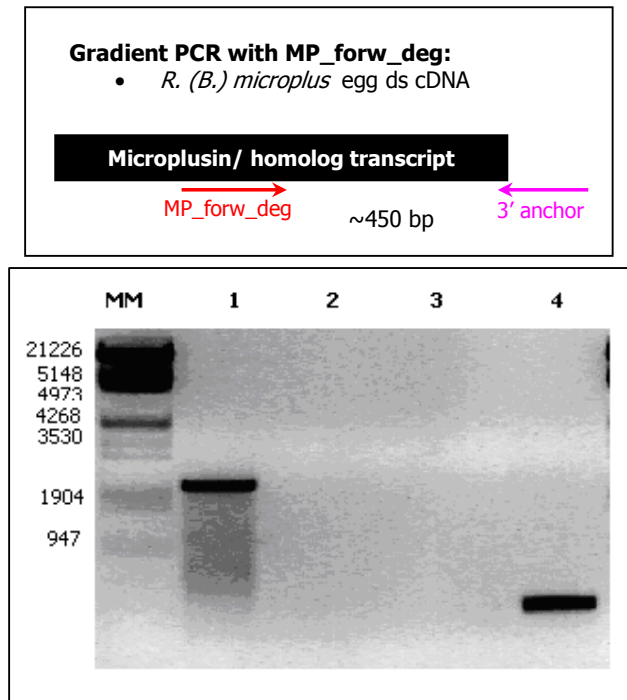
Figure 2.10: **Agarose-EtBr (1.5%) gel analysis of products of the step (gradient) PCR on** **_R.(B.) microplus_:** MM represents λ-phage DNA (EcoRI + HindIII digested) marker; Lane 1: MP_forw_deg + 5' PCR IIA; Lane 2: negative control (MP_forw_deg); Lane 3: negative control (3' anchor primer); Lane 4: positive control (actin) DNA.

As can be seen from lane 1 (Figure 2.10) a single band (~1900 bp) was produced by gradient PCR. The downward smear visible indicates that non-specific binding did indeed still occur to a certain extent, however, negative controls for the forward (lane 2) and reverse (lane 3) primers showed no bands indicating that non-specific binding by the primers was eliminated by the decrease in cycling at the reverse primers annealing temperature. Lane 4 represents the actin-positive control which in this case reinforces the fact that the reaction was efficient in facilitating amplification. Sequence analysis of the abovementioned bands revealed no significant similarity or identity to microplusin (data is not shown due to the fact that the alignments were insignificant). BLAST searches of the sequences obtained showed no significant homology to any known tick related peptides.

2.5.2.3 Amplification with Primer 1

Fogaca *et al.* (2004) designed a degenerate primer (Primer 1) based on the first seven amino acids of the mature microplusin peptide from *R. (B.) microplus*. In this study, this primer used in conjunction with the 3' anchor primer, was unsuccessful in producing any visible product from egg ds cDNA.
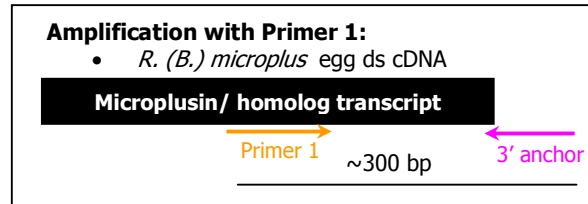
2.5.2.4 Taguchi PCR

The Taguchi method was used in an attempt to optimize conditions for the possible amplification of microplusin from *R.(B.) microplus* mixed life stage ds cDNa. This method combined all possible primer (MP_forw_deg), template and $MgCl_2$ concentrations.
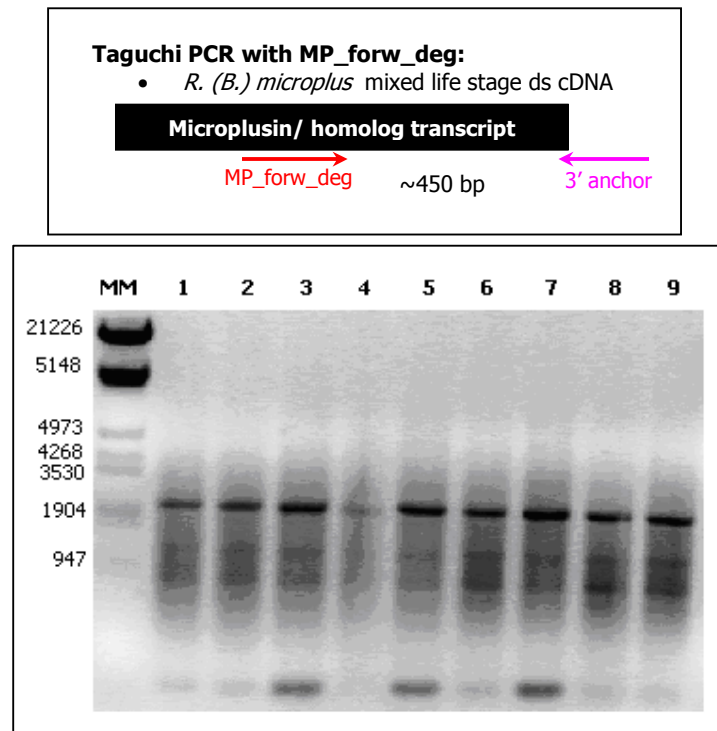
Figure 2.11: Agarose-EtBr (1%) gel analysis of Taguchi PCR products: MM represents λ-phage DNA (EcoRI + HindIII digested) marker; Lanes 1 to 9 represent reaction sets 1 to 9 respectively.

From Figure 2.11 it should be noted that combinations used during the Taguchi PCR were unable to produce significant differences between reactions in terms of specificity of bands

produced as would be expected by the use of Taguchi PCR. The 1900 bp band remained to be present and from previous reactions (Figure 2.10) this band was seen to arise as a result of non-specific binding and amplification of the 3' anchor primer. Downward smears too remained visible together with significant concentrations of primer dimers. Additionally, non-specific binding and amplification by the primer was seen as visible smears. Reaction 8 in lane 9 was chosen as the reaction conditions to be continued with (2 μl of template, 50 mM MP_forw_deg and 1.5 mM MgCl$_2$) due to the fact that this reaction showed the lowest dimers and highest concentration of product. It should be noted at this point that the increase in MgCl$_2$ concentration from 1 mM to 2.5 mM was successful in the elimination of primer dimers. The estimated maximum size of the microplusin transcript (including UTRs) is 450 bp. No work was continued on the 947 bp bands observed in Figure 2.11, as these products are significantly larger than the expected amplicon size. Furthermore, these bands were not reproducible upon repeated experiments.

2.5.2.5 Nested PCR with GSPs

Since the Taguchi PCR was performed using the degenerate forward primer, it was reasoned that the product could serve as template to be used with GSPs in an attempt to amplify a band of ~500bp.
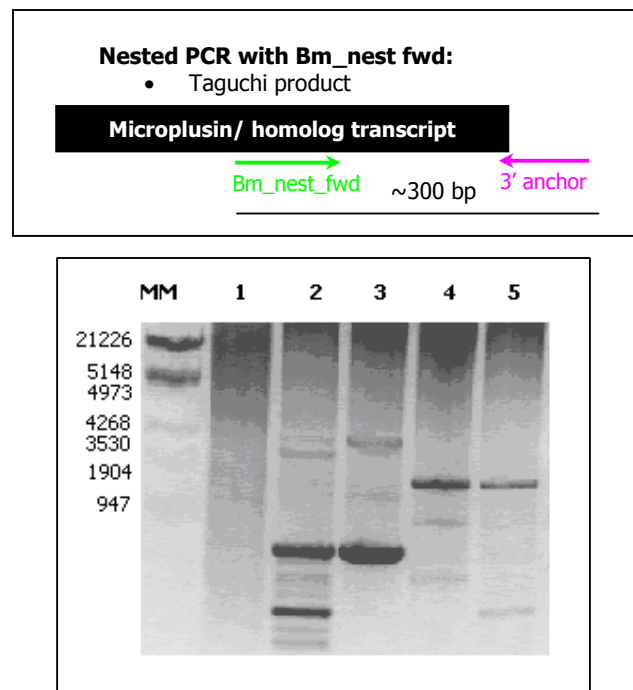
Figure 2.12: Agarose-EtBr (1.5%) gel analysis of products of the nested PCR on product from Taguchi reaction 8 (see table 2.6)**:** MM represents λ–phage DNA (EcoRI + HindIII digested) marker; Lane 1: taguchi 9; Lane 2: taguchi 9 and nested primers; Lane 3: negative control (Bm_nest_fwd); Lane 4: negative control (Bm_nest_rev); Lane 5: positive control (actin) DNA.

Lane 1 (Figure 2.12) represents the repeat of reaction 9 of the Taguchi PCR. The 2000 bp and 900 bp bands observed were due to non-specific binding and amplification by the reverse and forward primers, respectively. The unique ~500 bp band was unfortunately no longer obtained in repeated experiments.

2.5.2.6 PCR using combinations of the primers

Due to the inability of the Taguchi PCR to be repeated, it was reasoned that since the nested primers, Bm_nest_fwd and Bm_nest_rev, which are microplusin-gene specific, are to be used in a screening reaction with *R. (B.) microplus* whole adult cDNA as template, the product should theoretically be microplusin. For this reason, the following reactions included screening new template with combinations of gene-specific primer pairs. Optimal reaction conditions were found to be favoured by the inclusion of the Bm_nest_fwd and 3' anchor primer as forward and reverse primers, respectively. Figure 2.13 shows the reaction performed on *R. (B.) microplus* adult first strand cDNA. Egg and mixed life stages (used as an additional tissue source due to negative results obtained with other mentioned tissue) did not yield the correct product and so were excluded from this point on.
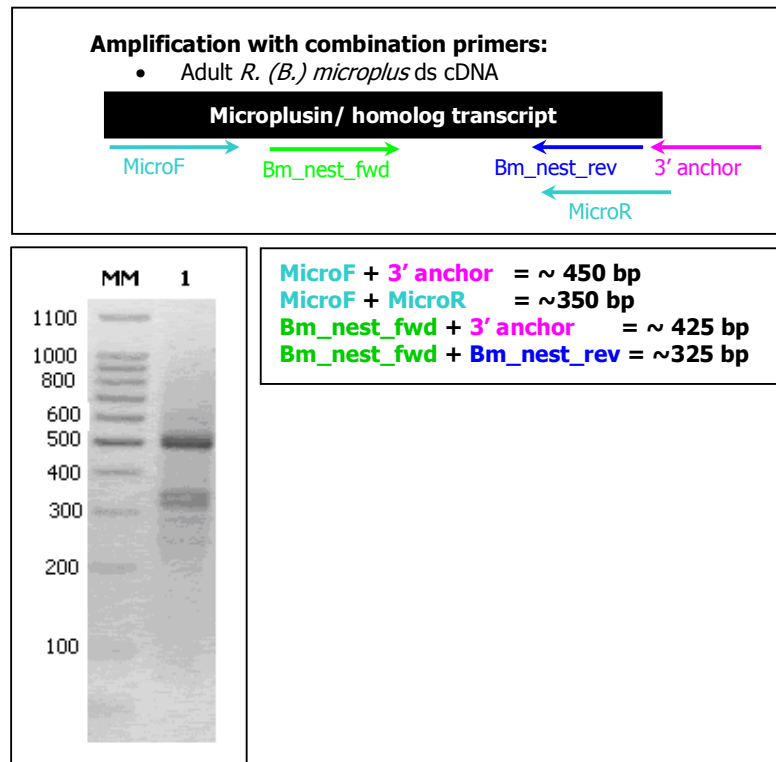
Figure 2.13: Agarose-EtBr (2.0%) gel analysis of products of the gene specific primer PCR using *R. (B.) microplus* adult ds cDNA as template: MM represents 100bp DNA ladder, lane 1: first strand screen using Bm_nest_fwd and Bm_nest_rev.

Figure 2.13 shows that 3 bands (two bands at 350 bp and one band at 500 bp) were produced in addition to a significant smear. The 350 bp and 500 bp bands were cut out of the agarose-EtBr gel, purified and used as template. Dilutions of this template indicated that the optimal dilution for reamplification of the 350bp and 500bp bands was 1 : 10 000 which allowed for the removal of primer dimers and low abundance non-specific products from the template. Figures 2.14 shows the results of this reamplification reaction.
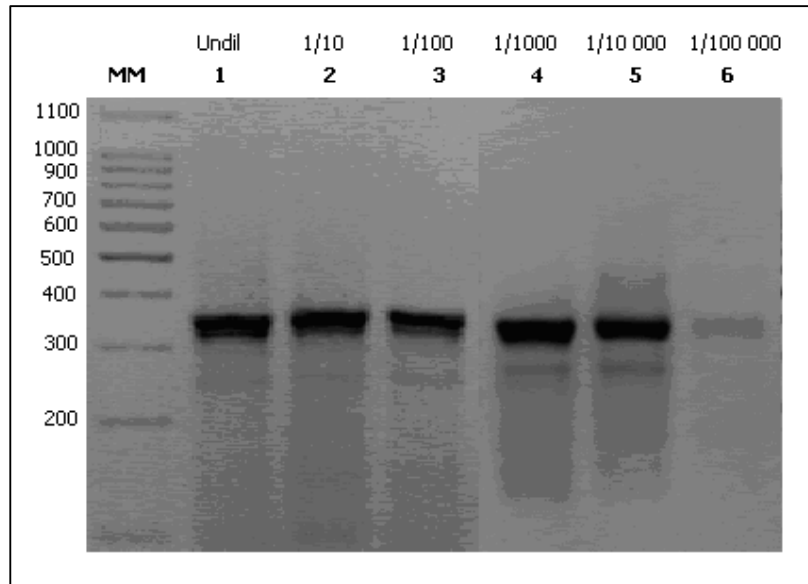
Figure 2.14: Agarose-EtBr (2.0%) gel analysis of products of 350bp band reamplification PCR: MM represents 100bp DNA ladder, lane 1: undiluted template, lane 2: 1 in 10 dilution, lane 3: 1 in 100 dilution, lane 4: 1 in 1000 dilution, lane 5: 1 in 10 000 dilution and lane 6: 1 in 100 000 dilution.

Following purification of the large scale 350 bp band (Figure 2.14), the product was ligated into the pGEM T Easy Vector system (Promega, Madison, WI, USA) and subsequent ligation products precipitated and electroporated into electrocompetent *E. coli* DH5α cells.

2.5.3 Colony PCR

In order to identify clones carrying recombinant plasmids, a colony PCR was performed using SP6 and T7 primers specific to the pGEM vector. A total of 45 colonies were picked and a total of 8 positive clones bearing the 350 bp band were identified. Five of the eight clones were used for plasmid isolation and sequencing reactions.

2.5.4 Sequencing of recombinant plasmids

A sequencing reaction was setup using in one instance the SP6 primer and in the second instance the T7 primer. Sequence information for clones 8 and 12 sequenced with the SP6 primer is shown in Figure 2.15 and 2.16.
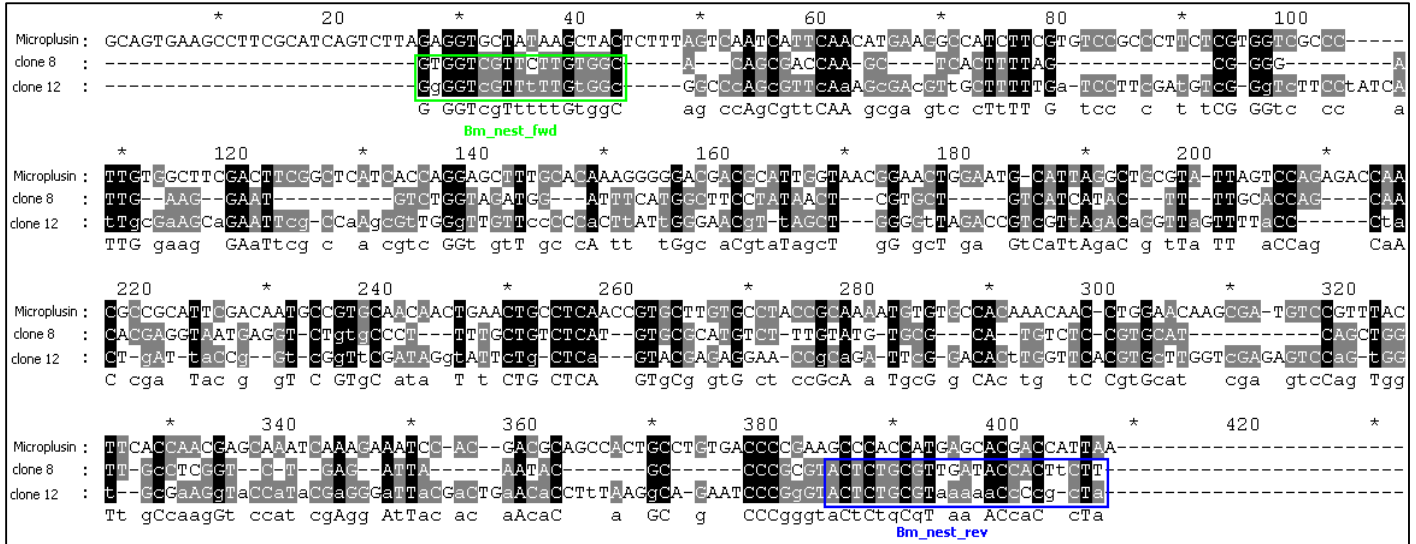
Figure 2.15: Alignment of the nucleotide sequence of colonies 8 and 12 with the known microplusin sequence: The region indicated in bright green is representative of the forward primer (Bm_nest_fwd), while the region indicated in blue is representative of the reverse primer (Bm_nest_rev).

The data presented in Figure 2.15 shows that the reaction was indeed primer driven, however, analysis of the translated nucleotide sequence in Figure 2.16 below further confirms that the sequences obtained are not those of microplusin homologs.
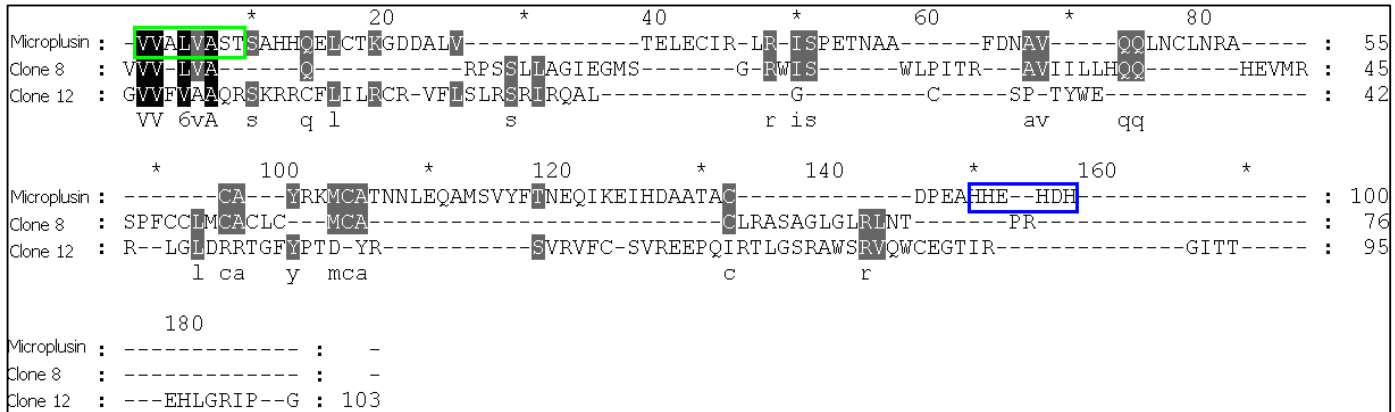
Figure 2.16: Alignment of the translated nucleotide sequence of colonies 8 and 12 with the known microplusin sequence: The region indicated in bright green is representative of the forward primer (Bm_nest_fwd), while the region indicated in blue is representative of the reverse primer (Bm_nest_rev) where regions in black indicate homology while grey regions indicate similarity.

53

From Figure 2.16, it is clear that there is no significant similarity between the suspected bands and native microplusin. Considering the fact that the tissue source was that of *R. (B.) microplus*, it is theoretically assumed that the nucleotide and amino acid sequence of any positive clone should show significant identity and similarity to microplusin. Seven alternative clones were sequenced, however sequence analysis showed lower significance than that seen for clones 8 and 12. For this reason, this data was excluded. From this, it may therefore be concluded that the 350 bp band is not microplusin.

2.5.5 PCR using combinations of primers on *O. savignyi* gut and salivary glands

An initial screening reaction using rTaq was unsuccessful in producing any visible product. This reaction was repeated using ExTaq due to the higher fidelity of ExTaq relative to rTaq. Additionally, ExTaq possesses an inherent proofreading ability and exonuclease activity in both the 5' to 3' and 3' to 5' directions. This means that a reaction catalyzed by ExTaq will be of higher specificity. Non specific amplification will be eliminated. The higher fidelity of the enzyme allows longer processing times and so prevention of truncations and better amplification of low abundance transcripts.

Amplification with Bm_nest_fwd:
- *O. savignyi* gut and salivary gland ds cDNA

Microplusin/ homolog transcript

Bm_nest_fwd   ~350 bp   3' anchor
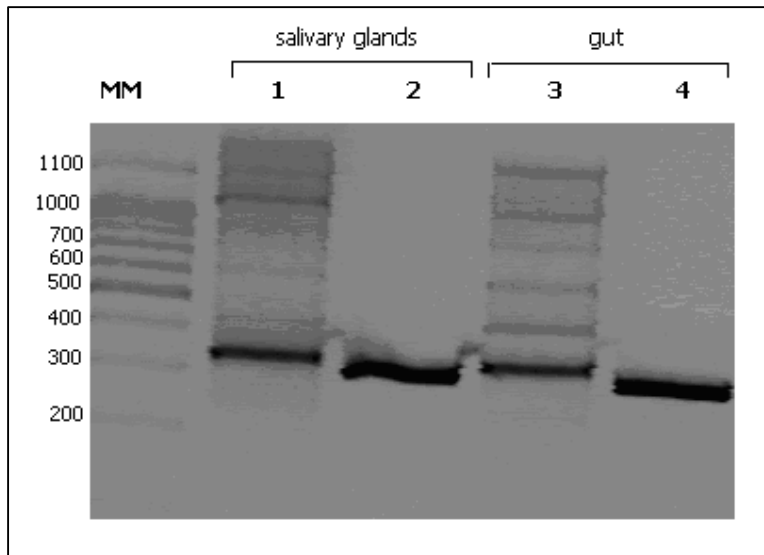
Figure 2.17: Agarose-EtBr (2.0%) gel analysis of screening of *O. savignyi* first strand cDNA with primer combination Bm_nest_fwd and 5' PCR IIA: lane 1: salivary gland first strand cDNA as template, lane 2: positive control (actin), lane 3: gut first strand cDNA and lane 4: positive control (actin).

It should be observed that first strand cDNA with the primer combination Bm_nest_fwd + 5' PCR IIA produces a band of 300 bp which was subjected to purification and reamplification (Figure 2.18).
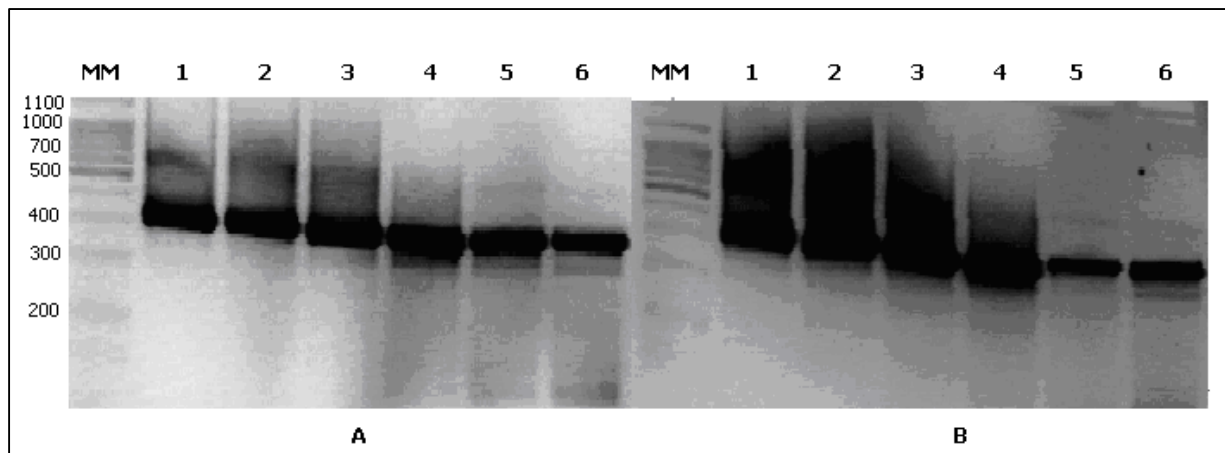
Figure 2.18:   Agarose-EtBr (2.0%) gel analysis of (A) salivary gland and (B) gut reamplification products of the *O. savignyi* 300bp band: MM represents 100bp DNA ladder, Lane 1: undiluted template, Lane 2: 1 in 10 dilution, Lane 3: 1 in 100 dilution, Lane 4: 1 in 1000 dilution, Lane 5: 1 in 10 000 dilution and Lane 6: 1 in 100 000 dilution.

Figure 2.18 shows that as dilution increases, high molecular weight DNA smearing, indicative of over-amplification, decreases. A 1/100 000 dilution was found to be optimal for reamplification of the 300 bp band from salivary glands and gut tissue and a large scale reamplification for both tissues was performed at this dilution. These bands were subjected to ligation and electroporation into electrocompetent DH5α cells. Positive colonies were sequenced. Nucleotide sequences showed no significant similarity or identity to the microplusin sequence. Figures 2.19 represents the translated nucleotide sequence obtained, aligned against microplusin. From the results, it may be concluded that the 300 bp band obtained by amplification using the microplusin specific primers on *O. savignyi* gut and salivary gland tissue, is not representative of microplusin.

BLAST searches revealed that clone 47 showed weak similarities to an *A. monolakensis* metalloprotease (42%) and the glycoprotein antigen Bm86 of *R. (B.) microplus* (30%). BLAST searches performed on the translated nucleotide sequence of clone 16 showed weak similarities to an *A. monolakensis* putative secretory protein (50%), an *A. monolakensis* metalloprotease (33%) and a member of the 7DB family of proteins of *A. monolakensis* (32%). These values are based upon similarity between a single isolated fragment of the sequence to isolated fragments of proteins mentioned and not full length sequences. For this reason, no conclusive identity may be given to the translated nucleotide sequence obtained.
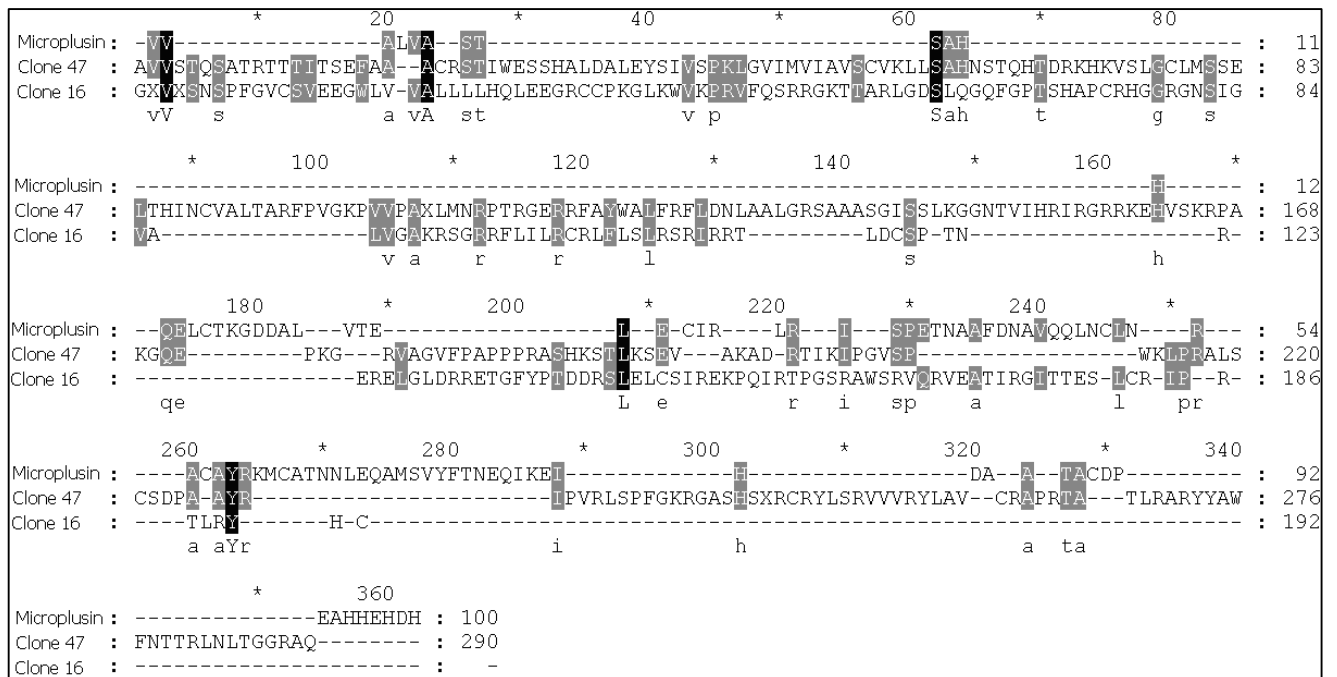
Figure 2.19: Alignment of the translated nucleotide sequences deduced from the 300bp band sequences: in the case of *O. savignyi* gut tissue (clone 47) and salivary gland tissue (clone 16). The sequence shown for microplusin begins at the site of the first nucleotide used in primer design.

2.5.6 PCR using MicroF/ MicroR and MonoF/MonoR

Finally, a second primer pair based upon the sequence of the *A. monolakensis* salivary gland microplusin-like antimicrobial peptide, was tested. An initial screening reaction produced bands of ~600 bp in both *R. (B.) microplus* adult cDNA as well as *O. savignyi* salivary gland cDNA. No band was present in *O. savignyi* gut tissue (Figure 2.20).

No primer-driven or non specific band was seen when screening with the MicroF/MicroR primer pair. This is contrary to results obtained by A. Nijhof (University of Utrecht). PCR involving the use of the MicroF and MicroR primers was repeated by A. Nijhof (University of Utrecht) following the method described in section 2.4.7.6. The template, however, was cDNA prepared from the fat body of fully engorged female *R. (B.) microplus* ticks. The product was sequenced (Figure 2.20) and shown to be microplusin.
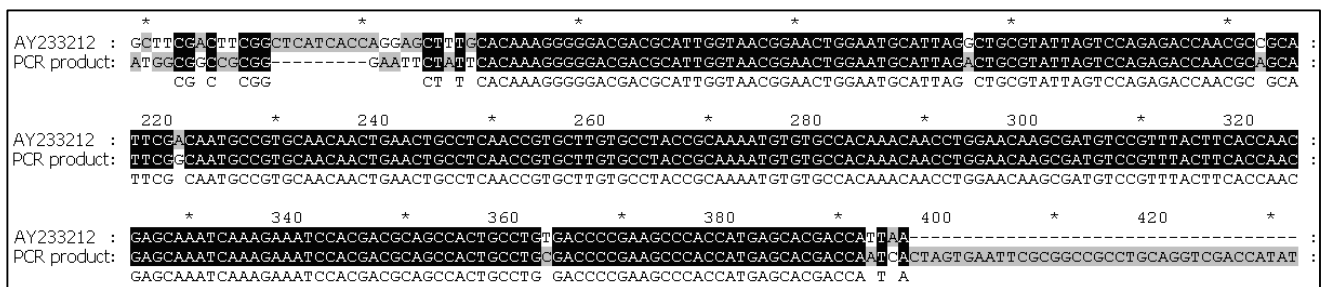
Figure 2.20: Alignment of the nucleotide sequence of the band obtained from the fat body of *R. (B.) microplus* adults using the MicroF and MicroR primer pair: AY233212 represents the known microplusin sequence as published by Fogaca *et al.,* in 2004 while microplusin represents the sequence under analysis.

Furthermore, Nijhof performed tissue expression profiling on several tissue types which included gut, salivary glands, ovaries, hemolymph, fat body, malpighian tubules as well as non-adult ticks. Significantly detectable quantities of the transcript was found only in the fat body of fully engorged adult female ticks.

Amplification with MonoF and MonoR:
- *O. savignyi* gut and salivary gland ds cDNA

Microplusin/ homolog transcript

MonoF   MonoR

~ 450 bp
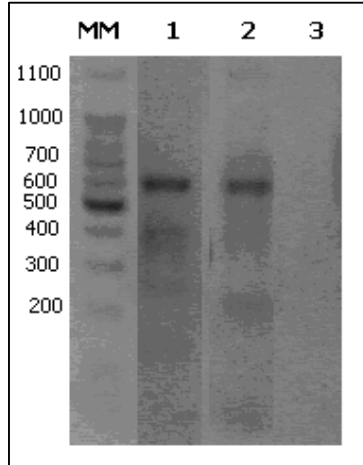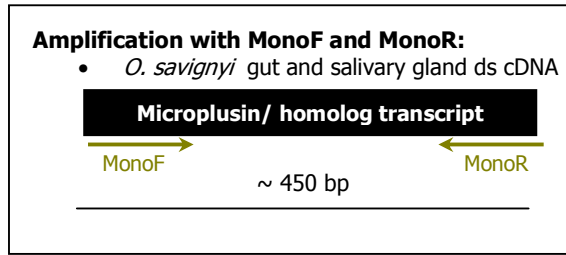
Figure 2.21: Agarose-EtBr (2.0%) gel analysis of screening of *R. (B.) microplus* adult cDNA and *O. savignyi* salivary gland and gut cDNA with the MonoF/MonoR primer pair: MM represents 100bp DNA ladder, lane 1: screen of *R. (B.) microplus* adult cDNA, lane 2: screen of *O. savignyi* salivary gland cDNA and lane 3: screen of *O. savignyi* gut cDNA.

Bands visible in Figure 2.21 were precipitated from the PCR reaction and subject to ligation and electroporation into electrocompetent DH5α cells. Positive colonies as determined by PCR screening were sequenced. The sequence of *R. (B.) microplus* showed that a non-specific product was produced by primers and for this reason, sequence data for this tick is omitted. Sequences obtained in the case of the band obtained from the *O. savignyi* salivary gland tissue, did not align to neither microplusin nor the *A. monolakensis* homolog (Figure 2.22).
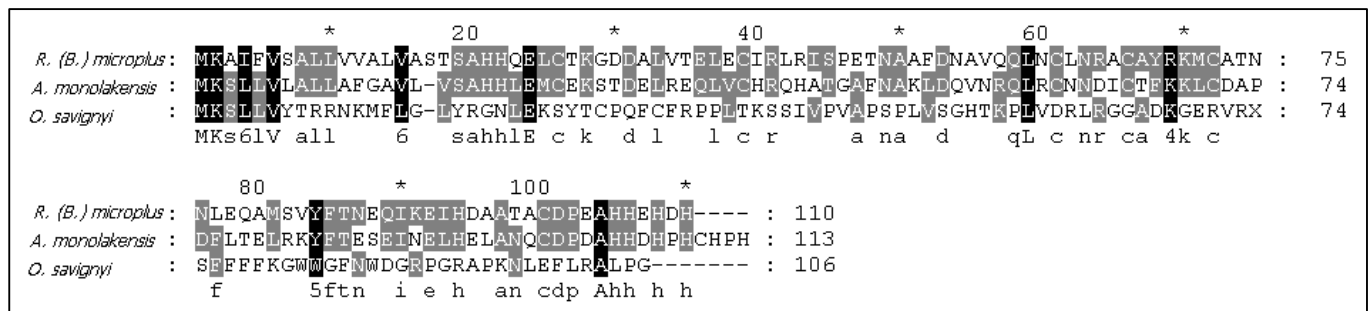
Figure 2.22: Alignment of translated nucleotide sequences of: *R. (B.) microplus* microplusin, the *A. monolakensis* microplusin-like salivary gland peptide and the sequence amplified from the salivary glands of *O. savignyi*.

2.6 Concluding remarks

Microplusin is a unique, non-defensin like AMP isolated from the ixodid tick, *R. (B.) microplus* (Fogaca *et al.*, 2004). This 10 kDa, cysteine-rich AMP shows anti Gram-positive activity and is specifically bacteriostatic against *Micrococcus luteus*. Since transcription of AMPs are induced by detection of a foreign invader, an understanding of the mode of action of such an AMP or homolog thereof, should theoretically allow for elucidation of a putative mechanism of survival of ticks following an immune challenge.

Since microplusin was initially identified from the ixodid tick *R. (B.) microplus,* this species was used as the positive control. If the reaction parameters are indeed functional, a negative result in terms of molecular identification of a microplusin homolog in the argasid tick, *O. savignyi*, could be accepted as conclusive. If however, the positive control shows sub-optimal results, a conclusive statement regarding the hypothesized presence of argasid homologs in *O. savignyi* may not be formulated.

Based on results obtained to date, no conclusive results were obtained with regards to the presence of a microplusin homolog in *O. savignyi*. The fact that the transcript was indeed successfully amplified from the fat body of *R (B.) microplus* indicates that the primer pair used during the study was successful in facilitating the amplification of this transcript by A. Nijhof (Utrecht, 2008). Several possibilities may allow for an explanation of the observations.

First, RNA used for this study was isolated from *R. (B.) microplus* eggs, a mixture of partially fed ticks of mixed life stages (including larvae and nymphs) and finally a mixture of all tissues from partially fed whole adult ticks. It may be possible that microplusin represents a low abundance transcript and hence was diluted in tissues used for the positive control, in contrast to using RNA isolated from the fat body of fully engorged female ticks where this organ is known to be enriched in microplusin. Nevertheless, cDNA produced was amplified by suppression PCR which functions to equalize transcript levels in a sample and eliminate the masking effect that higher abundance transcripts may show in contrast to low abundance transcripts which would amplify to a lower concentration under non-suppression PCR conditions. In these experiments, suppression PCR was afforded by the use of complementary anchor sequences. High abundance transcripts would form pan-handle like structures, thereby allowing amplification and normalization of low abundance transcripts. The optimal number of cycles during the amplification was determined as 20. Since

suppression PCR was used, a higher number of cycles does not directly correlate with a positive result.

Second, in ixodid ticks, the fat body is a diffuse organ of small size, while in argasid ticks, the fat body is distributed throughout the connective tissue, making isolation promlematic. For these investigations the fat body from fully engorged adult female ticks, was not available as no *R. (B.) microplus* colonies had been established at the University of Pretoria, at that time. It is therefore clear that the microplusin transcript (positive control) was not successfully amplified, simply due to the fact that inappropriate tissues were used. An area of improvement in order to circumvent this problem in future studies, is the establishment of a stable colony of these ticks as well as suitable feeding hosts and facilities as well as the use of intenal tissues of as many ticks as possible, as fat body alone cannot be isolated.

Alternatively, results obtained in this chapter may indicate an intricate mechanism of regulation of induction of synthesis of microplusin in response to physical or physiological stimulus. The results of A. Nijhof have revealed tissue specific expression of microplusin in the fat body of fully fed, adult female ticks as opposed to salivary glands, gut, ovaries, malpighian tubules and hemolymph tested. Fogaca *et al.,* showed in 2004 that the microplusin transcript is expressed in ovaries. The results of A. Nijhof showed no expression in ovaries. The work of A. Nijhof involved the use or real time PCR which shows a higher sensitivity to the level of expression as opposed to the presence of the transcript with end point PCR in the work of Fogaca *et al.* This may indicate stage specific induction where it may be hypothesized that the transcript is upregulated following fertilization or during the production of eggs. However, no conclusive evidence was found to substantiate any of the stage specific statements and must be readdressed in future studies.

The amplification of the microplusin from *R. (B.) microplus* as the positive control was inconclusive. However the internal positive control of individual PCR reactions (β-actin) was successfully amplified on repeated attempts indicating that poor RNA integrity or degradation of cDNA may be eliminated as reasons for lack of detection of the microplusin transcript.

Further studies should involve an investigation into the effect of feeding on the microplusin expression in *O. savignyi* as it is observed to be upregulated in *R. (B.) microplus* upon feeding. In order to successfully target the appropriate tissue expressing microplusin, an expression profile is essential prior to any attempts being made in the area of amplification of microplusin. Since the data obtained, by A. Nijhof, shows expression of the transcript only

in the fat body of fully fed adult female ticks and will allow the identification of a suitable positive control for future studies. The use of RNA isolated from ticks that have been challenged by Gram-positive and/or Gram-negative bacteria may provide insight into any further stimuli for upregulation of the transcript other than feeding. A search for suitable gene homologs at the level of genomic DNA will confirm the presence of homologs and warrant investigation of transcript levels at the level of mRNA.

Additionally, an argasid specific positive control should be included in experimentation, for example the salivary gland microplusin-like peptide of *A. monolakensis.*

These results imply that microplusin does not show basal levels of transcription. In order to confirm this possibility, expression profiles at specific times following feeding as well as in response to bacterial challenge should be compiled and compared.

In conclusion, it has been observed that the optimal positive control is the fat body of fully engorged adult female ticks. This serves as an indication of the tissue specific expression of the transcript in response to feeding. A suitable search for cross species homologs will therefore require the use of specific tissues obtained from fully fed adult female ticks.

Chapter 3:

The identification and molecular characterization of lysozyme from the argasid tick, *O. savignyi*

3.1 Introduction

Lysozyme (E.C.3.2.1.17) is classified as a ubiquitous enzyme (Liu *et al.*, 2006) catalyzing the hydrolysis of the β-1,4-glycosidic bond between amino sugars *N*-acetyl muramic acid (NAM) and *N*-acetyl glucosamine (NAG) which constitute the peptidoglycan layer of the cell wall of bacteria (Jolles & Holles, 1975, Bachali *et al.,* 2002). This activity directly contributes to the antibacterial properties of lysozyme. This enzyme is present across species including vertebrates, invertebrates, plants as well as phages (Matsumoto *et al.,* 2006). In vertebrates, the prominence of lysozyme is observed in secretory fluids of the body where it exhibits bactericidal activity.

In addition to its role in innate immunity, lysozyme expression is observed in the ruminant stomach. In this case, lysozyme has been implicated in digestion of bacteria which then provides the essential nitrogen and phosphorus required for milk production. For this reason, lysozyme has been divided into subtypes endowed with immunoprotective and/or digestive functions within vertebrates (Grunclova *et al.,* 2003).

3.1.1 *c*-Type lysozyme

Studies on lysozyme, prior to 1975, revealed the existence of two types of lysozyme, namely *c*-type (chicken type) and the *g*-type (goose type) in vertebrates. The well known example of the *c*-type family is hen egg white lysozyme (HEWL) (Figure 3.1), which exhibits a digestive function. These digestive *c*-type lysozymes differ from immunoprotective lysozyme by exhibiting high resistance against digestive proteases, possessing a characteristically lower number of basic amino acids which afford the molecule a lower pI (isoelectric point) in addition to an acidic pH optimum for activity (Grunclova *et al.,* 2003). The distribution of *c*-type lysozymes, with digestive roles, is summarized in Table 3.1.
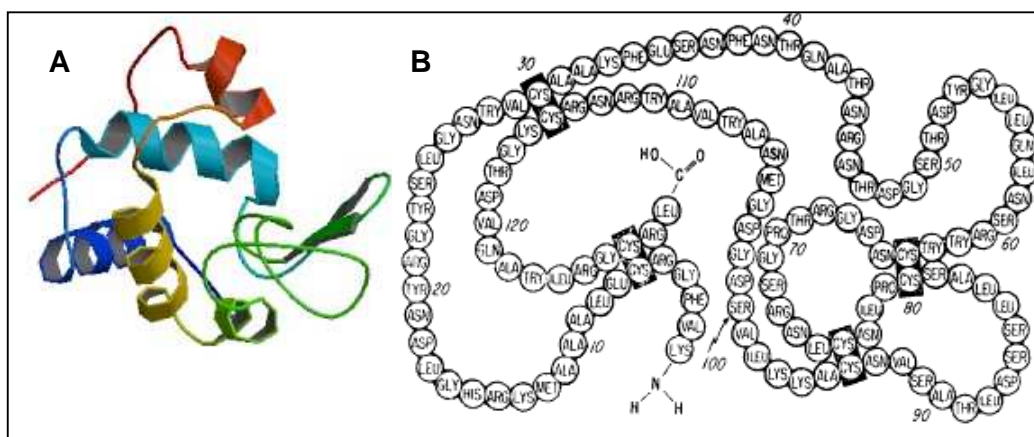
Figure 3.1: (A) Ribbon structure of hen egg white lysozyme (Protein data bank 1gxv), a member of the c-type family of lysozyme. **(B) Primary sequence of lysozyme** where darkened blocks surrounding the cysteine residues indicate disulfide bonds (Phillips 1976)

Table 3.1: Species distribution of the c-type lysozyme family (adapted from Bachali _et al.,_ 2002)

Species	Common name	Classification
Anas platyrhychos	Mallard duck	Vertebrata; Aves
Anopheles gambiae	African malaria mosquito	Arthropoda; Insecta; Diptera
Bombyx mori	Domestic silkworm	Arthropoda; Insecta; Lepidoptera
Bos taurus	Cow	Vertebrata; Mammalia; Ruminantia
Columba livia	Domestic pigeon	Vertebrata; Aves
Drosophila melanogater	Fruit fly	Arthropoda; Insecta; Diptera
Equus caballus	Horse	Vertebrata; Equidae
Gallus gallus	Chicken	Vertebrata; Aves
Heliothis virescens	Tobacco budworm	Arthropoda; Insecta; Lepidoptera
Homo sapiens	Human	Vertebrata; Mammalia
Hyalophora cecropia	Cecropia moth	Arthropoda; Insecta; Lepidoptera
Hyphantria cunea	Fall webworm moth	Arthropoda; Insecta; Lepidoptera
Manduca sexta	Tobacco hornworm	Arthropoda; Insecta; Lepidoptera
Musca domestica	House fly	Arthropoda; Insecta; Diptera
Mus musculus	Mouse	Vertebrata; Mammalia; Rodentia
Oncorhynchus mykiss	Rainbow trout	Vertebrata; Teleostei
Oryctolagus cunniculus	Rabbit	Vertebrata; Mammalia; Lagomorpha
Presbytis entellus	Hanuman langur	Vertebrata; Primates; Cercopithecidae
Rattus norvegicus	Rat	Vertebrata; Mammalia; Rodentia
Trichoplusia ni	Cabbage looper	Arthropoda; Insecta; Lepidoptera
Trichosurus vulpecula	Silver-grey bushtail possum	Vertebrata; Mammalia; Metatheria
Trionyx ganeticus	Turtle	Vertebrata; Trionychidae
Sus scrofa	Pig	Vertebrata; Mammalia; Suina
Dermacentor variabilis	Tick	Arthropoda; Arachnida: Ixodidae
Dermacentor andersoni	Tick	Arthropoda; Arachnida; Ixodidae
Ornithodoros moubata	Tick	Arthropoda; Arachnida; Argasidae

63

The Phillips mechanism (Figure 3.2) describes catalysis of the hydrolysis of the β-1,4-glycosidic bond between NAM and NAG by lysozyme, as studied in hen egg white lysozyme (Voet and Voet, 2004). Essential residues of the active site of HEWL, participating in the hydrolysis of the β-1,4-glycosidic bond, are Glu^{35} and Asp^{52}. Glu^{35} is situated within a hydrophobic pocket, while Asp^{52} is situated within a hydrophilic pocket. The characteristic pH of activity of HEWL is within the range of 3 and 8. For this reason, the side chain of Asp52 remains unprotonated during lysozyme activity while that of Glu^{35} is protonated. The reaction involves a general acid catalysis reaction where Glu^{35} is involved in transfer of the side chain proton to *O1* of ring E (in this case NAM). This leads to breakage of the $\beta-$1,4-glycosidic bond between ring D (NAG) and ring E (NAM) with associated release of ring E and formation of an oxonium ion intermediate (ring D). The oxonium ion is electrostatically stabilized by the unprotonated carboxyl group of Asp52. Addition of H_2O across the double bond of the oxonium ion leads to re-protonation of Glu^{35} and release of ring D. The end of the catalytic cycle is marked by release of ring D and restoration of the active site residues to the initial conformation (Voet and Voet, 2004).
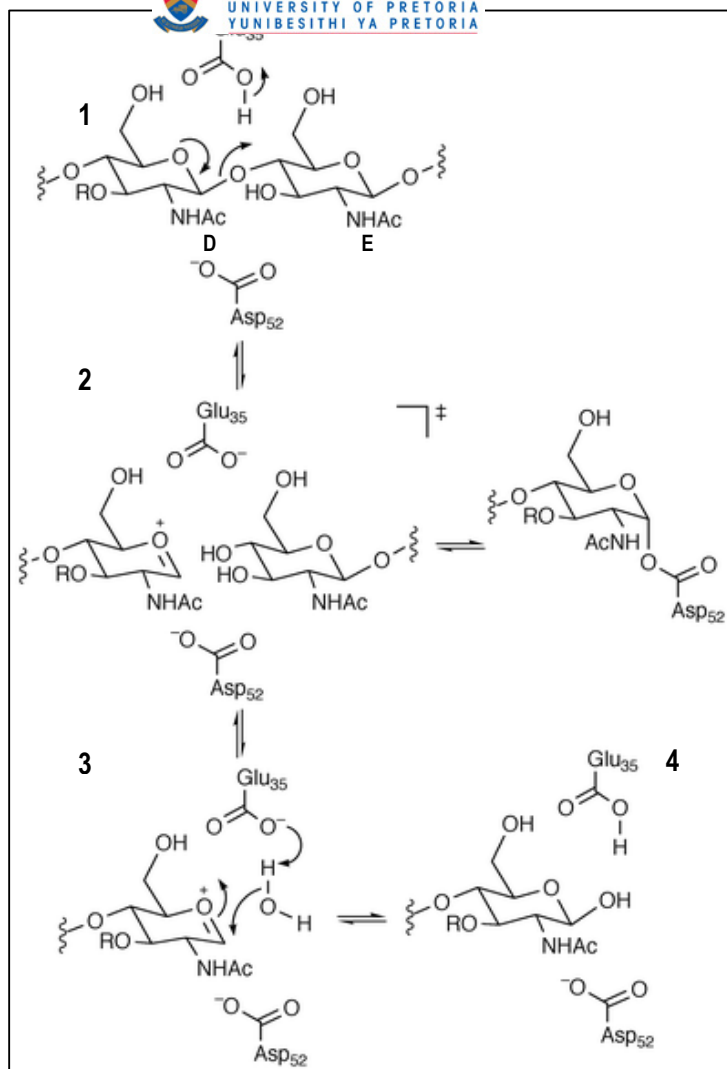
Figure 3.2: Reaction mechanism of c-type lysozymes which catalyze hydrolysis of the β–1,4-glycosidic bond between NAM and NAG of the peptidoglycan layer of bacteria: D and E represent the ring structures of NAM and NAG. General acid catalysis (1) leads to the release of the E ring (2) which accepted the proton of the active site Glu[35]. The D ring forms the reaction intermediate which is stabilized by the active site Asp[52]. Addition of H_2O to the stabilized oxonium ion (3) leads to completion of the catalytic cycle by release of the D ring (Bachali *et al.,* 2004).

3.1.2 *i*-Type lysozyme

In 1975, Jolles *et al.*, identified the *N*-terminal sequence of lysozyme of *Asteria rubens*, a starfish species. This discovery led to emergence of the invertebrate (*i*-type) family of lysozyme (Olsen *et al.*, 2003). The overall function of the *i*-type family of lysozyme is similar to that of the *c*-type family, i.e. a function in food digestion. In addition a similar three dimensional structure is observed within these families. Since the primary sequences of these proteins differ significantly the *c*- and *i*-type families of lysozyme represent functional rather than structural analogs (Bachali *et al.*, 2002). Within the *i*-type family, however, differential activity of digestion of bacterial cell wall components, as opposed to food ingested, show a direct correlation with species divergence, while it has been observed that these proteins are highly related at the level of primary sequence (Nilsen & Myrnes, 2001). Table 3.2 summarizes the distribution of the *i*-type lysozymes, across species.

Table 3.2: Species distribution of the *i*-type lysozyme family (adapted from Bachali *et al.*, 2002)

Species	Common name	Classification
Bathymodiolus azoricus	Hydrothermal-vent mussel	Mollusca; Bivalvia; Mytiloida
Bathymodiolus thermophilus	Hydrothermal-vent mussel	Mollusca; Bivalvia; Mytiloida
Caenorhabditis elegans	Nematode	Nematoda; Rhabditida
Calyptogena sp. 1	Cold-seep clam	Mollusca; Bivalvia; Veneroida
Calyptogena sp. 2	Cold-seep clam	Mollusca; Bivalvia; Veneroida
Chlamys islandica	Little scallop	Mollusca; Bivalvia; Pectinoida
Drosophila melanogaster	Fruit fly	Arthropoda; Insecta; Diptera
Hirudo medicinalis	Medicinal leech	Annelida; Clitellata; Hirudinea
Mytilus edulis	Blue mussel	Mollusca; Bivalvia; Mytiloida
Mytilus galloprovincialis	Mediterranean mussel	Mollusca; Bivalvia; Mytiloida
Penaeus (Litopenaeus) setiferus	White shrimp	Arthropoda; Crustacea; Decapoda
Penaeus (Litopenaeus) vannamei	Pacific white shrimp	Arthropoda; Crustacea; Decapoda
Tapes japonica	Mollusks	Mollusca; Bivalvia; Veneroida

As mentioned previously, two acidic residues namely Glu^{35} and Asp^{52} are present in the catalytic center of HEWL. To the contrary, in the *i*-type family Glu15 serves the function of the side chain proton donor (Glu^{35} of HEWL). Analysis of the primary sequence shows absence of Asp^{52} in HEWL, however this residue is conserved across most invertebrate species except the arthropods (Bachali *et al.*, 2002).

Mutational analysis on Asp52 involved transformation of this residue to either alanine, threonine, cysteine or serine. It was shown that activity of the lysozyme molecule was observed to be decreased by only 0.2% to 1.5% while overall activity of the molecule was maintained. For this reason, the function of the residue is seen to be primarily in assisting catalysis by means of facilitation of an electrostatic field when present in the unprotonated form. This form is then, as previously mentioned, involved in the stabilization of the oxonium ion (specifically an oxocarbonium ion) (Hashimoto *et al.,* 1996).

The *i*-type family is predominantly present in the protostome phylum including arthropods, annelids, nematodes and mollusks, while the *c*-type family is found in both deuterostomes as well as protostomes indicating a common ancestral lysozyme protein. This fact, together with the exon homologies between the families, indicates that the currently known families of lysozyme have arisen as a result of gene duplication or exon shuffling events early in the evolution of the species (Bachali *et al.,* 2002).

3.1.3 Tick lysozyme

In ticks, the storage organ for a bloodmeal is the midgut (Kopacek *et al.,* 1999) and digestion occurs intracellularly within epithelial cells of the gut (Grunclova *et al.*, 2003). Since digestion is intracellular, the lumen of the gut does not possess proteolytic enzymes and for this reason, the optimal temperature, pH and nutrient medium within the gut lumen provides the ideal conditions for the survival and replication of several different microorganisms (Kopacek *et al.,* 1999). The presence of lysozyme, eliciting bactericidal activity, could be beneficial to the survival of the tick following a bloodmeal and ingestion of bacteria.

Simser *et al*. (2004) identified an immune-responsive lysozyme in the ixodid tick species, *Dermacentor variabilis* and *D. andersoni.* A *D. variabilis* hemocyte library was utilized in the identification of a *c*-type lysozyme which then assisted homology cloning resulted in the identification of a a homolog of this gene in the DAE100 cell line of *D. andersoni.* A comparison of major physicochemical properties of the known *Dermacentor* lysozyme molecules is presented in Table 3.3.

Table 3.3: Main physiochemical properties of the ixodid tick lysozymes of *D. variabilis* and *D. andersoni*

Property	*D. variabilis* lysozyme	*D. andersoni* lysozyme
Full length gene	670 bp	629 bp
Open reading frame	420 bp	420 bp
Cleavage of signal peptide site	Alanine 16 and Lysine 19	Alanine 16 and Lysine 19
Number of amino acids	121	121
pI	9.97	9.91
Molecular weight (Da)	13869	13881

These tick lysozyme molecules exhibited upregulation following immune challenge with *E. coli*. Expression levels were observed to peak 72 hours post-inoculation and levels returned to baseline 96 hours post-inoculation (Simser *et al.,* 2004)

The observation that gut contents of engorged adult female *O. moubata* ticks facilitated antimicrobial activity led to isolation of lysozyme from this argasid tick species (Kopacek *et al.,* 1999). The full length coding sequence consists of 609 bp. Following cleavage of a 22 amino acid signal sequence, a mature protein of 124 amino acids and a molecular weight of 14037.75 Da is produced. The pI of this protein is approximately 8.16. Tissue expression profiling revealed the presence of lysozyme in hemocytes and midgut, while comparatively low levels of expression were observed in ovaries, salivary glands and malpighian tubules.

Sequence analysis of these ixodid and argasid tick lysozyme molecules indicate a high similarity to the *c*-type family of lysozyme with the conserved 8 cysteine residues forming the associated four disulfide bonds. In the *O. moubata* lysozyme sequence the active site residues are represented by Glu^{33} and Asp^{51} (corresponding to Glu^{35} and Asp^{52} of HEWL) (Kopacek et al., 1999). Therefore, it is hypothesized that the catalytic function of tick gut lysozyme is analogous to that of HEWL. Highest levels of expression of *O. moubata* lysozyme was found in the midgut 16 hours post-feeding and these elevated levels remained stable for approximately 5 days post-feeding. Baseline levels of lysozyme were restored to that of unfed ticks within approximately 2 weeks following feeding. Analysis of lysozyme activity of the midgut and hemolymph revealed high levels of lytic activity within the midgut content and significantly lower levels within hemolymph. However, this hemolymph activity is assumed to be due to a possible contamination with midgut contents during tissue isolation (Kopacek *et al.,* 1999).

Further divergence within the *c*-type lysozyme family led to emergence of the H-branch of lysozyme during phylogenetic analyses of *c*-type lysozyme sequences across species. Figure 3.3 shows that several invertebrates belong to the H-branch, including *D. melanogaster* and *Anopheles gambiae*.
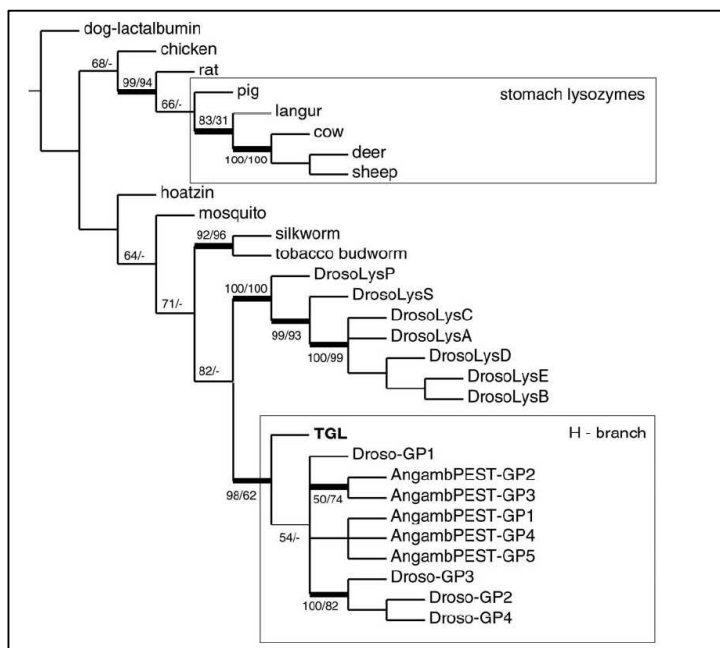
Figure 3.3: Phylogenetic tree showing relationships between known c-type lysozyme molecules (Grunclova *et al.*, 2003). Digestive lysozymes are indicated in the uppermost square while the H-branch of c-type lysozymes are indicated in the lower square.

Tick gut lysozymes possess a Histidine 40 and Histidine 52 residues in both ixodid and argasid ticks replacing a highly conserved tyrosine residue at corresponding positions (Grunclova *et al.,* 2003 and Simser *et al.,* 2004). For this reason, it was implicated that tick lysozyme falls within the H-branch.

In general, lysozyme is seen to be upregulated in ixodid tick species in response to bacterial challenge by Gram-negative bacteria. In contrast, upregulation is observed in response to feeding in argasid tick species. At this point, it may be assumed that tick lysozyme may be induced in response to physiological stresses which include injury or bacterial challenge as well as responses induced during and post-blood feeding. It can therefore be hypothesized that tick lysozyme exhibits either a bactericidal and/or a digestive function due to upregulation in response to bacterial challenge or uptake of a bloodmeal in ixodid and argasid ticks, respectively.

Furthermore, catalytic residues differ from the prototype of the *c*-type lysozyme family (HEWL). Since phylogenetic analysis revealed the presence of lysozyme in several species

an attempt was made to identify a homologous lysozyme molecule in the argasid tick, *O. savignyi*. Molecular characterization of this molecule, in terms of:

1. identity to known arthropod (tick) lysozyme molecules,
2. stimulus of induction and
3. analysis of putative catalytic residues to facilitate classification, was attempted.

3.2 Hypothesis

Lysozyme has been implicated in immunoprotective and/or digestive roles in several arthropod species including the ixodid (*D. andersoni and D. variabilis*) and argasid (*O. moubata*) ticks. It is hypothesized that a homologous lysozyme molecule is present in the gut of the argasid tick, *Ornithodoros savignyi,* where it is induced during feeding.

3.3 Aims

To identify a lysozyme transcript in the gut of the argasid tick, *O. savignyi* and determine the tissue expression profile of this transcript. Additionally, an attempt will be made to characterize lysozyme into the H-branch of the *c*-type lysozyme family by means of sequence analysis.

3.4 Materials and Methods

3.4.1 Ticks: dissection and hemolymph collection

O. savignyi ticks were collected from the Northern Cape (Upington) by the sifting of sand and stored in sand at room temperature. Dissections were performed as described in section 2.4.2 and midgut, salivary glands and ovaries were collected. Hemolymph collection was facilitated by immobilization of ticks on double-sided tape, with the ventral surface exposed. A 30 gauge needle was used to puncture the first pair of coxae at the base of the trochanter. Application of moderate pressure on the ventral surface of the tick allowed for the leakage of hemolymph, which was collected and immediately placed into Tri-Reagent (Sigma-Aldrich).

3.4.2 RNA isolation

RNA was isolated from tissues collected during dissection (midgut, salivary glands and ovaries). The protocol followed is described is section 2.4.3.

3.4.3 cDNA synthesis

cDNA used for 3'- RACE was synthesized using the SMART II A oligonucleotide on the 5' end and a unique poly T anchor on the 3' end. Alternatively, cDNA used for 5'- RACE was synthesized using a unique poly G anchor on the 5' end and the 3' SMART CDS Primer II A supplied by the kit, on the 3' end. This was done since it was found in chapter 2 that the CDS primer sequence provided by the cDNA synthesis kit facilitates non-specific binding and amplification.

As starting material, 500 ng of RNA isolated from the midgut was used. To this 12 pmoles/μl (of a 10 mM stock) of the poly T anchor primer (GCT ATC ATT ACC ACA ACA CTC (T)18VN) and 12 pmoles/μl (of a 7 mM stock) of the SMART IIA oligonucleotide (AAG CAG TGG TAT CAA CGC AGA GTA CGC GGG) was added. DEPC-water was then added to a final volume of 64 μl. The 64 μl reaction mixtures were spun briefly in a microcentrifuge and incubated at 65°C for 2 minutes in a thermal cycler (Perkin Elmer Gene Amp PCR system 2400). This step allowed for denaturation of secondary structures in the RNA sample. Following incubation, samples were placed on ice immediately for 5 minutes in order to prevent reformation of secondary structures and so facilitate specific annealing of the poly T anchor primer, downstream. To each reaction tube, 20 μl 5X First strand buffer, 2 μl 100 mM dithiothreitol (DTT), 10 μl 50 X dNTPs (10 mM) (Roche Diagnostics, Indianapolis, USA), 100 U RNase inhibitor (Promega, Madison, WI, USA), 500 U Superscript III reverse transcriptase (Invitrogen, Carlsbad, CA) and 5 μl DEPC-water were added. Reaction mixtures were mixed by gentle pipetting and spun down in a microcentrifuge. This was followed by incubation at 42°C for 90 minutes in the Perkin Elmer Gene Amp PCR system 2400. At the end of the incubation period, 2 μl (0.5M) EDTA (ethylene diamine tetra-acetate) was added to terminate the reaction. Amplification of the abovementioned ss cDNA to was performed as described in section 2.4.5.

3.4.4 Primer design

The nucleotide and amino acid sequences obtained for the known argasid and ixodid lysozyme reading frames were aligned using Clustal X as described in section 2.4.6. These sequences included the *D. andersoni* lysozyme molecule (accession number: AY207371), *D. variabilis* lysozyme (accession number: AY183671) and *O. moubata* lysozyme precursor (accession number: AF425264). The alignments (Figures 3.5 and 3.6) were visualized and analyzed for similarity and identity using GeneDoc (Version 2.6.003, a multiple sequence alignment editor and shading tool). This allowed for the identification of suitable regions

showing high similarity across species, which were used to design a degenerate primer representative of lysozyme and a possible homolog in *O. savignyi*. Furthermore, since the lysozyme gene sequence of the argasid tick, *O. moubata* is known, it was hypothesized that gene specific primers based on this sequence will facilitate the amplification of a homologous lysozyme sequence from *O. savignyi*.

3.4.5 Polymerase chain reaction (PCR)

3.4.5.1 Amplification using the degenerate primer

The PCR reaction was setup with 100 ng of gut ds cDNA to which 2 μl of the 10 X ExTaq buffer (Mg^{2+} included), 2 μl of dNTPs (2.5 mM each), 50 pmoles of the degenerate primer (Deg_Lys_F1, Table 3.4) and 10 pmoles of the poly T anchor primer were added. The final reaction volume was constituted to 20 μl by means of water.

Initial denaturation at 94°C was allowed for 7 minutes followed by incubation at 80°C for 30 seconds. At this point 1.25 U of ExTaq (5 U/μl) in the corresponding buffer was added to each reaction tube. The reaction was allowed to proceed for 25 cycles at 94°C for 30 seconds, 55°C for 30 seconds and 72°C for 2 minutes. A final extension at 72°C was allowed to proceed for 7 minutes following which the reactions were maintained at 4°C.

3.4.5.2 Nested PCR using *O. moubata* gene specific primers

Product obtained after PCR using the degenerate primer was used with *O. moubata* gene specific primers. Template (100 ng), 2 μl of the 10 X ExTaq buffer (Mg^{2+} included), 2 μl of dNTPs (2.5 mM each), 10 pmoles of the gene specific forward primer (Lys F1) and 10 pmoles of the three alternate gene specific reverse primers (Lys 1R, Lys 2R or Lys 3R (Table 3.4) in individual reactions were added. The final reaction volume was constituted to 20 μl by means of water.

Initial denaturation at 94°C was allowed for 7 minutes followed by incubation at 80°C for 30 seconds. At this point 1.25 U of ExTaq in the corresponding buffer was added to each reaction tube. The reaction was allowed to proceed for 30 cycles at 94°C for 30 seconds, 50°C for 30 seconds and 72°C for 2 minutes. A final extension at 72°C was allowed to proceed for 7 minutes following which the reactions were maintained at 4°C The product of this reaction was analysed on a 2.0% agarose-ethidium bromide gel.

3.4.5.3 3'-RACE using *O. moubata* gene specific primers

Once the central ~300 bp of the *O. savignyi* lysozyme was identified, the identification of the 5' and 3' ends remained. Using the central sequence obtained, a gene specific forward primer within the 3' region of the fragment was designed. This primer, Lys 1R fwd (Table 3.4), when used in conjunction with the poly T anchor primer mediated amplification of the 3' end of the lysozyme transcript. The reaction involved the use of 100 ng of gut ds cDNA from field collected, unfed ticks, as template, to which 2 μl of the 10 X ExTaq buffer (Mg^{2+} included), 2 μl dNTPs (2.5 mM each), 10 pmoles of the gene specific forward primer (Lys 1R fwd) and 10 pmoles of the poly T anchor primer were added. The reaction was constituted to a final volume of 20 μl using H_2O.

Initial denaturation at 94°C was allowed for 7 minutes followed by incubation at 80°C for 30 seconds. At this point 1.25 U of ExTaq in the corresponding buffer was added to each reaction tube. The reaction was allowed to proceed for 30 cycles at 94°C for 30 seconds, 55°C for 30 seconds and 72°C for 2 minutes. A final extension at 72°C was allowed to proceed for 7 minutes following which the reactions were maintained at 4°C. The product of this reaction was cloned and sequenced following the procedures described in sections 2.4.8 - 2.4.15.

3.4.5.4 5'-RACE

The sequence obtained during 3'- RACE was used for the design of a gene specific reverse primer suitable for 5'-RACE. This primer, Lys F1R (Table 3.4), when used in conjunction with the poly G anchor primer (Table 3.4) amplified a fragment representative of the 5' end of the mRNA transcript. The reaction involved the use of 100 ng of gut ds cDNA from unfed ticks, as template, to which 2 μl of the 10 X ExTaq buffer (Mg^{2+} included), 2 μl dNTPs (2.5 mM each), 10 pmoles of the gene specific forward primer (Lys F1R) and 10 pmoles of the poly G anchor primer were added. The reaction was constituted to a final volume of 20 μl using water.

Initial denaturation at 94°C was allowed for 7 minutes followed by incubation at 80°C for 30 seconds. At this point 1.25 U of ExTaq in the corresponding buffer was added to each reaction tube. The reaction was allowed to proceed for 30 cycles at 94°C for 30 seconds, 58°C for 30 seconds and 72°C for 2 minutes. A final extension at 72°C was allowed to proceed for 7 minutes following which the reactions were maintained at 4°C. The product of

this reaction was cloned and sequenced following the procedures described in sections 2.6.8-2.6.15.

3.4.6 Tissue expression profiling

In order to study the changes in expression of the lysozyme transcript in response to various stimuli, a tissue expression profile was produced using semi-quantitative real time PCR (RT-PCR).   Since real time PCR represents a quantitative approach, an internal standard is required in order to quantify the expression of a target (gene of interest) relative to a known concentration of the standard.   Due to the lack of elucidation of a household gene in *O. savignyi* an internal standard (human B-cell receptor RNA) was used.   Since tick tissues do not possess any known homolog to this sequence, it may be safely assumed that the target (lysozyme) expression may be quantified relative to the internal standard or spike.

3.4.6.1 Tick feeding and dissections

For these experiments, 20 adult female *O. savignyi* ticks with a net weight of ~150 mg were placed in a sieve, gently rinsed with water and allowed to dry on tissue paper.   Ticks were then fed artificially on cattle blood obtained from the Experimental Farm (University of Pretoria) (Ethical number EC022-08).   Blood was collected in 10 ml BD Vacutainer tubes (BD Biosciences-Plymouth, UK) containing 170 IU of lyophilized heparin.

Blood collected in this manner was stored at 4°C for 4 days or placed at -20°C for long term storage.   The artificial feeding system was optimized by A. Nijhof (University of Utrecht) and is shown in Figure 3.4 below.
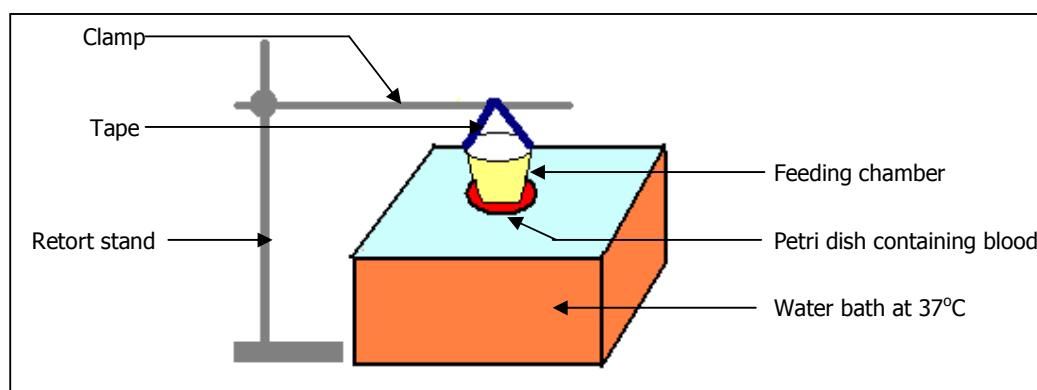
Figure 3.4: Diagrammatic representation of the artificial feeding system

Washed ticks were placed into the feeding chamber (plastic container of which the base was removed and replaced with parafilm fastened with an elastic band) which was then fastened to a clamp attached to the retort stand. The height was adjusted in order for the feeding chamber to merely touch the meniscus of the blood (40 ml) in the Petri dish which had been pre-heated to $37^{\circ}C$. The Petri dish was stabilized in the water bath by placement upon a glass bottle filled with water. The temperature of the water bath was constantly maintained at $37^{\circ}C$.

For the purposes of this experiment native blood (no bacteria added) was used in addition to blood infected with Gram-positive bacteria alone or blood infected with a combination of Gram-positive and Gram-negative bacteria.

Gram-positive *(Bacillus subtilis)* and Gram-negative *(E. coli)* were grown in 10 ml of LB-Broth overnight at $30^{\circ}C$ with shaking (250 rpm). When an OD_{600nm} of 1 for *B. subtilis* and *E. coli* was reached, 250 μl of the cell suspension was centrifuged at 3000 X g for 15 minutes followed by washing twice with sterile PBS (phosphate buffered saline), pH 7.5. Cells were then resuspended in PBS.

In general an OD_{600nm} of 1 represents an estimated total of 1×10^{9} bacterial cells/ml. The aliquot of the overnight culture used (250 μl) therefore contained 2.5×10^{8} bacterial cells. Final resuspension was performed using 1 ml PBS thereby producing a cell solution of 2.5×10^{8} bacterial cells/ml. A final volume of 400 μl of this cell suspension was added to 40 ml of blood (Buresova *et al.,* 2006)*.*

At 16 hours post feeding hemolymph was collected and ticks were dissected for midgut, salivary glands and ovaries.

3.4.6.2 RNA isolation

For the tissue expression profile to be generated, RNA was isolated (section 2.4.3) from the hemolymph (including hemocytes), salivary glands, midgut, and ovaries of fully engorged adult female *O. savignyi* ticks fed on native blood and ticks fed on blood infected with either Gram-positive bacteria *(B. subtilis)* alone or a combination of Gram-positive *(B. subtilis)* and Gram-negative *(E. coli)* bacteria.

Additionally, RNA was isolated from the hemolymph, midgut, salivary glands and ovaries of unfed adult female *O. savignyi* ticks. RNA was isolated in three batches of five ticks each in order to obtain biological triplicate values.

3.4.6.3 cDNA synthesis

RNA (500 ng), 1 ng of the spike RNA (human B-cell receptor (N.A Olivier, ACGT Microarray Unit, University of Pretoria)), 12 pmoles of the poly T primer and 12 pmoles of the $p(dN)_6$ (random hexamer primer) (obtained from Whitehead Scientific, Cape Town) and H_2O was added to a final volume of 11 μl. Tubes were briefly centrifuged and incubated at 70^oC for 10 minutes, followed by cooling on ice for 2 minutes.

To each tube, 4 μl of 5X first strand buffer, 1 μl of 10 mM dNTPs, 2 μl of 0.1 M dithiothreitol (DTT), 40 U of RNase inhibitor and 200 U of Superscript III reverse transcriptase was added. Tubes were again centrifuged and incubated at 42^oC for 90 minutes. The enzyme was thereafter inactivated by incubation at 70^oC for 10 minutes. cDNA samples were stored at -70^oC.

3.4.6.4 Real time PCR

Prior to real time PCR, the cDNA was diluted 5 times and the reaction for each batch of the biological triplicate was performed in duplicate using both spike-specific primers, as well as lysozyme-specific primers.

To decrease technical error, two master mixes were prepared using, in the first case, 0.5 μl of the Lys F1R (10 pmoles/μl) primer and 0.5 μl of the Lys 1F (10 pmoles/μl) primer, and in the second case 0.5 μl of the forward (10 pmoles/μl) and 0.5 μl of the reverse spike-specific primers (10 pmoles/μl). In addition to the primers, the master mix contained 5 μl of the Roche SYBR I master mix (containing SYBR Green, Taq polymerase, dNTPs and $MgCl_2$) and 3 μl of nuclease free water (supplied with the master mix). This mix (9 μl each) was then was then pipetted into the real time PCR plate followed by the addition of 1 μl sample templates corresponding to isolated tissues of unfed, fed and bacterially challenged ticks.

After pipetting, the plate was centrifuged at 2000 X g for 2 minutes. PCR was performed on the Roche Light Cycler 480 System. The cycling procedure allowed for activation of the Taq DNA polymerase at 95^oC for 5 minutes followed by 45 cycles of denaturation at 95^oC for 3

seconds, annealing of primers at 55°C for 7 seconds and extension at 72°C for 3 seconds. Fluorescence was detected during the extension step.

In order to generate a melting curve, the reaction was subsequently allowed to incubate at 95°C for 30 seconds, 55°C for 30 seconds followed by a continuous acquisition at 95°C. Finally, the reaction was allowed to cool to 40°C.

3.4.6.5 Real time PCR data analysis

Due to the lack of known and proven household genes in ticks, the expression levels of lysozyme were compared to an internal standard (spike) to allow semi-quantitative profiling.

Software of the Roche Light Cycler 480 system was used for relative quantification where the samples containing the spike primers were designated as the reference while the experimental samples containing the lysozyme primers were designated as the target. C_T values were calculated by the software and analysis was performed using Microsoft ® Excel. Data was then analysed using a Student's t-Test assuming unequal variances.

3.5 Results and discussion

3.5.1 Primer design

The know argasid and ixodid tick lysozyme sequences of *O. moubata, D. variabilis* and *D. andersoni* were aligned and analysed for regions of similarity, as indicated in Figures 3.5 and 3.6. A degenerate primer (Deg_Lys_F1) was designed by Dr. C. Maritz-Olivier (University of Pretoria, Department of Biochemistry). It was proposed that amplification using this primer in addition to the poly T anchor primer (see cDNA synthesis) present on the 3' terminals of the produced cDNA, should theoretically lead to the amplification of an *O. savignyi* lysozyme sequence.
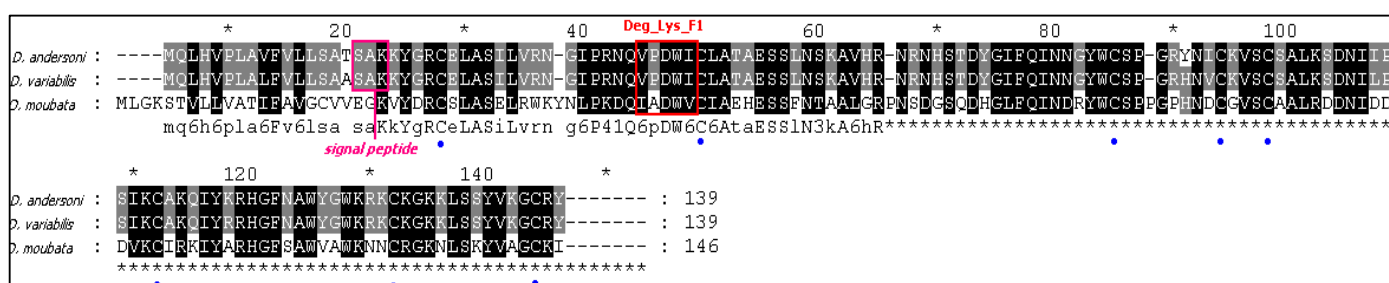
Figure 3.5: Alignment of the amino acid sequences of the known ixodid and argasid tick lysozyme molecules: The region indicated in red was used for the design of the forward degenerate primer (Deg_Lys_F1). Blue dots indicate the 8 typically conserved cysteine residues while the region of cleavage of the signal peptide is indicated in pink.
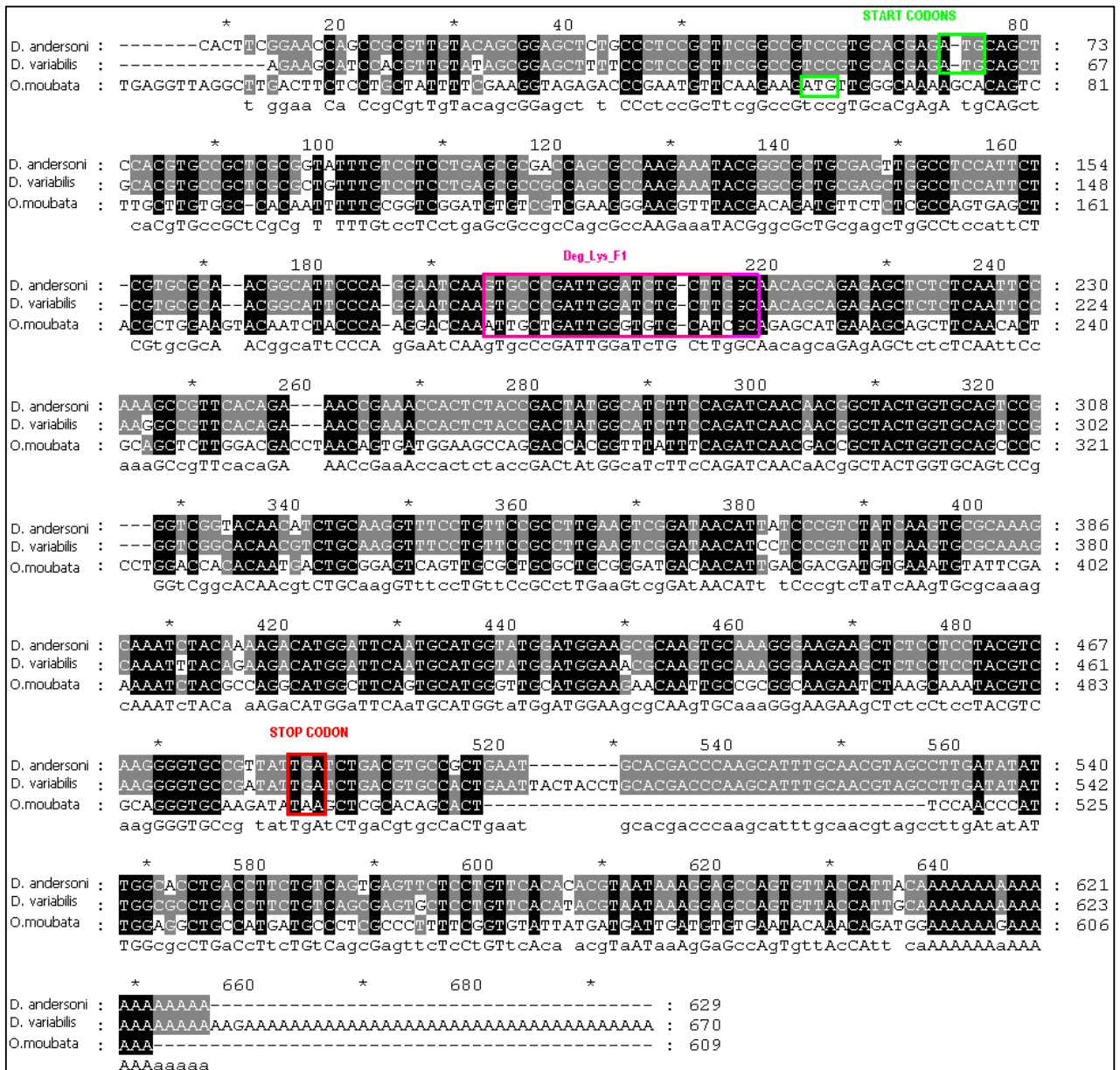
Figure 3.6: Alignment of the nucleotide sequences of the known ixodid and argasid tick lysozyme molecules: The start codons of the respective transcripts are indicated in bright green while the *O. moubata* stop codon is indicated in red. The region indicated in pink represents that used for the design of the degenerate primer Deg_Lys_F1.

The lack of success using the degenerate primer, Deg_Lys_F1 prompted the need for the design of gene specific primers based upon the *O. moubata* lysozyme sequence alone. The reasoning for the design of each of these primers is given below and the regions used have been annotated in Figure 3.7.
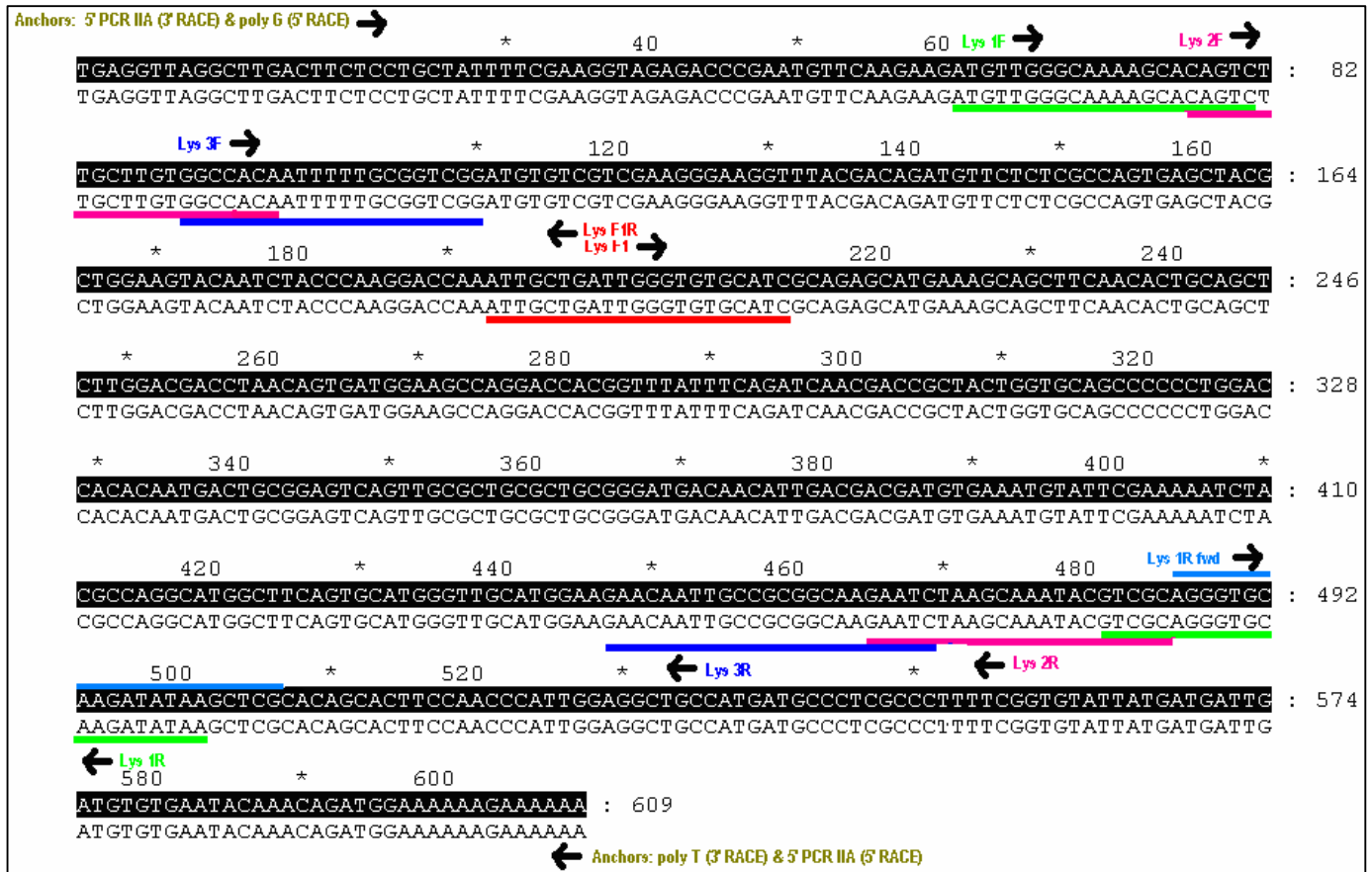
Figure 3.7: Nucleotide sequence of *O. moubata* lysozyme (accession number AF425264): Regions used for the design of the gene specific primers are underlined with the 5′ to 3′ direction of the primer indicated in the direction of the black arrow. The regions of the anchor primers used during cDNA synthesis are indicated at the 5′ and 3′ terminals in olive green.

LysF1 (gene specific to the *O. moubata* sequence) was designed in the same position as the degenerate primer, Deg_Lys_F1. This primer when used in conjunction with the overlapping reverse primers should yield the central fragment of the lysozyme transcript. Overlapping primers included Lys 1R, Lys 2R and Lys 3R were based on the sequence of the 3′ region of the *O. moubata* transcript.

In order to amplify the 3′ terminal of the transcript, the abovementioned Lys 1R fwd primer was designed in the region of the Lys 1R primer. This primer when used in conjunction with the poly T anchor primer should theoretically amplify the 3′ terminal of the transcript. Lys F1R was designed in the region of Lys F1 in order to amplify the 5′ terminal of the transcript

in addition to the 5' overlapping primers. These overlapping primers include Lys 1F, Lys 2F and Lys 3F suitable for nested PCR. Alternatively, the Lys F1R primer may be used in conjunction with the unique poly G anchor in order to amplify out the 5' terminal of the transcript.

Table 3.4 summarizes the degenerate and gene specific primers designed for the amplification of the *O. savignyi* lysozyme homolog.

Table 3.4: Primers designed for the amplification of *O. savignyi* lysozyme based on the nucleotide sequence of *O. moubata* lysozyme (where R represents A or G, Y represents C or T, I represents inosine and H represents A, C or T)

Primer name	Nature	Sequence (5' --> 3")	Melting temperature (ºC)	Application
Deg_Lys_F1	Degenerate	RTT GCT GAY TGG RTI TGY HTI GC	60.00	3'-RACE
Lys F1	Gene specific	ATT GCT GAT TGG GTG TGC ATC	56.00	3'-RACE
Lys 1R	Gene specific	TTA TAT GTT GCA CCC TGC GAC	55.00	3'-RACE nested PCR
Lys 2R	Gene specific	GCG ACG TAT TTG CTT AGA TTC	52.00	3'-RACE nested PCR
Lys 3R	Gene specific	GAT TCT TGC CGC GGC AAT TGT TC	59.00	3'-RACE nested PCR
Lys 1R fwd	Gene specific	AGG GTG CAA GAT ATA AGC TCG	60.00	3'-RACE
Lys F1R	Gene specific	GAT GCA CAC CCA ATC AGC AAT	60.00	5'-RACE
Lys 1F	Gene specific	ATG TTG GGC AAA AGC ACA GTC	57.00	5'-RACE nested PCR
Lys 2F	Gene specific	CAG TCT TGC TTG TGG CCA C	57.00	5'-RACE nested PCR
Lys 3F	Gene specific	GCC ACA ATT TTT GCG GTC GG	58.00	5'-RACE nested PCR

3.5.2 Identification of the central ~300bp region

The initial reaction involved screening of ds cDNA of unfed tick gut tissue, with the degenerate primer (Deg_Lys_F1). Typical of degenerate primers, the reaction is one of lower specificity for the target gene of interest, compared to when using gene specific primers, i.e. numerous bands were visible after 3'-RACE. For this reason, the PCR products of the degenerate primer PCR was used as a template in a nested PCR primed by gene specific primers in an attempt to amplify the correct lysozyme sequence. Figure 3.8 represents the product of the screening reactions using the nested primers.
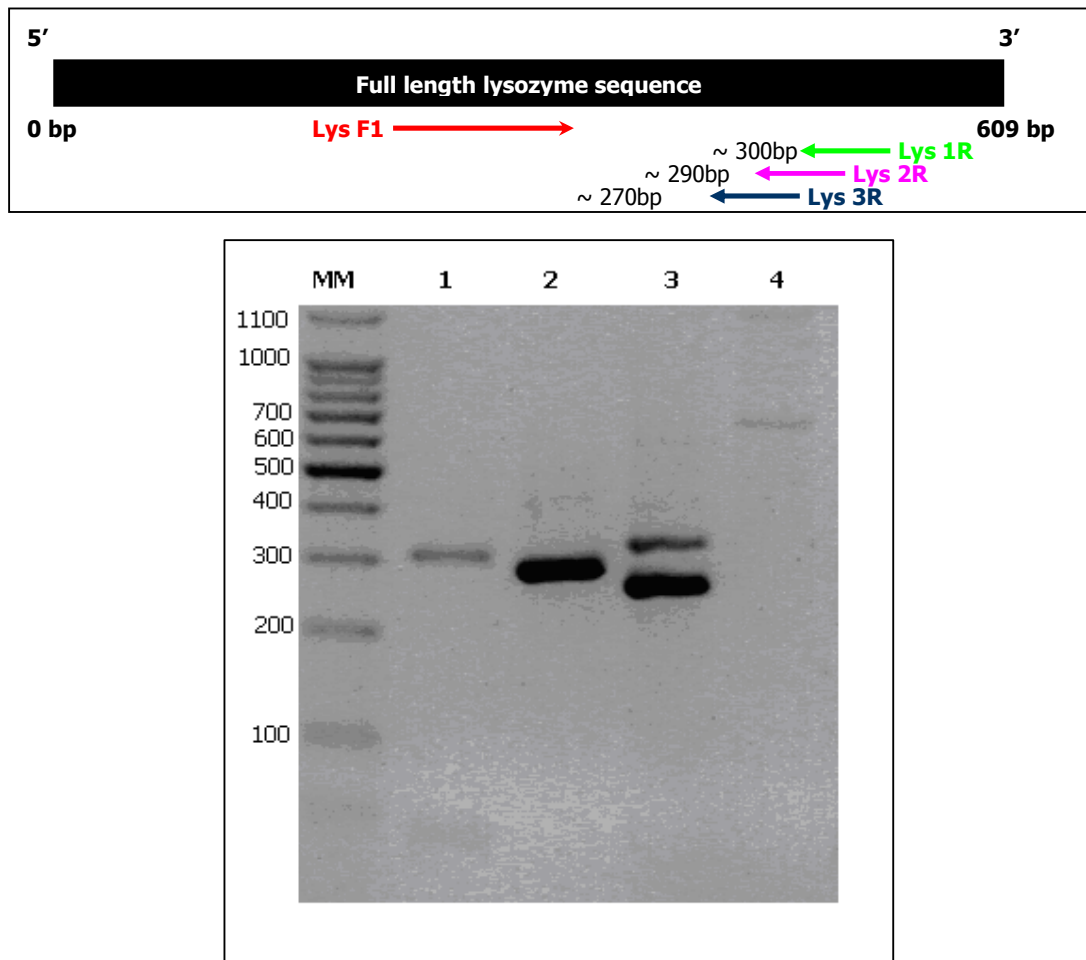
Figure 3.8: Agarose-EtBr (2.0%) gel analysis of nested PCR products: MM: 100 bp DNA ladder; Lane 1: screen with Lys F1 and Lys 1R; Lane 2: Lys F1 and Lys 2R; Lane 3: Lys F1 and Lys 3R; Lane 4: degenerate screen on gut tissue. The primers used in the PCR and the estimated expected sizes of the PCR products are shown above the gel photo.

As can be seen in lane 4 (Figure 3.8), screening with the degenerate primer produced two faint bands of approximately 1100 bp and 700 bp, in addition to a smear. This reaction solution (1 μl) was used as template in a reaction using the nested gene specific primers. These alternate primer pairs were designed to be overlapping, the expected sizes of the bands should show incremental increases.

The product (300 bp) of the nested primer reactions shown in lane 1 (figure 3.8) was precipitated and ligated into the pGEM T Easy Vector System. This specific band was chosen as it represented the largest stretch of sequence obtained with the primer pairs mentioned. Furthermore, the product in lane 3 showed the presence of a non-specific band of approximately 310 bp. Lane 2 shows ta band of ~ 290 bp, as expected. Following electroporation and plating of transformants, colony PCR revealed several positive colonies which were sequenced.

Clone number 45 (representative of the 300 bp band in lane 1 of Figure 3.8) was sequenced with the T7 primer and showed the highest identity (95%) to *O. moubata* lysozyme.
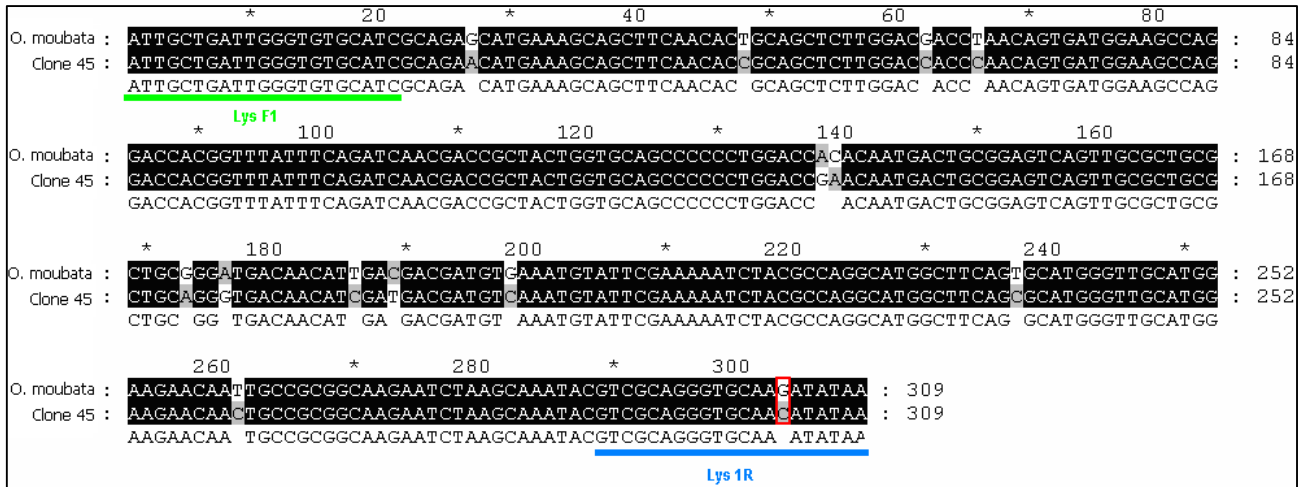
Figure 3.9: Nucleotide sequence alignment of clone 45 against the *O. moubata* lysozyme sequence: The 5' region underlined in bright green represents the region of binding of the forward primer (Lys F1) and the 3' region underlined in bright blue represents the region of binding of the reverse primer. The mutation indicated in red was forced during PCR due to a primer mismatch.

The nucleotide sequence obtained shows a 95% identity to the *O.moubata* lysozyme sequence. It should be noted at this point that the fragment was generated by means of amplification using the Lys 1R reverse primer indicating that the degenerate primer alone was inefficient, but produced the ideal result when combined with the use of nested PCR. Suppression PCR is used for the equalization of low abundance and high abundance transcripts during cDNA synthesis. It is clear, from amplification using the degenerate primer that suppression PCR does not produce ideal conditions. The transcript was only successfully amplified through the use of nested PCR. These findings may indicate that, in ticks, nested PCR represents a more efficient approach towards favourable amplification.

Alternate overlapping primers were designed internal to the Lys 1R primer. For the purposes of sequencing, largest fragment was used.

The regions highlighted in black (Figure 3.9) indicate the regions of identity between the *O. moubata* and *O. savignyi* sequences. Regions in grey and/or white indicate the nucleotide position at which base mutations have occurred during PCR. The mutation indicated in red in Figure 3.9 is a point mutation that was forced during the PCR due to a single base mismatch in the primer that was used. However, several more clones should be sequenced before the explanation of point mutations or errors incorporated during PCR may be considered valid. The final TAA beginning at position 307 is the stop codon for translation.

The corresponding amino acid sequence obtained (Figure 3.10) shows a 93% identity and 95% similarity to the *O. moubata* lysozyme sequence. Histidine 52 (position 30 in this alignment) shows the characteristic histidine of the H-branch of lysozymes, underlined in pink. This position in the case of the ixodid tick species *D. andersoni* and *D. variabilis* is occupied by a tyrosine residue. The presence of the histidine residue at a position, as observed in the case of *O. moubata*, allows for the grouping of the *O. savignyi* lysozyme into the H-branch of the *c*-type lysozyme family.
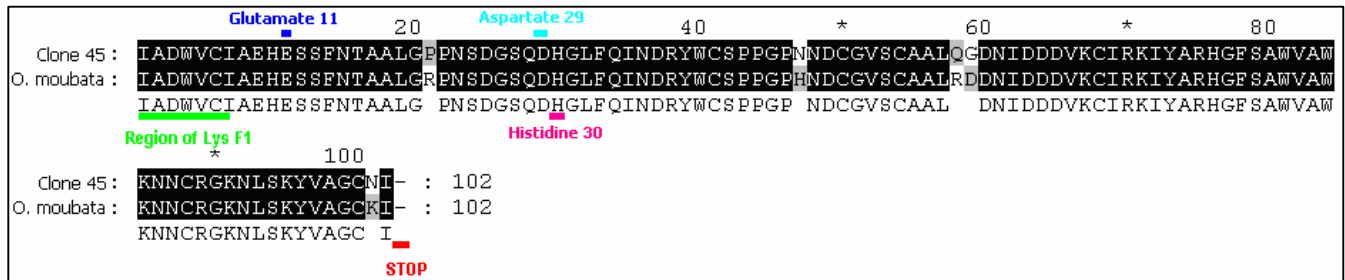
Figure 3.10: Translated nucleotide sequence alignment of clone 45 against *O. moubata* lysozyme C-terminal amino acid sequence: The active site glutamate and aspartate residues are indicated at position 11 (dark blue) and position 29 (light blue) respectively. Histidine 30 is indicated in bright pink while the position of the Lys F1 primer and the stop codon are indicated in bright green and red, respectively.

Furthermore, based upon the data available for the *O. moubata* lysozyme sequence, the Glu[33] (indicated in blue at position 11 in this alignment) and the Asp[51] (indicated in light blue at position 29 in this alignment) residues represent the active site residues involved in the catalytic activity of the molecule (Figure 3.2). The protein terminates at the isoleucine residue at position 101 in this alignment.

Despite the conservation of the active site residues and His[52], 5 specific differences in amino acids are observed. Amino acids of similar polarity are indicated by the red dots in Figure 3.10. However, the differences that are observed would be detrimental for protein folding and solubility, for example the arginine to proline substitution at position 21. If this were indeed a true mutation, the characteristic cyclic structure of the side chain of proline, would completely disrupt the native fold of the protein, changing the overall conformation of the molecule and so impact the conformation of the active site of *O. savignyi* lysozyme when compared to that of *O. moubata*. Therefore, it is highly unlikely that these are true mutations. The lysine to asparagine mutation at position 101 has already been accounted for by the single nucleotide mismatch of the Lys 1R primer. Figure 3.9 shows substitutions in the nucleotide sequence which have been attributed to possible errors incorporated during PCR. This would therefore account for the amino acid differences observed in Figure 3.10.

Before conclusive analysis, repetition of amplification and sequencing of this band in order to confirm if these are indeed true mutations or errors incorporated during PCR is essential.

The availability of the central ~300 bp sequence of lysozyme allowed for the design of a gene specific forward primer in the 3' end of this fragment suitable for 3'-RACE. This primer when used in conjunction with the poly T anchor primer produced the approximately 200 bp band observed in Figure 3.11 below.
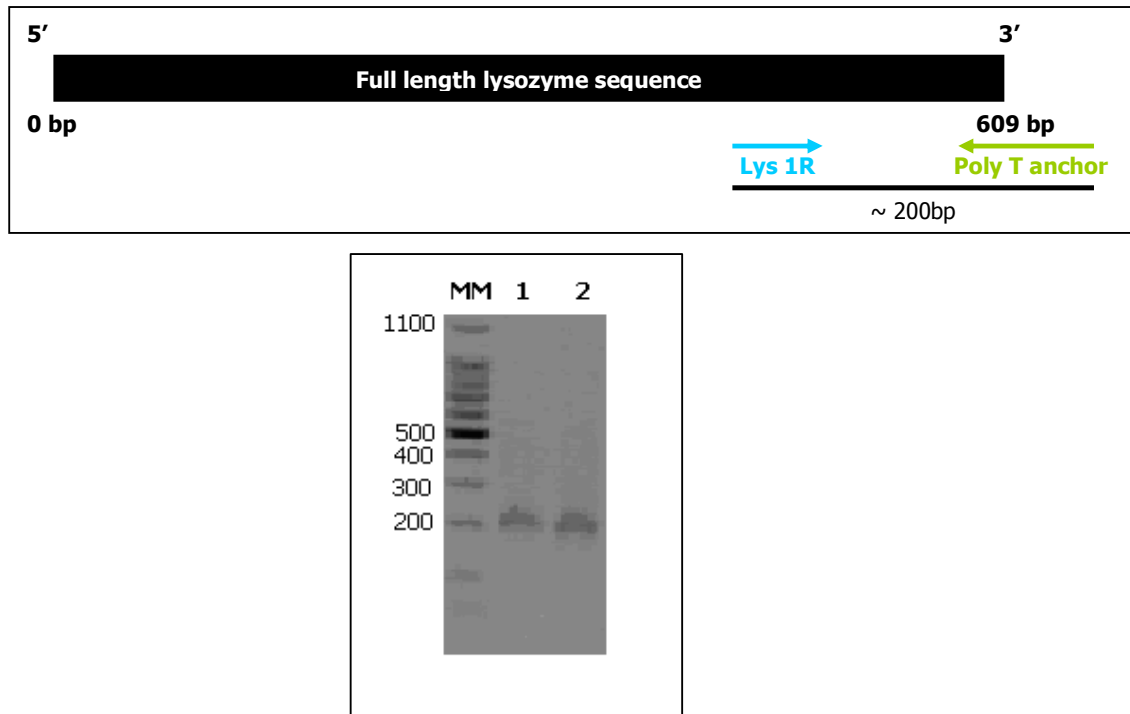
Figure 3.11: Agarose-EtBr (2.0%) gel analysis amplification of the 3' ends of lysozyme: MM: 100bp DNA ladder; Lanes 1 and 2: bands obtained by screening with Lys 1R fwd and the poly T anchor in duplicate reactions. The primers used in the PCR and the estimated expected sizes of the PCR products are shown above the gel photo.

The product of the screening reaction as seen in Figure 3.11 was pooled, precipitated and subsequently ligated into the pGEM T Easy Vector System. Following electroporation and plating of transformants, a colony PCR revealed positive clones containing the correct size of the insert. Clones 18, 20 and 22 were sequenced using the T7 primer and the results are presented in Figure 3.12.
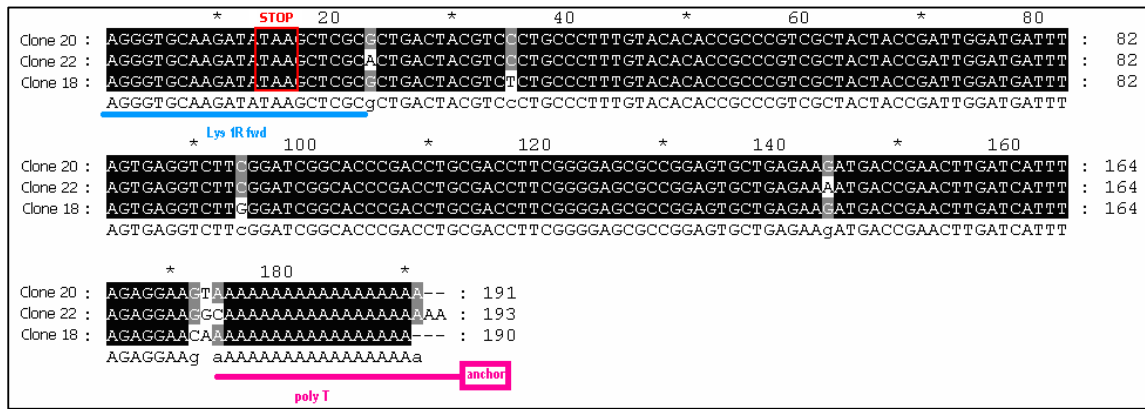
Figure 3.12: Nucleotide alignment of clones representative of the 3' UTR of O. *savignyi* lysozyme: The region underlined in bright blue represents the forward primer that was designed based on the previously derived central sequence of *O. savignyi* lysozyme.

As observed in Figure 3.12, each sequence reveals differences in single nucleotides. These differences may be due to errors misincorporated during PCR or true isoforms. Repeated sequencing of this region would confirm a final 3'-UTR (untranslated region) sequence.

Figure 3.13 shows the fully constructed 3' end of the *O. savignyi* lysozyme transcript. It should be noted that the previously derived amino acid sequence (Figure 3.10) terminates at the stop codon. Therefore, the sequences presented in Figure 3.12 represent the 3' UTR of the transcript. For this reason, the sequence was not translated to the corresponding amino acids for comparison to the *O. moubata* sequence and the comparison presented in Figure 3.13 is merely based on nucleotides.
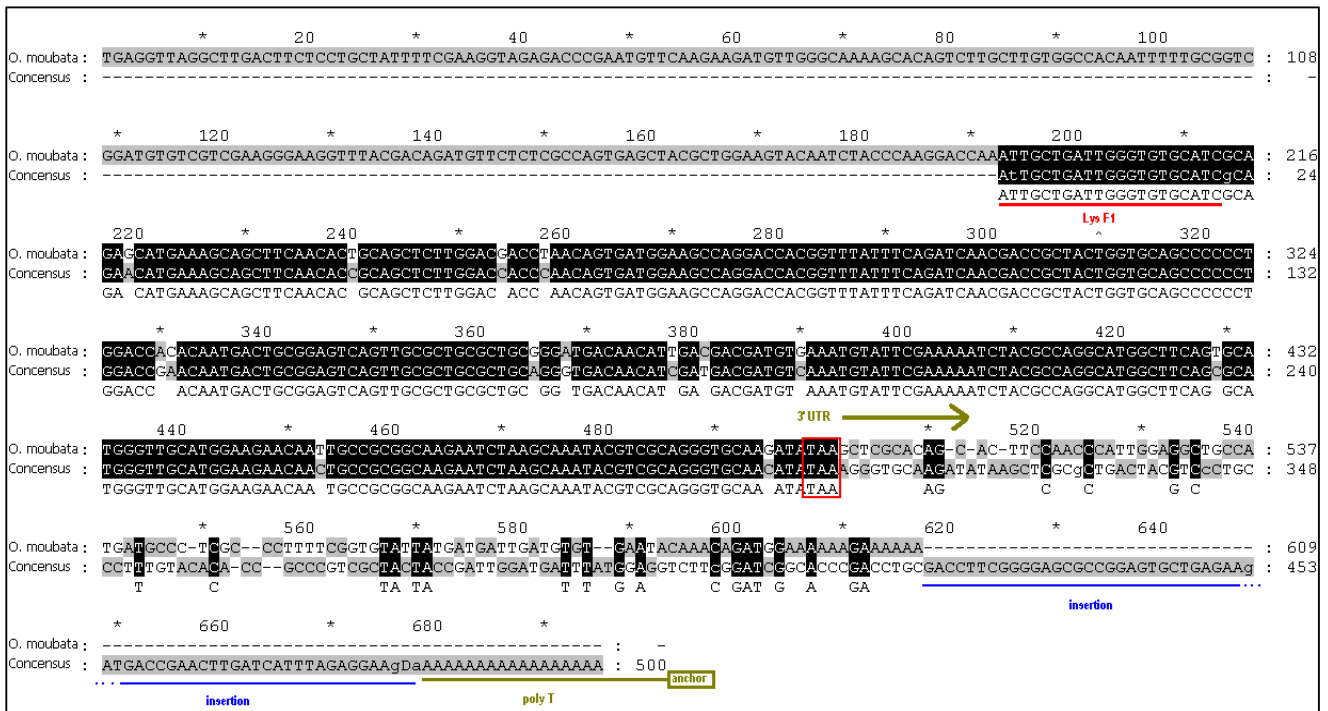
Figure 3.13: Nucleotide sequence of *O. savignyi* and *O. moubata* lysozyme sequences: The 5' region highlighted in bright red indicates the region of the forward primer Lys F1. The stop codon for translation is indicated in the red block. The UTR region of *O.savignyi* is that of a consensus obtained from clones 18, 20 and 22.

In Figure 3.13 an insertion of approximately 60 bp is seen in the 3' UTR (underlined in blue). This region upstream of the poly A tail may theoretically be involved in differential regulation of the transcript in the different species.

Youheng *et al.*, (2009) showed that transiently expressed antimicrobial peptides in *Drosophila* are differentially regulated by changes in the stability of mRNA due to the presence or absence of elements in the 3' UTR. The peptides investigated include cecropin (anti Gram-positive and antifungal activity) and diptericin (anti Gram-negative activity). A unique *cis*-acting ARE (AU-rich element) in the 3' UTR of the cecropin transcript was identified. Further immunoprecipitation studies revealed that this element facilitates an interaction with the RNA destabilizing protein Transactor Tis II. This interaction leads to degradation of the cecropin transcript. This finding has shed light on the faster decay of cecropin relative to diptericin.

The work of Kelly *et al.*, (2008) showed that the presence of a CPE-like (cytoplasmic polyadenylation element-like) sequence in the 3' UTR of the long chain *S*-crystallin peptide leads to expression of this transcript in a dark-adapted octopus while the CPE-like sequence is seen to be absent in the short chain *S*-crystallin and α-tubulin peptides typically expressed in the light-adapted octopus. The abovementioned literature indicates that the insertion

shown in the *O. savignyi* 3' UTR may be essential for the regulation of the transcript in response to differing physiological or environmental stimuli. However, in order to confirm this statement, further investigation will be required which may include mutational or deletion analysis of the region mentioned.

3.5.4 Identification of the 5' end of *O. savignyi* lysozyme

The availability of the central ~300 bp sequence of lysozyme allowed for the design of a gene specific reverse primer in order to perform 5' RACE. This primer is the reverse complementary sequence of the Lys F1 primer which when used in conjunction with the poly G anchor primer produced an approximately 80 bp band (Figure 3.14).
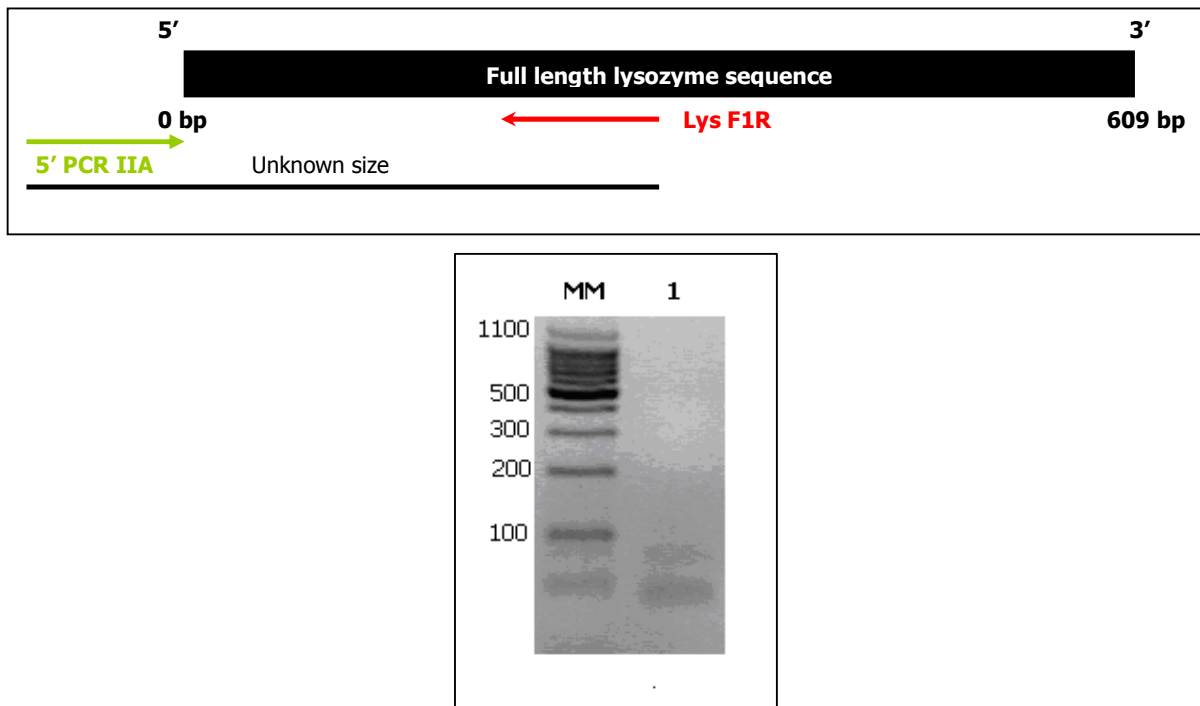
Figure 3.14: Agarose-EtBr (2.0%) gel analysis of 5' RACE products: Lane 1: 100bp DNA ladder; Lanes 2 and 3: band obtained by screening with Lys F1R and the poly G anchor. The primers used in the PCR are shown above the gel photo.

The product of the screening reaction as seen in Figure 3.14 was precipitated and subsequently ligated into the pGEM T Easy Vector System. Following electroporation and plating of transformants, a colony PCR revealed eight positive clones (1-4, 9-10, 36 and 45) which were sequenced.

The sequence obtained for the 5' end of the putative *O. savignyi* lysozyme sequence was coupled to the sequence of the 3' region of the ORF of *O. savignyi* lysozyme in order to

produce the sequence shown in Figure 3.15 (where the lower case letters indicate ambiguous nucleotides on the chromatogram which were determined manually due to poor sequencing results).
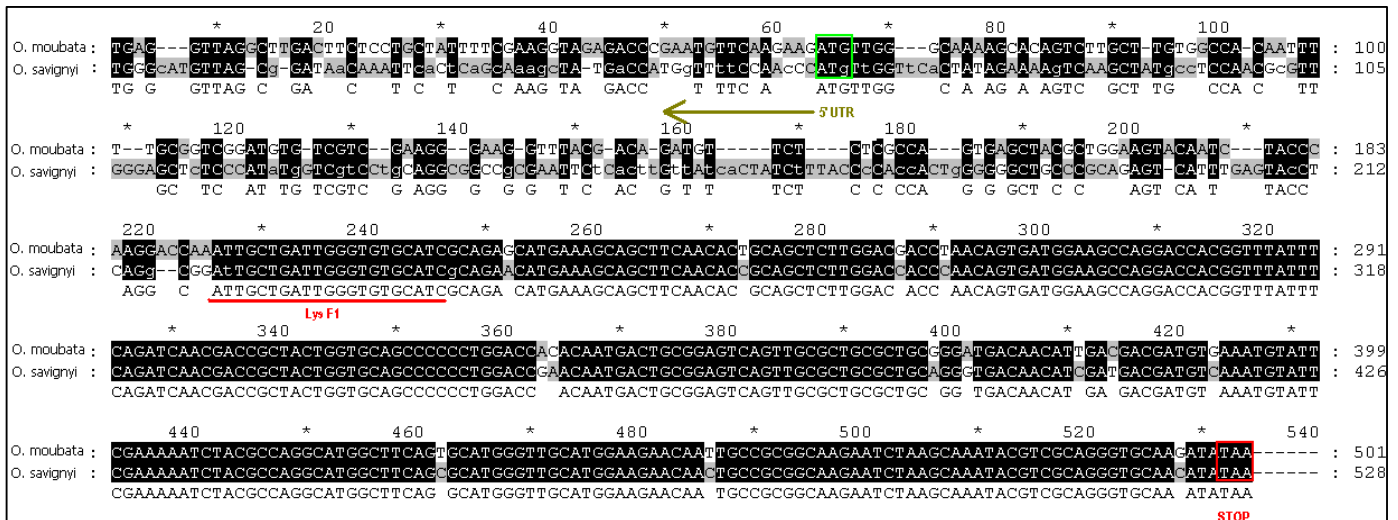
Figure 3.15: Comparison of the 5' UTR and ORF of *O. moubata* (AF425264) and *O. savignyi* lysozyme: The start codon is indicated in green while the stop codon is indicated in red. The region of the Lys F1 primer is shown in red. The 5' UTR is indicated in olive green.

Comparison of the central and 3' end of the coding sequence of the *O. moubata* and *O. savignyi* lysozyme transcripts (Figure 3.9) shows a high percentage of identity (95%), as expected. In Figure 3.15, however, the overall identity of the sequences drops significantly when including 5' RACE results. It is observed that the 5' terminal of the *O. savignyi* transcript differs significantly from that of the *O. moubata* sequence. This can be closer analysed upon comparison of the translated nucleotide sequences (Figure 3.16 A).

The translated nucleotide sequence (obtained from the sequencing of 1, 3 and 8 clones for the central, 3' UTR and 5' regions, respectively) of the *O. savignyi* lysozyme was used in position specific iteration BLAST (PSI-BLAST). A total of 284 significant sequences were returned showing high identity to the Lyz1 superfamily, with regards to the active site residues as well as the Ca^{2+} binding domains (Figure 3.16 B).

A
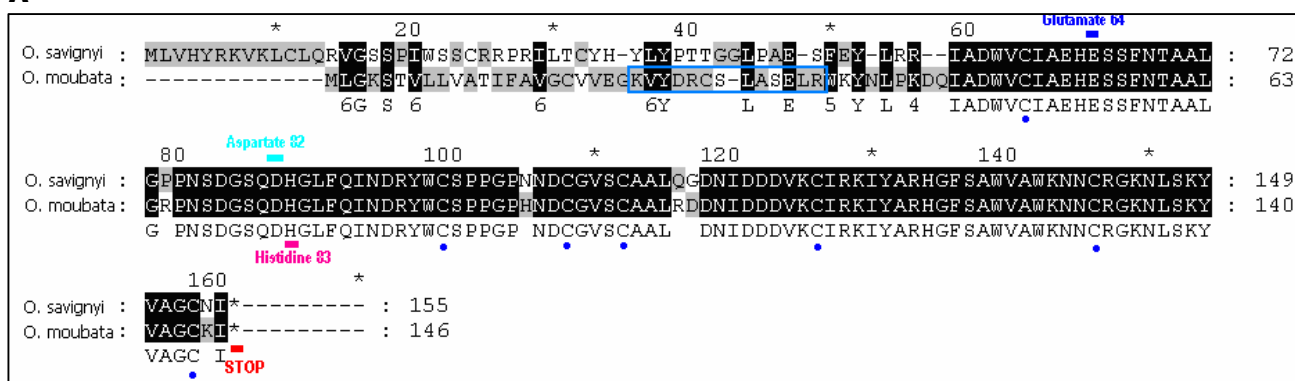
B
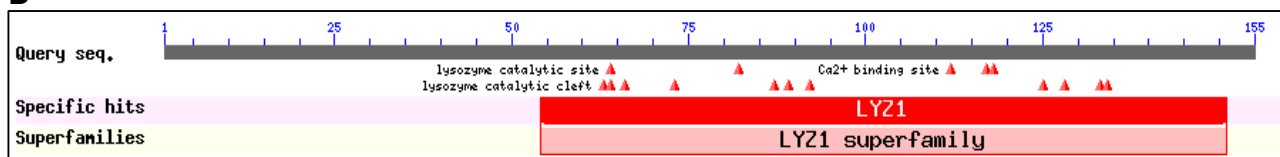
Figure 3.16: **A. Comparison of the translated nucleotide sequences of the open reading frames of the *O. moubata* and *O. savignyi* lysozyme molecules:** The active residues, Glu[64] (dark blue) and aspartate 82 (bright blue) are shown in addition to histidine 83 (pink) and the point of termination of the protein (red). The blue dots indicate the conserved cysteine residues. The cleavage of the signal peptide occurs between residues 22 and 23 in *O. moubata* and the N-terminal of the *O. moubata* lysozyme molecule as well as the DRCSLA motif characteristic of digestive lysozyme molecules, is enclosed within the blue block. **B. Illustration of the position specific (domain) identity of PSI-BLAST hits:** The query sequence represents the *O. savignyi* lysozyme sequence. It should be observed that the query sequence matches the catalytic sites as well as the Ca^{2+} binding sites of members of the LYZ1 superfamily of lysozyme molecules

The amino acid sequences in Figure 3.16A shows significant differences between both members of the argasid tick family. The sequencing of 3 clones for the elucidation of the 3' UTR revealed the differences observed in Figure 3.13. Since this region is not within the coding sequence, no changes were observed with regards to the amino acid sequence. Furthermore, Figure 3.16B shows the conservation of the active site residues identified in *O. savignyi* lysozyme with that of other species identified by PSI-BLAST.

With regards to the 5' sequence, however, differences are already observed at the nucleotide level within the coding sequence (Figure 3.15). It is therefore unlikely that the sequence obtained is the correct 5' end of the *O. savignyi* lysozyme. Despite a calculated 65% identity (63% between ixodid and argasid ticks) at the amino acid level, such drastic changes can not be attributed to evolutionary divergence.

Figure 3.5 shows the 8 strictly conserved cysteine residues across both the argasid and ixodid tick species. In Figure 3.16, only 7 of these cysteine residues are present in the correct position; all outside the region identified during 5' RACE.

Biochemical characterization of tick gut lysozyme (TGL) has shown that this molecule possesses an N-terminal amino acid sequence (K-V-Y-D-R-C-S-L-A-S-E-L-R) (Figure 3.16) and shows high identity to vertebrate digestive lysozymes. Furthermore, the DRCSLA motif typical of digestive lysozymes (Grunclova *et al.*, 2003) is clearly indicated in the *O. moubata* sequence in Figure 3.16; but also absent from the 5' RACE region.

The translated nucleotide sequence of the *O. savignyi* 5' terminal shows neither all 8 conserved cysteine residues, nor the correct cleavage site or the characteristic motif of digestive lysozymes. For this reason and from the results observed in Figure 3.16 it is confirmed that the 5' sequence of the *O. savignyi* lysozyme molecule was not successfully elucidated.

3.5.5 Tissue expression profile of *O. savignyi* lysozyme

In ticks, stimuli for induction of transcription include feeding as well as bacterial challenge. Depending upon the functional importance of a gene product within a specific tissue under stimulatory conditions, differences in expression are expected.

In the case of *O. moubata,* the highest levels of expression were seen following feeding in the hemocytes and midgut with much lower levels of expression in ovaries, salivary glands and malpighian tubules (Kopacek *et al.,* 1999). Furthermore, lysozyme expression was seen to peak 16 hours post obtaining a blood meal (Grunclova *et al.,* 2003). The high level of expression observed in the hemolymph was assumed to be due to possible contamination by midgut contents during the collection of hemolymph, although this effect was seen only following feeding.

The situation in ixodid ticks differs slightly. In 2004, Simser *et al.* observed that lysozyme expression occurs at the highest levels in hemocytes followed by the midgut, ovaries, salivary glands and malpighian tubules. Furthermore, lysozyme expression in partially fed *D. variabilis* ticks was upregulated in response to hemocoel inoculation with the Gram-negative *E. coli*. The highest level of expression was observed at 72 hours post inoculation.

The tissue expression profile that presents itself in terms of *O. savignyi* (Figure 3.17) suggests that the expression of *O. savignyi* lysozyme is constitutive in the midgut and ovaries. This is due to the fact that no significant differences are observed following feeding and/or bacterial challenge.
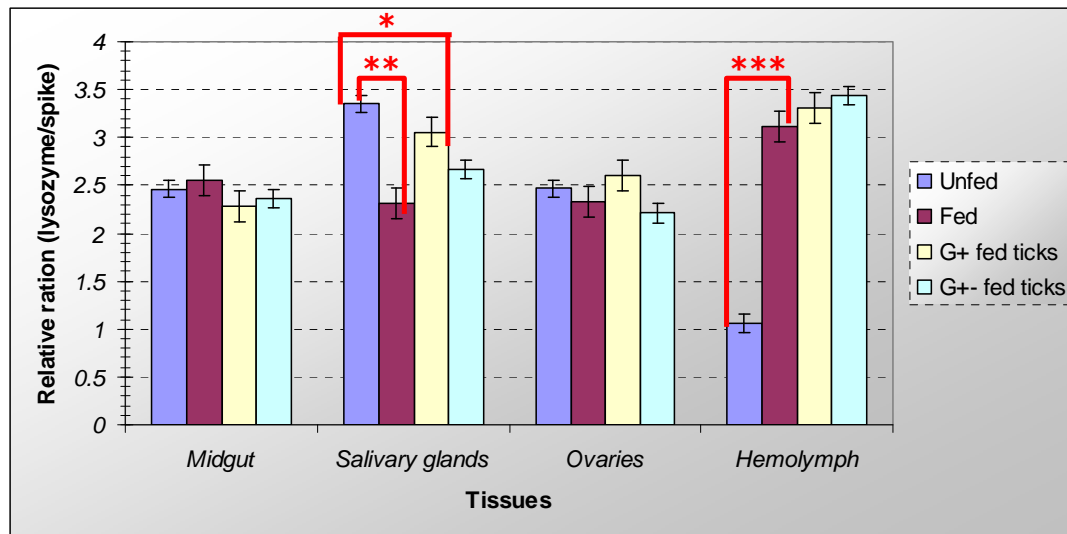
Figure 3.17: Tissue expression profile of lysozyme: Profiles were constructed using adult female unfed, fed on sterile blood, fed on Gram-positive infected blood and fed on mixed Gram-positive and Gram-negative infected blood ticks. (n=3) (* = 1 x 10^{-5}, ** = 4.5 x 10^{-7} and *** = 5.4 x 10^{-7} as calculated using Microsoft Excel).

A statistically significant (P=5.4X10^{-7}) three-fold upregulation of lysozyme expression is observed in hemolymph following feeding. The response seen in the case of ticks fed on Gram-positive bacteria or a combination of Gram-positive and Gram-negative bacteria is approximately equivalent to that observed in fed ticks indicating that the observed response is primarily due to feeding and not bacterial ingestion. This is similar to findings in *O. moubata*.

With regards to salivary glands, it is observed that a higher level of expression occurs in unfed ticks and feeding on Gram-positive infected blood showed a higher level of expression relative to samples where ticks were fed on sterile blood or blood infected with a combination of Gram-positive and Gram-negative bacteria. The Student t-Test shows that the difference between unfed and fed samples is indeed statistically significant (P-value of 4.5X10^{-7}). A P-value of 1.6X10^{-5} was calculated for the Gram-positive bacteria fed samples. This result is therefore statistically significant. It is proposed that lysozyme possesses a role in feeding. In salivary glands, it is observed that feeding leads to a decrease in the levels of the lysozyme transcript. Since several physiological changes occur in salivary glands of ticks following feeding, it may be assumed that the typical upregulation of salivary gland specific peptides shifts the equilibrium of transcription to favour these peptides, while the expression of peptides of low functional importance, in this case, lysozyme, shows a marked decrease. In the case of ticks fed on Gram-positive bacteria, it is seen that there is less down-regulation of the transcript. This may suggest that lysozyme is involved in the elicitation of

an antimicrobial response against Gram-positive bacteria. This response is however only observed in salivary glands.

Several differences are observed when comparing the tissue expression of lysozyme in *O. moubata* and *O. savignyi*. First, the highest level of expression in *O. moubata* was found to be in the midgut while in *O. savignyi* the highest level was observed in salivary glands. Second, in *O.* moubata feeding increased the mRNA levels in the salivary glands and showed no effect in the hemocytes, while the converse is seen for *O. savignyi*. The response of transcript levels following bacterial ingestion was not previously investigated in *O. moubata* and so this work for *O. savignyi* represents a unique observation with regards to argasid ticks.

The situation observed for *O. savignyi* may differ from that observed in *O. moubata* for several reasons. In the case of *O. moubata,* the feeding history of the ticks was known since laboratory cultured ticks were used. The *O. savignyi* ticks were collected from the wild and so the feeding, injury and bacterial challenge history is unknown. This fact may contribute to the differences observed between these species. Furthermore, the induction of lysozyme in response to bacterial challenge in this case by ingestion has not been investigated in argasid ticks. This work therefore represents the first indication of the argasid response of lysozyme to bacterial ingestion.

3.6 Concluding remarks

Lysozyme is classified as an enzyme catalyzing the cleavage of the β-1,4-glycosidic bond linking NAM and NAG in the peptidoglycan cell wall of bacteria, thereby eliciting antibacterial activity. In ticks, feeding is a non-sterile process, since several different microorganisms may be ingested during the bloodmeal. The presence of lysozyme in the midgut therefore could provide antibacterial protection against any bacteria that may be ingested.

In the ixodid tick *D. variabilis* and *D. andersoni* cell lines co-cultured with *E. coli*, lysozyme was seen to be upregulated in response to challenge with Gram-negative *(E. coli)* bacteria (Simser *et al.,* 2004) while in the argasid tick *O. moubata*, lysozyme was upregulated in the midgut in response to feeding (Kopacek *et al.,* 1999).

In *O. moubata*, the active site residues are identified as Glu^{33} and Asp^{51} while a His residue at position 52 replaces the Tyr residue at the corresponding position in hen egg white lysozyme. This allows for the classification of tick lysozyme into the H-branch of lysozymes. The partial amino sequence (ie. excluding the 5′ sequence) of the *O. savignyi* lysozyme reveals 71% similarity and 65% identity to that of *O. moubata* revealing the presence of homologous lysozyme molecule in these closely related species. The active site residues (Glu^{64} and Asp^{82}) as well as the unique His residue at position 83 are conserved. This allows for the classification of *O. savignyi* lysozyme into the H-branch of lysozymes.

In this chapter, a partial sequence of the *O. savignyi* lysozyme homolog was identified. As shown in Figure 3.16, the 5′ sequence obtained is not representative of a homologous sequence. This is due to the lack in conservation of the typical 8 cysteine residues as well as the characteristic motif of digestive lysozymes and the site of cleavage of the signal peptide. Both *O. moubata* and *O. savignyi* are closely related species that show recent species divergence (Mans *et al*., 2003) and such drastic mutations are not likely. Furthermore, the work of Herbeck *et al.* (2005) revealed that the dispensability and functionality of a protein determines evolution within closely related species. Lysozyme, due to its antimicrobial function, is regarded indispensable and of high functionality. This alone confirms that it is unlikely that the 5′ sequence obtained in this chapter is due to evolution of lysozyme at the time of divergence between *O. moubata* and *O. savignyi*. Further PCR of this region using alternate reverse primers and overlapping 5′ primers, as used for the elucidation of the central sequence, may prove successful.

It should be noted that the degenerate primer alone was inefficient when used alone, however, did produce the correct transcript when combined with the use of nested PCR. It is clear that amplification using a degenerate primer does not produce ideal conditions. The transcript is indeed present however is only successfully amplified through the use of nested PCR. These findings may indicate that nested PCR represents a more efficient approach towards favourable amplification.

Further investigations on the elucidation of the *O. savignyi* lysozyme sequence should include the sequencing of several more clones in order to confirm the sequences obtained and disprove the claim of induced mutations during analysis. Furthermore, new primers should be designed for the 5' region of the transcript.

The tissue expression profile in *O. savignyi* reveals constitutive expression of lysozyme in the midgut and ovaries, with no statistically significant differences between fed (uninfected) and bacteria-fed ticks. With regards to the hemolymph, the response seen in the case of ticks fed on Gram-positive bacteria or a combination of Gram-positive and Gram-negative bacteria is essentially equivalent to that observed in fed ticks indicating that the observed response is primarily due to feeding and not bacterial ingestion. This pattern of expression was observed in the case of defensin as well (Chapter 4). A statistically significant ($P=5.4 \times 10^{-7}$) upregulation of lysozyme expression is observed in hemolymph following feeding. In the case of salivary glands, the levels of expression decreases following feeding. This may be attributed to the fact that lysozyme functions in the digestion of bacterial cell walls. During feeding, several other essential genes may be upregulated in the salivary glands and no energy is expended on the transcription of lysozyme if the molecule is not essential in this organ at this time.

Additionally, an increase in the levels of the transcript was observed in salivary glands in response to feeding on Gram-positive bacteria. This is in direct contrast to the data published for ixodid ticks, where lysozyme expression in salivary glands is upregulated in response to Gram-negative bacteria. This may be attributed to the fact that in this case, *O. savignyi* ticks were fed artificially on blood containing bacteria. In the case of *D. variabilis*, *E.coli* was inoculated into the hemocoel of ticks. This difference in the route of entry may allow for a possible explanation of the differences observed. The data obtained does not allow any conclusive statement regarding this phenomenon, however it may be suggested that a possible synergism or transcriptional linkage occurs between an AMP targeting Gram-positive bacteria and lysozyme (Sonenshine & Hynes, 2008). This would theoretically

translate to the fact that as the intracellular levels of this proposed AMP is increased, so too are the levels of lysozyme increased.

However, the presence of mRNA does not directly correlate to the presence of active protein. For this reason, a future perspective would include simple protein assays which will allow for correlation of expression levels with differing stimuli of induction.

Alternatively, the data may suggest a differential mechanism of antibacterial activity elicited by lysozyme, contrary to the currently available knowledge on the topic. However, further investigations will be required in order to confirm such possibilities.

Chapter 4:

In vivo functional analysis of lysozyme and defensin in the argasid tick, *O. savignyi*

4.1 Introduction

The identification and molecular characterization of immunoprotective and immune responsive candidates have become a prominent feature in the field of tick research. Chapter 3 focused on the identification and molecular characterization of one such candidate, lysozyme from the soft tick while two defensin isoforms have already been identified in *O. savignyi*, in 2007 (M.E. Botha, University of Pretoria, Biochemistry). In order to assess the contribution of these candidates to *O. savignyi* innate immunity, specialized techniques are required.

RNA interference (RNAi) is characterized as a reverse genetic approach facilitating a functional investigation of a gene or the outcome of hindering its expression (de la Fuente *et al.,* 2007). This mechanism is based on the fact that double stranded RNA (dsRNA) of the gene of interest which is injected intracellularly, activates the enzyme Dicer to bind to the dsRNA and cleave it into 20-25 base pair fragments, so-called siRNA (small interfering RNA). The guide strand (strand involved in binding to the target mRNA) is then bound to a second protein complex called RISC (RNA induced silencing complex) which then binds to the target mRNA. Argonaute, the catalytic domain of the complex , is involved in the actual cleavage of the mRNA and the subsequent silencing of expression of the mRNA. The anti-guide strand is degraded during the activation of the RISC complex.

A model for the mechanism of RNAi in ticks (Figure 4.1) has been based upon investigations into *D. melanogaster,* the model organism for insects (Kavi, 2005).
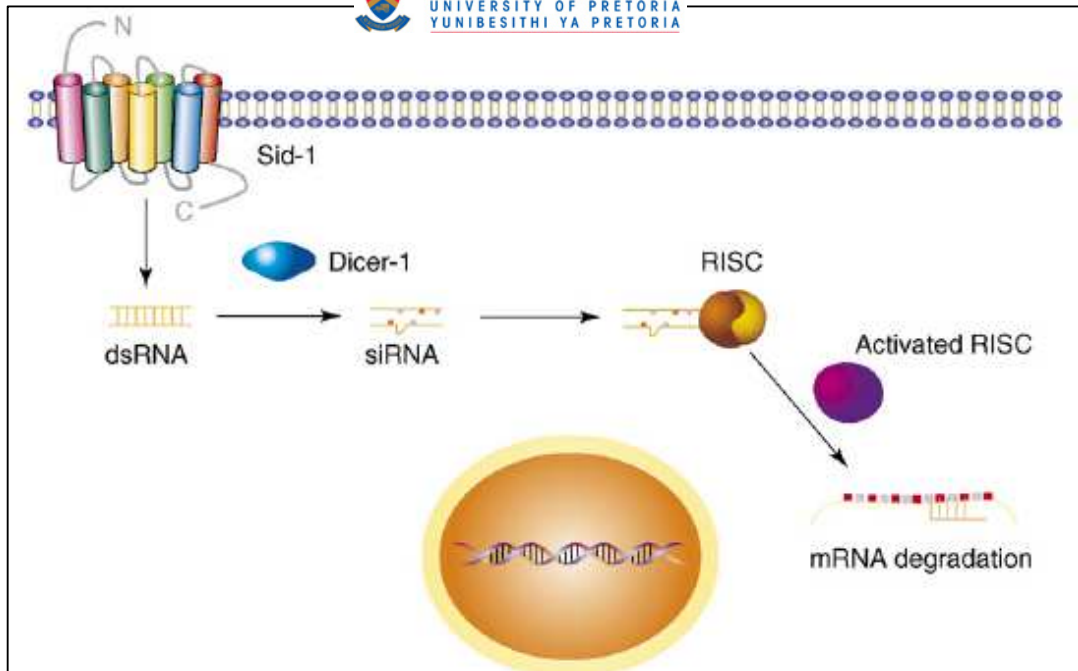
Figure 4.1: Diagrammatic representation of the proposed mechanism of RNAi in ticks (de la Fuente *et al*., 2007)**:** Sid-1 represents the putative membrane bound protein involved in the transport of dsRNA into a cell. Activated Dicer-1 is then involved in the cleavage of the dsRNA into 20-25nt long fragments known as siRNA. The guide strand, complementary to the sequence of the target mRNA then binds to the RISC complex which facilitates binding and cleavage of the target mRNA.

dsRNA may be administered to ticks in a variety of ways including injection of the dsRNA directly into the body cavity, soaking or incubation of a wounded tick (usually induced by the severing of a coxa), capillary feeding with dsRNA-containg blood or *in vivo* viral production of the dsRNA (de la Fuente *et al.,* 2007). Several attempts have been made at the silencing of ixodid genes. The method and outcome (observed phenotype) are summarized in Table 4.1.

In ticks, the major region for digestion has been characterized as the digestive cells of the midgut epithelium. Tick feeding is a non sterile process and the ingested bloodmeal comprises the optimal composition and temperature for the survival of microorganisms. For this reason, it is essential that ticks devise a mechanism of eradication or neutralization of these microbes (Kopacek *et al.*, 1999).

Table 4.1: Summary of RNAi studies in ixodid ticks (de la Fuente *et al.*, 2007)

Tick species	Target gene[a]	Delivery of dsRNA[b]	Phenotype
Study of tick gene function			
Amblyomma americanum	Histamine-binding protein (HBP)	Soaking of salivary glands Injection in ticks	Reduction of histamine-binding activity in salivary glands and aberrant tick feeding pattern
A. americanum	Synaptobrevin	Soaking of salivary glands	Inhibition of PGE$_2$-stimulated anticoagulant protein secretion by isolated salivary glands
A. americanum	nSec1	Soaking of salivary glands Injection in ticks	Reduction in anticoagulant protein release by salivary glands and aberrant tick feeding
A. americanum	Synaptobrevin cystatin	Soaking of salivary glands Injection in ticks	Inhibition of tick feeding and reduced tick weight
A. americanum	Subolesin (4D8)	Injection in ticks	Reduction in tick survival, weight and oviposition
Ixodes scapularis	Salp14	Microinjection in ticks	Reduction in anticoagulant activity in salivary glands and reduction in tick weight
I. scapularis	Salp14	Microinjection into nymphal ticks	Reduction in mRNA levels but no effect on tick feeding
I. scapularis	Actin	Microinjection and injection in ticks	Inhibition of tick feeding and reduction in tick weight
I. scapularis	Subolesin (4D8)	Injection in ticks	Reduction in tick weight and oviposition
I. scapularis	5' nucleotidase (4F8)	Injection in ticks	Reduction in tick survival, weight and oviposition
I. scapularis	Semliki Forest virus (SFV) replicon	Infection of ISE6 cells with recombinant SFV expressing viral suppressors	Suppression of RNAi induced by SFV replicon
I. scapularis	Subolesin (4D8)	Soaking of IDE8 cells	Reduction in mRNA levels
Haemaphysalis longicornis	Cubilin-related serine proteinase (HISP)	Microinjection in ticks	Reduction in tick weight
H. longicornis	Follistatin-related protein (FRP)	Microinjection in ticks	Reduction in tick oviposition
H. longicornis	Longepsin	Injection in ticks	Reduction in mRNA and protein levels
Rhipicephalus sanguineus	Subolesin (4D8)	Injection in ticks	Reduction in tick survival, weight and oviposition
R. sanguineus	Rs86 (homologue of Bm86)	Injection in ticks	Reduction in tick weight and oviposition
Dermacentor variabilis	Subolesin (4D8)	Injection in ticks	Reduction in tick survival, weight and oviposition. Diminished reproductive performance and absence of viable offspring
Dermacentor marginatus	Subolesin (4D8)	Injection in ticks	Reduction in tick survival, weight and oviposition
Boophilus microplus	Subolesin (4D8)	Injection in unfed and replete ticks	Reduction in tick survival, weight and oviposition. Abnormal egg development. Systemic RNAi on tick progeny
B. microplus	Bm86	Injection in unfed and replete ticks	Systemic RNAi on tick progeny
B. microplus	Bm91	Injection in unfed and replete ticks	Systemic RNAi on tick progeny
Characterization of tick–pathogen interface			
I. scapularis	TROSPA	Microinjection into nymphal ticks	Reduction in infection and transmission of *B. burgdorferi*
I. scapularis	Salp15	Microinjection into nymphal ticks	Reduction in the capacity of tick-borne *B. burgdorferi* to infect mice
I. scapularis	Salp16	Microinjection into nymphal ticks	Reduction of survival of *A. phagocytophilum* in ticks
I. scapularis	Salp14	Microinjection into nymphal ticks	Reduction in mRNA levels but no effect on acquisition of *A. phagocytophilum* and *B. burgdorferi*
I. scapularis	Isac	Nymph capillary feeding	Reduction in tick weight and infection with *B. burgdorferi* and affected expression of salivary gland and non-salivary gland proteins
D. variabilis	Subolesin (4D8)	Injection in ticks	Reduction in tick infection by *A. marginale*
Screening and characterization of tick protective antigens			
I. scapularis	cDNA pools	Injection in ticks	Reduction in tick weight and oviposition
R. sanguineus	Subolesin (4D8) and Rs86	Injection in ticks	Synergistic effect on tick weight and oviposition

4.1.1 Defensins

These AMPs, found in species ranging from vertebrates to invertebrates are typically characterized as small cationic AMPs of approximately 45 amino acids (Bulet *et al.,* 2004). Defensins possess 6 characteristic cysteine residues which are involved in the formation of 3 disulfide bridges. In general, defensins are found in the mucosal cells of the small intestines, phagocytes of mammals and the hemolymph of insects (Ganz *et al.,* 1995). Defensins may be divided into three major families (Figure 4.2):

Classical defensins

These mammalian defensins have been found to be stored in secretory cells, phagocytes as well as Paneth cells. The overall structure of these peptides is a triple stranded β-sheet connected to an orthogonally projecting β-hairpin hydrophobic finger. Classical defensins are typically active at concentrations of 1-100 μg/ml against both Gram-positive and Gram-negative bacteria, mycobacteria, fungi and some enveloped viruses (Ganz *et al.,* 1995).

β-defensins

Peptides of this family consist of 38 to 42 amino acid residues and include the bovine tracheal antimicrobial peptide (TAP), the bovine neutrophil β-defensin (BNβD) as well as gallicin of chicken leucocytes. The activity of β-defensins is directed against both Gram-positive and Gram-negative bacteria at an effective concentration of 10-100 μg/ml (Ganz *et al.,* 1995).

Insect defensins

These defensin peptides are usually upregulated in response to injury or by the penetration of Gram-positive bacteria. Cells of the fat body are predominantly responsible for the synthesis and secretion of these 38-45 amino acid peptides. The overall structure of these peptides involves an α-helix linked to an antiparallel β-sheet by a connecting loop (Ganz *et al.,* 1995).

The overall mechanism of action of insect defensins has been postulated to be mediated by channel formation within microbial membranes, resulting in membrane depolarization, the inhibition of cellular respiration or the depletion of ATP and cell death (Arrieta *et al.,* 2006).

Figure 4.2: Ribbon structures of the α- and β-defensins of mammals as well as the insect defensins (Hoffmann *et al.*, 1999)**:** The α- and β- defensins clearly show the three β-sheets involved in the formation of these structures. In insect defensins, the typical two β-sheets linked via loops to an α-helix is evident.

4.1.2 Tick lysozyme and defensin

As mentioned in chapter 3, lysozyme is classified as an enzyme catalyzing the cleavage of the β−1,4-glycosidic bond linking NAM and NAG in the peptidoglycan cell wall of bacteria, thereby eliciting antibacterial activity (Nakajima *et al.,* 2003). *D. variabilis* lysozyme expression was upregulated in response to hemocoelic injection of *E. coli* while in *O. moubata* lysozyme expression was upregulated in response to feeding.

In ixodid ticks, the major activity of defensins is against Gram-positive bacteria, however activity against Gram-negative bacteria and eukaryotic pathogens is also observed. In argasid ticks, the analysis of the four defensin isoforms indicated upregulation of these isoforms following a bloodmeal. Furthermore, specific activity against *Staphylococcus aureus* was observed. Table 4.2 summarizes the recently discovered tick defensins.

Table 4.2: Tick defensins

Tick	Defensin	Life stage or organ	Induced by:	Reference
D. variabilis	Varisin	Hemolymph	*Borrelia burgdorferi*	Sonenshine *et al.*, 2003
H. longicornis	Longicin	All life stages and hemolymph, midgut, fat body, salivary glands and ovaries	Gram positive bacteria, fungi and *Babesia sp.*	Tsuji *et al.*, 2007
A. hebraeum	Defensin peptide 1	Constitutive expression in all tissues	Feeding	Lai *et al.*, 2004
	Defensin peptide 2	Hemolymph	Gram positive bacteria	
A. americanum	Americin	Constitutive expression in all tissues and life stages	Spirochetes	Todd *et al.,* 2007
H. longicornis	*Hl* gut defensin	Midgut	Gram positive bacteria	Zhou *et al.*, 2007
	Hl salivary gland defensin	Salivary glands		
D. variabilis	Defensin 2	Midgut and fat body	*Rickettsia montanensis*	Ceraul *et al.*, 2003
O. moubata	Isoforms A-D	Constitutive in midgut, fat body and ovaries	Bloodmeal, *Staphylococcus aureus*	Nakajima *et.al.*, 2002

In the argasid tick, *O. moubata*, an upregulation of the defensin gene was observed due to septic injury (injection of bacteria or bacterial cell wall components) (Nakajima *et al.,* 2003). Four isoforms (A, B, C and D) have been identified to date.   The molecular weights are approximately 4 kDa and following the cleavage of a signal peptide, the mature isoforms contain 6 cysteine residues involved in the formation of 3 disulfide bridges stabilizing the 37 amino acid mature peptide (Nakajima *et al.,* 2001). All four isoforms (A, B, C and D) were seen to be upregulated at approximately 4 hours post blood meal while upon hemocoelic injection of bacteria, only isoforms A and B were upregulated indicating unique regulation mechanisms.   It has been shown that the *O. moubata* defensin is able to disrupt the membrane potential of cells within a period of 30-60 minutes, which is referred to as the "slow killing effect" (Nakajima *et al.,* 2002).

4.1.3 RNAi mediated silencing of tick defensins

Hynes *et al.* (2008) attempted the RNAi mediated silencing of varisin, an ixodid defensin from *D. variabilis*. Analysis of silencing in hemocytes by means of real time PCR showed that the transcript was indeed silenced (>99%). A radial immunodiffusion assay using *M. luteus,* hemolymph and various tissue extracts of silenced ticks, revealed that growth of this

microorganism was uninhibited in the presence of extracts from varisin silenced ticks. Interestingly, hemolymph of varisin silenced ticks was able to inhibit the growth of *M. luteus* (although varisin was successfully silenced) indicating the presence of additional anti-microbial activity. This antimicrobial activity was attributed to lysozyme which is known to be expressed by hemocytes of *D. variabilis*. Johns *et al.,* (2001) showed that lysozyme, in combination with varisin was able to enhance the overall antimicrobial activity of varisin and strengthen a synergistic effect between these two antimicrobials in ixodid ticks.

Furthermore, Sonenshine & Hynes, (2008) suggested synergism in the activity of tick defensins and lysozyme. The abovementioned work of Johns *et al.,* (2001) and Hynes *et al.,* (2008) suggests that the antimicrobial activity that remains following the silencing of varisin may be attributed to the expression of lysozyme by the hemocytes. For this reason, an attempt will be made to silence both defensin and lysozyme of the argasid tick, *O. savignyi* and analyse the effect on tick survival.

4.2 Hypothesis

Silencing of *O. savignyi* defensins or lysozyme will affect the survival of bacterially-challenged ticks (Gram-positive, Gram-negative and a combination of Gram-positive and Gram-negative bacteria). Furthermore, it is hypothesized that co-silencing of both antimicrobials will have an effect of higher significance in bacterially challenged ticks compared to individual silencing.

4.3 Aims

1. To determine the tissue expression profile of defensins in *O. savignyi*
2. To silence *O. savignyi* defensins and lysozyme using *in vivo* RNAi
3. To assess the phenotype of silenced ticks after feeding and bacterial challenge

4.4 Materials and Methods

4.4.1 Primer design

Tissue expression profiling was performed using real time PCR with gene specific primers. Gene specific primers were designed using the two defensin isoforms of *O. savignyi* sequenced by Ms M.E. Botha (2007), and the lysozyme sequence identified in chapter 3. RNAi Upper represents an initial primer which was designed for the incorporation of the T7 site into the fragment selected. Due to the futile attempts at obtaining significant product from defensin (as only low concentration of template was purified following amplification), RNAi Upper New and RNAi Lower were designed for the incorporation of the T7 site flanking the region selected for RNAi. The primers designed for real time analysis include RNAi L- (with the same sequence as RNAi lower without the T7 flanking sequence) and Def RTF.

T7 Lys F1 and T7 Lys R1 represent the primers that were designed for the incorporation of the T7 site flanking the region selected for RNAi of *O. savignyi* lysozyme. In the abovementioned primer sequences, the italicized underlined sequence represents the T7 sequence. The primers designed for real time analysis included Lys F1R and Lys 1F.

Figure 4.3 illustrates the estimated position of the primers while Table 4.3 lists the sequences and melting temperatures of the abovementioned primers.
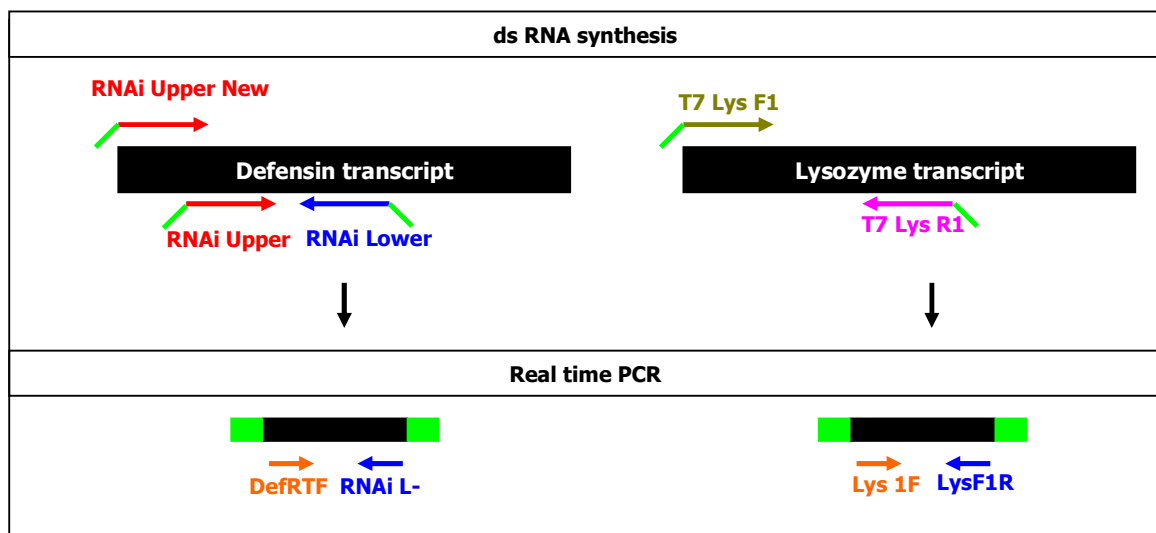
Figure 4.3: Diagrammatic representation of the estimated position of the primers used for ds RNA synthesis and real time PCR. The green overhangs represent the T7 sequence

Table 4.3: List of primers used in the incorporation of T7 sites and for real time PCR: the italicized and underlined segments represent the fragment of the T7 sequence

	Primer name	Nature Use	Sequence (5' --> 3")	Melting temp (°C)
Defensins	RNAi Upper	Gene specific (dsRNA synthesis)	_taa tac gac tca cta tag_ GCT ACA AAG GAG GCT ACT GC	63
	RNAi Upper New	Gene specific (dsRNA synthesis)	_taa tac gac tca cta tag_ GTC CGT TTA ATC AGT ACC AGT	68
	RNAi Lower	Gene specific (dsRNA synthesis)	_taa tac gac tca cta tag_ TTA CAT GTC TGC TTG AAC GC	61
	RNAi L-	Gene specific (real time PCR)	TTA CAT GTC TGC TTG AAC GC	58
	Def RTF	Gene specific (real time PCR)	ATT TCC CCA GAG TCC GCC GT	61
Lysozyme	T7 LysF1	Gene specific (dsRNA synthesis)	_taa tac gac tca cta tag gg_ ATT GCT GAT TGG GTG TGC ATC	64
	T7 LysR1	Gene specific (dsRNA synthesis)	_taa tac gac tca cta tag gg_ TAT CTT GCA CCC TGC GAC G	65
	Lys F1R	Gene specific (real time PCR)	GAT GCA CAC CCA ATC AGC AAT	60
	Lys 1F	Gene specific (real time PCR)	ATG TTG GGC AAA AGC ACA GTC	57

4.4.2 Preparation of defensin DNA template for dsRNA synthesis

Primers with flanking T7 sequences (Figure 4.3) were used for the amplification of the selected region of the transcript for dsRNA synthesis. Since the T7 polymerase is a DNA dependent RNA polymerase, these incorporated sites will allow for binding of the polymerase to DNA template and subsequent production of dsRNA. The following method describes the incorporation of these T7 sequences into the regions of interest.

Recombinant pGEM T Easy vector containing the gut defensin (isoform 1) was obtained from Ms M.E. Botha (University of Pretoria, Department of Biochemistry). According to the MEGAscript RNAi Kit (Ambion Inc., USA), the optimal amplification profile is obtained by manipulation of the annealing temperature of the T7 primers. It was suggested that the initial 5 cycles of the amplification profile allow annealing at the melting temperature of the (gene-specific fragment of the primer + 5°C) and the remaining cycles be performed at the melting temperature of the total primer i.e. (gene specific + T7 sequence + 5°C). The template for the reaction was a dilution series of the plasmid ranging from undiluted to 1/100 000 and the protocol performed involved the use of 10 ng of plasmid containing the defensin insert to which 2 μl 10 X rTaq buffer (Mg^{2+} included), 2 μl of dNTPs (2.5 mM each), 10 pmoles of the RNAi upper primer and 10 pmoles of the RNAi lower were added. The final reaction volume was constituted to 20 μl by addition of water. Initial denaturation at 94°C

was allowed for 7 minutes followed by incubation at 80°C for 30 seconds and subsequent addition of 1.25 U of rTaq in the corresponding buffer was added to each tube. The reaction was allowed to proceed for 5 cycles at 94°C for 30 seconds, 55°C for 30 seconds and 72°C for 2 minutes. A second set of 30 cycles was allowed at 94°C for 30 seconds, 66°C for 30 seconds and 72°C for 2 minutes A final extension at 72°C was allowed to proceed for 7 minutes and the reactions were stored at 4°C. The product of this reaction was analysed on a 2.0% agarose-ethidium bromide (EtBr) gel.

The optimal reaction was scaled up to 6 tubes of 25 µl volumes each, pooled and precipitated as follows: A tenth of the volume of 3M NaOAc (pH 5) was added to the PCR product in addition to three volumes of 100% EtOH. The resulting solution was mixed and centrifuged briefly. Tubes were then incubated at -70°C overnight. Tubes were centrifuged at 16000 X g for 45 minutes at 4°C and the supernatant was discarded followed by the addition of 300 µl of 70% EtOH. The solution was vortexed briefly and centrifuged at 16000 X g for 45 minutes at 4°C. This was followed by three successive wash steps where 300 µl of 70% EtOH was added and the solution was centrifuged at 16000 X g for 15 minutes, 10 minutes and 5 minutes respectively at 4°C. Following discard of the final supernatant, pellets were dried in a vacuum concentrator (Bachoffer, Germany) and redissolved in 10 µl dddH$_2$O. The concentration of a 10 times dilution was determined using the Gene Quant and the remaining template DNA was stored at -20°C.

4.4.3 Defensin dsRNA production

This reaction was performed using T7 RNA polymerase from *E. coli* BL21/pAR 1219 (Nucleoside-triphosphate: RNA nucleotidyltransferase (DNA-directed) (Roche Diagnostics GmbH, Mannheim, Germany).

The reaction setup below (Table 4.4) indicates the standard reaction that was used as the initial reaction which was subject to optimization. The reaction was setup using rNTPs obtained from the RiboMax Kit (Promega, Madison, WI, USA). Additionally, a control reaction was set up in parallel using the control DNA template provided by the MEGAScript kit (Ambion Inc., Texas, USA) which produces a 500 bp dsRNA fragment.

Table 4.4: Standard reaction setup for the production of defensin dsRNA

Reagent	Reaction Volume (μl)
Template (1 μg/μl)	1
rNTPs (from the RiboMax Kit)	1
Buffer (10 X concentration)	2
T7-RNA polymerase (20 U/μl)	2
RNase Inhibitor (40 U/μl)	0.5
DEPC-H$_2$0	to a final volume of 20 μl

The reaction was set up at room temperature and was subsequently incubated at 37°C for 2 hours following which the RNA polymerase was inactivated at 65°C for 5 minutes. Samples were then subjected to digestion analysis as presented in section 4.4.4.

The standard reaction as shown in Table 4.4 was successful in the production of dsRNA. Further attempts were then made to increase the concentration of dsRNA produced by the reaction. Table 4.5 indicates the reaction conditions and reagent volumes of the reactions performed in an attempt to optimize the concentration of dsRNA produced.

Table 4.5: The steps performed in an attempt to optimize the concentration of dsRNA produced

Optimization Reaction	Standard parameter	Optimized parameter
A	40 U enzyme, 2 hour incubation	80 U enzyme, 6 hour incubation
B	1 μg template	3 μg template
C	40 U enzyme	80 U enzyme

From the abovementioned optimization reactions, it was found that the ideal reaction conditions included an increase in template concentration and a 2 hour incubation at 37°C. This reaction was scaled up and the resulting product was treated with 5 U DNase (in order to remove any contaminating DNA template) as well as with 5 U RNase (in order to remove any ssRNA). Succeeding this digestion reaction at 37°C for 2 hours, the remaining dsRNA was purified by lithium acetate (LiOAc) precipitation as described in 4.4.5.

4.4.4 Digestion of contaminating ssRNA and residual template DNA

The principle of this reaction relies upon the fact that dsRNA is resistant to digestion by an RNase enzyme. The digestion reactions were set up as shown in Table 4.6.

Table 4.6: Reaction setup performed for digestion analysis

Reagent	Undigested reaction volume (μl)	DNase digested reaction volume (μl)	RNase digested reaction volume (μl)
dsRNA	5	5	5
DNase (5 U/μl)	0	1	1
RNase (5 U/μl)	0	0	1
Water	5	4	3
Total volume	**10**	**10**	**10**

The reaction presented in section 4.4.2 was repeated with the RNAi upper new primer and the use of the ExTaq DNA polymerase.

4.4.5 Precipitation of defensin dsRNA

Following the digestion of template DNA with DNase and ssRNA with RNase, the remaining dsRNA was purified by precipitation with LiOAc. Conventionally, lithium chloride (LiCl) is used as the precipitating agent, however it is known that the chloride ions, which may remain following precipitation, will inhibit downstream enzymatic reactions. For this reason, LiCl was replaced by LiOAc. The Li$^+$ ions are available for binding to the anionic RNA molecule and the replacement of the Cl$^-$ ion by the OAc$^-$ ion prevents inhibition of downstream reactions.

To the 20 μl dsRNA synthesis reaction products, half the volume (i.e. 10 μl) of LiOAc (pH 5.0) was added in addition to 300 μl of 100% EtOH. The solution was mixed by pipetting up and down and brief vortexing after which an overnight incubation at -70°C was performed.

Following this incubation period, tubes were centrifuged at 16000 X g for 45 minutes at 4°C. The supernatant was discarded followed by the addition of 300 μl of 70% EtOH. The solution was vortexed briefly and centrifuged at 16000 X g for 45 minutes at 4°C. This was followed by 3 successive wash steps where 300 μl of 70% EtOH was added and the solution was centrifuged at 16000 X g for 15 minutes, 10 minutes and 5 minutes, respectively, at 4°C. Following the discarding of the final supernatant, the product was dried in a vacuum concentrator (Bachoffer, Germany) and the resulting dried precipitate was redissolved in 10 μl DEPC-H$_2$O. The concentration of a 10 times dilution was determined using the Gene Quant and the remaining dsRNA was stored at -70°C.

4.4.6 Lysozyme dsRNA synthesis

Recombinant pGEM T Easy containing the gut lysozyme (clone 45, chapter 3) was used as the template for dsRNA synthesis using a similar protocol to that described in section 4.4.2. Plasmid (10 ng) containing the lysozyme insert to which 2 µl 10 X ExTaq buffer (Mg^{2+} included), 2 µl of dNTPs (2.5 mM each), 10 pmoles of the T7 Lys F1 primer and 10 pmoles of the T7 Lys R1 primer were added. The final reaction volume was constituted to 20 µl by means of addition of H_2O. Initial denaturation at 94^oC was allowed for 7 minutes followed by incubation at 80^oC for 30 seconds. At this point 1.25 U of ExTaq in the corresponding buffer was added to each reaction tube. The reaction was allowed to proceed for 5 cycles at 94^oC for 30 seconds, 57^oC for 30 seconds and 72^oC for 2 minutes. A second set of 30 cycles were allowed at 94^oC for 30 seconds, 65^oC for 30 seconds and 72^oC for 2 minutes   A final extension at 72^oC was allowed to proceed for 7 minutes after which the reactions were maintained at 4^oC. The products of this reaction was analysed on a 2.0% agarose-ethidium bromide (EtBr) gel.

The optimal dilution was found to be 1 in 100 000 and so this reaction was scaled up and dsRNA was synthesized, digested with DNase and RNase and precipitated as described in sections 4.4.4 and 4.4.5.

4.4.7 Gene silencing in *O. savignyi*

In the case of silencing in the ixodid ticks Kocan *et al.* (2008) injected a final effective concentration of $5X10^{10}$ to $5X10^{13}$ molecules of dsRNA. Since no published data is available on the silencing of genes in argasid ticks, a starting point for effective injection concentration was based upon this study in ixodid ticks.

The number of molecules of dsRNA is calculated using the average molecular weight of a base pair and the spectrophotometrically determined concentration of the dsRNA as follows:

$$\text{No. of molecules} = \frac{\frac{ng}{ml}}{\text{no. of base pairs} \times 660} \times 6 \times 10^{23}$$

*where 6×10^{23} is Avogadro's constant.

The silencing experiment was based upon three fed groups of ticks injected with both defensin dsRNA alone, lysozyme dsRNA alone or a combination of both defensin and

lysozyme dsRNA (Table 4.6). The control group was injected with DEPC water, since the dsRNA was dissolved in DEPC water.

Table 4.7: Table summarizing the groups proposed for the large scale RNAi experiment

Solution injected	Fed (native bovine blood)	Fed (*2.5X10^{8}cells/ml, Gram-positive infected bovine blood)	Fed (*2.5X10^{8}cells/ml, Gram- positive and negative infected bovine blood)
Control (DEPC water)	25 ticks	25 ticks	25 ticks
Defensin	25 ticks	25 ticks	25 ticks
Lysozyme	25 ticks	25 ticks	25 ticks
Combination	25 ticks	25 ticks	25 ticks

* as estimated in chapter 3

4.4.8 Injection of ticks

Adult female *O. savignyi* ticks (25) of a net weight of 150 mg were placed in a sieve, gently rinsed with water and allowed to dry on tissue paper. For the purposes of injection in this study, ticks were ventrally immobilized on double sided tape attached to a petri dish. A microscope was used to assist in visualization of the tick anatomy. An initial point of injection was introduced by means of insertion of a 23 gauge needle into the site of interest. A 10 μl Hamilton syringe (25 gauge needle) was then used to inject 5 μl of the respective dsRNA solutions into the previously inflicted point of injection with an effective concentration of 5x10^{13} molecules. The point of injection was then wiped gently with 100% EtOH in order to prevent infection. Ticks were monitored for mortality for 24 hours at 22°C prior to artificial feeding as in section 3.4.6.1.

4.4.9 Hemolymph collection

Ticks were immobilized on double-sided tape, with the ventral surface exposed. A 30 gauge needle was used to puncture the first pair of coxae at the base of the trochanter. The application of moderate pressure on the ventral surface of the tick allowed for the leakage of hemolymph. The hemolymph was collected and immediately placed into TRI-Reagent for later RNA isolation. In ticks that were fed, hemolymph was collected 16 hours post-bloodmeal.

4.4.10 Tick dissections

Within each respective group, 15 ticks were used for dissection where five ticks constituted a batch, thereby producing dissection samples in biological triplicate. In order to obtain tick organ or tissue samples for RNA isolation, ticks were dissected 16 hours post bloodmeal as described in section 2.4.2.

4.4.11 Real time PCR

Total RNA was isolated from tick tissues and organs using the protocol described in section 2.4.3. cDNA was synthesized (as described in section 3.4.6.3) in the presence of a spike (human B-cell receptor), due to the lack of an argasid household gene.

For the purposes of the real time procedure, cDNA that was synthesized was diluted 5 times and the reaction for each batch of the biological triplicate was performed in duplicate to serve as technical repeats. The reaction was set up using 1 μl of diluted cDNA to which 0.5 μl of the forward (10 pmoles/μl) primer, 0.5 μl of the reverse (10 pmoles/μl) primer, 5 μl of the Roche SYBR I master mix and 3 μl of nuclease free water (supplied with the master mix) was added forming a final reaction volume of 10 μl. This reaction represents the general setup of an individual reaction. For the purposes of the experiment, a master mix including in the first case, lysozyme specific primers, in the second case, defensin specific primers and in the third case spike specific primers were added to the Roche SYBR I master mix and nuclease free water (see table 4.3 for primer sequences). This master mix (9 μl) was then pipetted into the required wells of a 384 well real time PCR plate followed by the addition of individual templates of the isolated tissues of unfed, fed and bacterially challenged ticks.

Once the reactions were successfully pipetted into the wells, the plate was centrifuged at 2000 X g for 2 minutes. PCR was performed on the Roche Light Cycler 480 System (University of Pretoria, Department of Genetics). The cycling procedure allowed for activation of the Taq DNA polymerase at 95°C for 5 minutes followed by 45 cycles of denaturation at 95°C for 3 seconds, annealing of primers at 55°C for 7 seconds and extension at 72°C for 3 seconds at which point detection of fluorescence occurred. In order to generate a melting curve, the reaction was subsequently allowed to incubate at 95°C for 30 seconds, (annealing temperatures of 55°C for 30 seconds in the case of the lysozyme primers and 58°C for the defensin primers) followed by a continuous acquisition at 95°C.

Finally, the reaction was allowed to cool at 40°C for 30 seconds marking the end of the PCR run.

4.4.12 Relative quantification of real time PCR data

The software of the Roche Light Cycler 480 system was used for relative quantification where the samples containing the spike primers were designated as the reference while the experimental samples containing the lysozyme or defensin primers were designated as the target. The C_T values were calculated by the Roche Light Cycler 480 software and analysis was performed using Microsoft ® Exel. Data was then analysed using a Student's t-Test assuming unequal variances.

4.4.13 Observation of phenotype

Since 15 ticks were used for dissections, depending on the number of ticks that fed, approximately 10 remained for phenotype observation (mortality, ovipositioning, viability of eggs). These ticks were placed in sterilized sand of approximately 20 cm depth and maintained at room temperature to allow ovipostioning.

4.5 Results and discussion

4.5.1 Preparation of the defensin DNA template

The RNAi primers designed with a 5' flanking T7 sequence were used to amplify a dilution series of the defensin insert, selected for RNAi studies, out of the pGEM T Easy Vector (Promega, Madison, WI, USA).
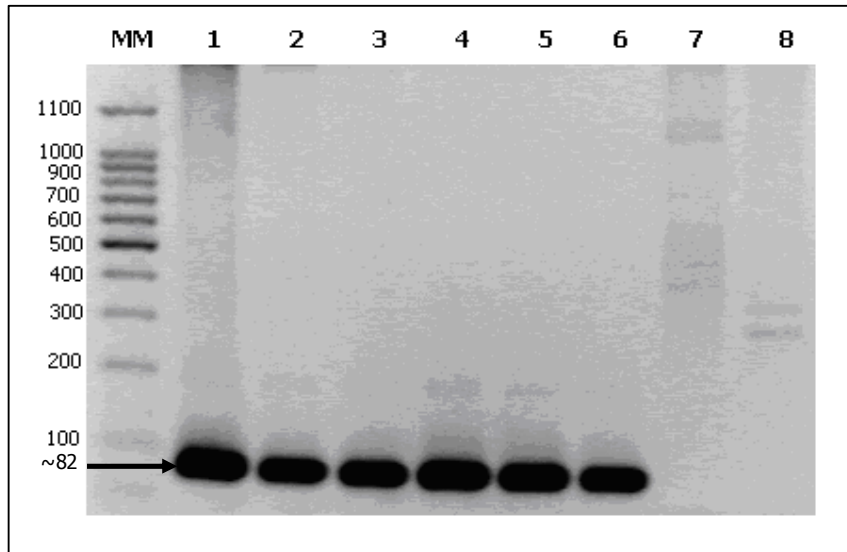
Figure 4.4: Agarose-EtBr (2.0%) gel analysis of incorporation of the T7 sequence into the selected defensin fragment: MM represents 100bp DNA ladder, lane 1: undiluted plasmid, lane 2: 1 in 10 dilution, lane 3: 1 in 100 dilution, lane 4: 1 in 1000 dilution, lane 5: 1 in 10 000 dilution, lane 6: 1 in 100 000 dilution, lane 7: negative control (RNAi upper) and lane 8: negative control (RNAi lower).

From Figure 4.4 it is evident that an increase in the dilution resulted in a decrease in non specific binding and amplification as bands additional to the expected ~82 bp, present in lanes 1-6 decreased in intensity with an increased dilution. The optimal dilution therefore was found to be 1/100 000. This reaction was repeated 5X, pooled and used as template for dsRNA.

Complete RNase digestion of all product, indicated that ssRNA was produced. This may be due to the fact that the initial template concentration in the RNA synthesis reaction was insufficient, facilitating a sub-optimal reaction. The low yield of the template DNA following purification was assumed to be due to the fact that the minimal fragment size purified by the kit is approximately 100 bp. The fragment of interest was, however, only 82bp in length and a significant quantity of the product could be lost during purification. For this reason a new

primer (RNAi upper New) was designed allowing for the amplification of template DNA of approximately 112 bp.

The reaction producing dsRNA was repeated with the RNAi upper new primer and the use of the ExTaq DNA polymerase. It was found that a 1 in 100 000 dilution was successful in yielding the 112 bp band. This reaction was scaled up to 6 tubes of 25 µl volumes each of which 5 µl of each reaction product was analyzed on a 2.0% agarose-EtBr gel (Figure 4.5) and the remaining samples were pooled and purified using ethanol precipitation.
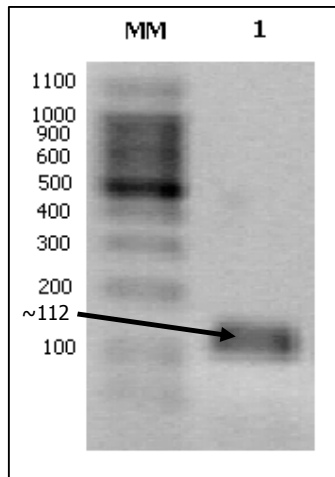

Figure 4.5: Agarose-EtBr (2.0%) gel analysis of large scale incorporation of the T7 site into defensin using RNAi upper NEW: MM represents 100bp DNA ladder, lane 1: large scale T7 incorporation into defensin fragment

4.5.2 Synthesis of dsRNA

The product shown in Figure 4.5 was used for dsRNA synthesis. The RNA produced was subjected to RNase digestion to allow digestion of ssRNA. The reactions were optimized with regards to reaction time, template volume as well as enzyme concentration (as shown in Figures 4.6-4.8). The standard reaction (as suggested by manufacturer) involved a 2 hour incubation at 37°C with 1 μg template.
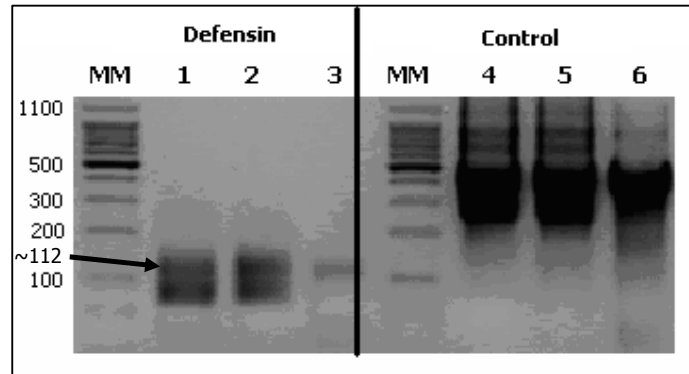
Figure 4.6: Agarose-EtBr (2.0%) gel analysis of digestion of RNA: Lanes 1-3 represent defensin dsRNA, while lanes 4-6 represent the control dsRNA of the MEGAScript Kit control of 500bp). MM represents 100bp DNA ladder, lane 1: undigested dsRNA, lane 2: DNase digested dsRNA, lane 3: DNase and RNase digested dsRNA, lane 4: undigested control dsRNA, lane 7: DNase digested dsRNA, lane 6: DNase and RNase digested dsRNA

In lanes 1 and 2 numerous bands are clearly visible. Following DNase digestion (lane 2), these bands remain. It is observed that upon RNase digestion (lane 3) the second band of lower molecular weight is eliminated. This band was representative of ssRNA and the characteristic faster motility of ssRNA on a gel is observed, as expected as two separate bands prior to digestion. Optimization of the reaction was required due to the fact the reaction favoured was unidirectional indicating that proper annealing of dsRNA that was synthesized.

The second optimization step involved an increase in the reaction time as well as enzyme concentration. The reaction was performed as a 6 hour incubation at 37°C with 1 μg template and 80 units of enzyme.
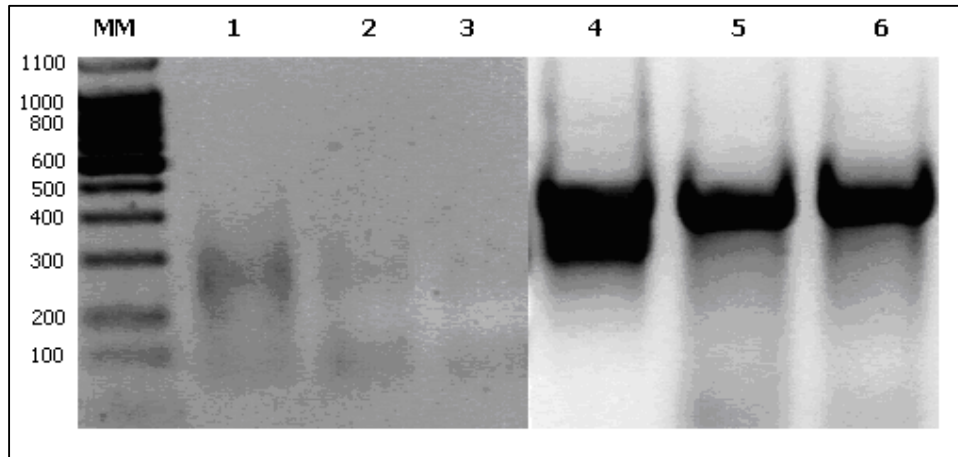
Figure 4.7: Agarose-EtBr (2.0%) gel analysis of digestion of RNA produced under optimization conditions, with DNase and RNase: Lanes 1-3 represent defensin dsRNA, while lanes 4-6 represent the dsRNA of the MEGAScript Kit control of 500bp. MM represents 100bp DNA ladder, lane 1: undigested dsRNA, lane 2: DNase digested dsRNA, lane 3: DNase and RNase digested dsRNA, lane 4: undigested control dsRNA, lane 5: DNase digested dsRNA, lane 6: DNase and RNase digested dsRNA

Results of a similar pattern to that observed in Figure 4.7 are seen in this case as well. Two bands are present prior to RNase digestion. However, upon RNase digestion the concentration of dsRNA produced is extremely low and barely visible on the gel. The control reaction in lanes 4-6 show no significant difference to the results obtained in Figure 4.6 hence it can be concluded that an increase in enzyme concentration does not result in an increase of product as would be expected. The effect of template concentration was subsequently evaluated using an increased template concentration with 2 hour incubation at 37°C with 3 μg template and 40 U enzyme.
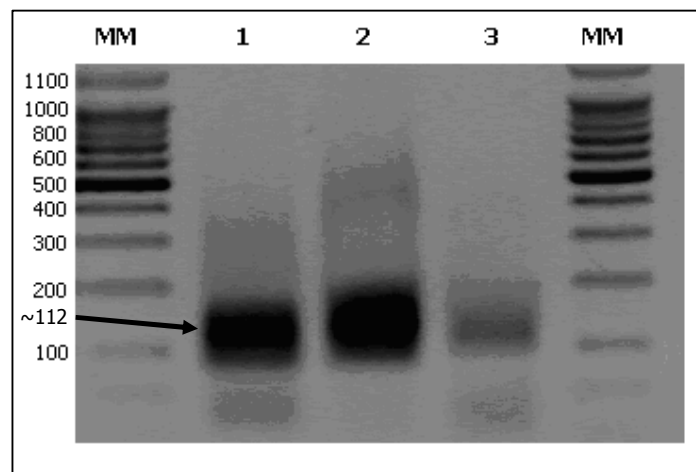

Figure 4.8: Agarose-EtBr (2.0%) gel analysis of digestion of defensin dsRNA produced under template concentration optimization conditions, with DNase and RNase: MM represents 100bp DNA ladder, lane 1: undigested dsRNA, lane 2: DNase digested dsRNA, lane 3: DNase and RNase digested dsRNA

From Figure 4.8, it is clear that an increase in template volume correlates with an increase in product concentration. A final optimization increasing both the template volume and enzyme concentration was unsuccessful since DNase and RNase digestion left no visible product on the gel. This may be explained by the fact that sufficient annealing, of the two complementary strands of RNA, did not occur. This produced a low concentration of dsRNA and a high concentration of ssRNA which is completely digested following RNase digestion. This may be improved by the production of each ssRNA in separate tubes, addition of these strands to a single tube, followed by complete denaturation at $\sim 95^{\circ}$C and subsequent cooling to allow for renaturation and efficient annealing of the strands.

The optimization reactions therefore indicate that the higher the concentration of template the higher the product concentration with a constant enzyme concentration of 40 U. The optimal reaction was thereafter scaled up and the product was purified using LiOAc precipitation. The concentration of the RNase-digested dsRNA following precipitation is given below in Table 4.8.

Table 4.7: Table showing the concentration of dsRNA obtained following precipitation (where the reaction was analysed on a 2.0% agarose gel, as presented in figure 4.8)

Reaction tube	A260/280	ng/μl
A	1.7	1324
B	1.8	1559
C	1.7	1800

4.5.3 Preparation of the lysozyme DNA template

Gene-specific primers bearing a 5' T7 overhang were designed and used to incorporate a T7 site into the 5' and 3' ends of the lysozyme fragment selected for dsRNA synthesis. The product of this reaction once optimized with ExTaq DNA polymerase producing the ~300 bp band as expected, is shown in Figure 4.9 below.
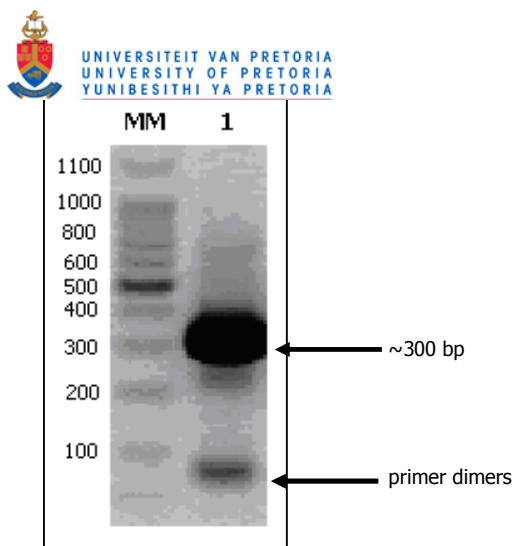
Figure 4.9: Agarose-EtBr (2.0%) gel analysis of T7 incorporation into the lysozyme DNA fragment: MM represents 100bp DNA ladder, lane 1 represents the product of the incorporation of the T7 sequence into the lysozyme fragment of interest.

Lane 1 above shows high concentrations of the band of interest however significant additional bands at approximately 250 bp as well as 90 bp. These bands could not be eliminated through optimization. As seen in chapter 3, the 5' sequence of the lysozyme transcript was not successfully identified. The primer used for the incorporation of the T7 sequence was designed in this region. At this point it should therefore be noted that non-specific amplification is possible and confirmed in the results observed above. The dsRNA synthesis reaction was continued as described below.

4.5.4 Lysozyme dsRNA synthesis and digestion analysis

The reaction shown in Figure 4.9 was scaled up to 10 tubes, pooled and precipitated. The product was then used in a dsRNA synthesis reaction (as optimized previously for the defensin molecule). The results below in Figure 4.10 show the digestion analysis of the initial (test) reaction.
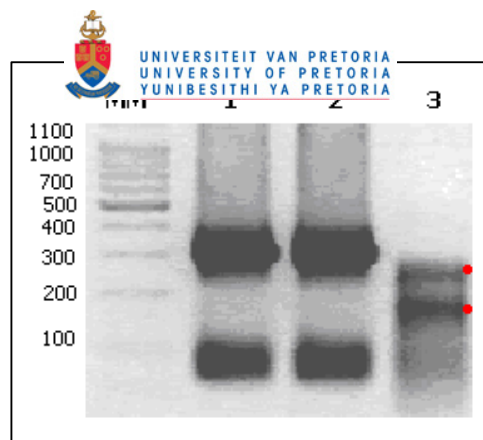
Figure 4.10: Agarose-EtBr (2.0%) gel analysis of digestion of RNA with DNase and RNase: MM represents 100bp DNA ladder, lane 1: undigested dsRNA, lane 2: DNase digested dsRNA, lane 3: DNase and RNase digested dsRNA. The bands produced are indicated by the red dots

From the results above, it can be seen that a band of approximately 300 bp representative of dsRNA is produced, however contaminating bands are also present. This may be explained by the use of the primer in the indeterminate region of the 5' end of the lysozyme sequence, as mentioned previously. The concentration of residual template DNA as well as ssRNA is relatively high however, the concentration of the dsRNA is sufficient. This reaction was then scaled up and the product was precipitated using LiOAc precipitation (as for the defensin molecule). The dsRNA produced was used for injection into ticks.

4.5.5 Tissue expression profile of defensin

In order to assess the functionality of a gene following RNAi mediated silencing, it is essential to possess prior knowledge on the expression of the gene during native conditions and in response to stimuli. For this reason, the tissue expression profile of the defensin molecule was investigated. The relative quantification software of the Roche Light Cycler 480 system was used in order to analyze the data obtained. Microsoft ® Excel was then used to generate the tissue expression profile (Figure 4.11). The statistical significance of the data sets was determined using a Student's t-Test assuming unequal variances.

Figure 4.11: Tissue expression profile of defensin: in adult female unfed, fed (sterile blood), fed (Gram-positive infected blood and fed (Gram-positive/negative infected blood) ticks (*= 8.3×10^{-7}, ** = 3.08×10^{-8} and *** = 7.4×10^{-12}, as calculated using Microsoft Excel)

Figure 4.11 suggests that the expression of defensin in the midgut is unaffected by feeding as unfed and fed samples show the same level of expression. It was, however, observed that expression is significantly upregulated in response to the feeding (P=7.5×10^{-6}) in hemolymph. Identical results were obtained upon ingestion of a combination of Gram-positive and Gram-negative bacteria, indicating that upregulation is due to the ingestion of gram positive bacteria alone. From these results it is hypothesized that defensin is not directly involved in digestion but rather exhibits an antimicrobial response when the tick is exposed to Gram-positive bacteria.

A similar pattern of regulation to that observed in the midgut is seen in the case of the ovaries. (with regards to lysozyme (Chapter 3)). The tissue expression profile revealed constitutive expression of lysozyme in the midgut and ovaries (same as for defensin) but no statistically significant differences between fed (sterile) and bacteria fed ticks with regards to the hemolymph).

In salivary glands, it is observed that feeding leads to a decrease in the levels of the defensin transcript (P=3.08×10^{-8}). This may be due to the fact that no digestive role is elicited by the salivary glands. Since several physiological changes occur in salivary glands of ticks following feeding, it may be assumed that the typical upregulation of salivary gland specific peptides shifts the equilibrium of transcription to favour these peptides while the expression of peptides of low functional importance, in this case, defensin, shows a marked decrease

(similar to lysozyme, in the case of salivary glands, the levels of expression also decreased following feeding). Additionally, an increase in the levels of the transcript was observed in salivary glands in response to feeding on Gram-positive bacteria. In the case of ticks fed on Gram-positive bacteria, it is seen that there is a statistically significant upregulation of the transcript ($P=8.3X10^{-7}$). This once again suggests that defensin is upregulated in response to Gram-positive bacteria.

This data suggests that feeding alone can greatly upregulate the expression of the defensin molecule ($P=7.4X10^{-12}$) in the hemolymph. As mentioned in the introduction, defensins are synthesized and stored in secretory cells and phagocytes. Since the hemolymph sample contained hemocytes, this observation may be attributed to the fact that upon feeding the rate of transcription of genes is, in general, upregulated (Nakajima Y. *et.al.*, 2002). Similar levels were observed in samples where bacteria were ingested; indicating upregulation due to feeding and not as a result of bacterial challenge.

The results obtained therefore suggest constitutive expression of defensin in the midgut and ovaries under normal physiological conditions. Significant upregulation in salivary glands, in response to Gram-positive bacteria was observed while hemolymph is the only tissue showing upregulation following feeding. This indicates that expression of defensin is differently regulated in different tissues.

4.5.6 Evaluation of silencing by real time PCR

No statistically significant knockdown of the defensin nor lysozyme transcript was observed. P-values were calculated in instances where the bar graphs indicate possible silencing, however no significant statistical data was obtained. The complete set of bar graphs obtained from the analysis is however presented in appendix A.

It was seen in Figure 4.10, that the lysozyme dsRNA produced consisted of two bands following RNase digestion. This was explained by the fact that the 5' primer was designed in the indeterminate 5' region of the lysozyme transcript (Chapter 3). The total effective concentration of specific lysozyme dsRNA was therefore lower than the calculated 5×10^{13} molecules. Overall, the lack of success of silencing of both the defensin and lysozyme transcripts may be the result of the overall effective concentration of dsRNA injected being insufficient to allow for complete or sufficient silencing of the transcripts of interest or uptake of dsRNA into the cells did not occur. For matters of practicality, however, the dose at this

point may not be increased since the reactions optimized allowed for the injection of 5.0×10^{13} molecules of dsRNA. In the study based on the silencing of varisin (defensin) in the ixodid tick, *Dermacentor variabilis*, Kocan *et al.* (2008) successfully silenced the transcript through the injection of a final effective concentration of dsRNA of 5×10^{10} - 5×10^{13} molecules of dsRNA. In the experiments performed, a total volume of 5 μl of dsRNA was injected and a further increase in this volume would compromise the ticks.

4.5.7 Observation of phenotype

Mortality of ticks was observed across groups following a 21 day observation period, however, due to the low efficiency of silencing of the chosen transcripts, the observations may not be directly correlated with the effects of silencing. Table 4.9 below illustrates the survival rates of ticks in the respective groups.

Table 4.9: Table illustrating the mortality rate of ticks (%): The % mortality equals number of dead ticks divided by total number of ticks observed for phenotype (5 ticks per group, 3 groups, therefore a total of 15 ticks)

dsRNA injected	% mortality		
	Fed (uninfected blood)	Fed (gram positive infected)	Fed (gram positive and gram negative infected)
Control (DEPC water injected)	0	25	75
Defensin	33	0	33
Lysozyme	33	20	40
Combination	25	0	0

It should be noted that the group size observed was statistically insignificant (>5 ticks) and was dependent upon the number of ticks that fed. A larger group size would be of higher statistical significance. This alone allowed for significant variation between groups and for this reason, the rate of mortality should not be considered as conclusive evidence of silencing. Furthermore, the observed calculated mortalities should not be considered to be a true reflection of the effect of silencing, as it is observed from the silencing data that no statistically significant silencing of the transcripts occurred. The mortality may therefore be described as non-specific and possibly the result of injury during injection.

4.6 Concluding remarks

A tissue expression profile allows for the assessment of the induction of transcription of a gene in response to a given stimulus. The tissue expression profile of defensin reveals that the transcript is primarily induced following ingestion of Gram-positive bacteria. Furthermore, in the hemolymph, defensin transcription seems to be induced by feeding. The same was observed in the case of lysozyme.

RNAi facilitates an *in vivo* functional analysis of genes within a system. In this case the defensin transcript as well as the lysozyme molecule of *O. savignyi* was analyzed for the respective functional role in digestion and/or immunoprotection of the tick following ingestion of Gram-positive bacteria or a combination of Gram-positive and Gram-negative bacteria.

In order to assess the overall response to injection as well as to ensure that mortality was not observed due to injection, a control (DEPC-H_2O) injected group was used. Injected ticks were then fed on native blood, blood infected with Gram-positive bacteria or blood infected with a combination of Gram-positive and Gram-negative bacteria. This was done in order to assess the role of the transcripts in response to the abovementioned stimuli. A future perspective that requires investigation includes the effect of ingestion of Gram-negative bacteria alone.

Statistically significant silencing was not observed. This may be the result of the overall effective concentration of dsRNA injected being insufficient to allow for complete or sufficient silencing of the transcripts of interest. Furthermore, the dsRNA that was produced against the lysozyme transcript showed the presence of two bands. This indicates that of the population of molecules injected, fewer than calculated specific molecules were able to successfully target the lysozyme transcript *in vivo*.

It was expected that the midgut would show the most reliable effect of silencing due to the fact that this is the primary site of transcription of these transcripts. Transcript levels in hemocytes would also be decreased allowing for growth and replication of microorganisms in the hemolymph with the observation of higher mortality rates. Little or no silencing would occur in the ovaries and it has been suggested that structures such as ovaries, salivary glands and possibly the fat body are unable to engage in the uptake of dsRNA due to the tight membrane bound encasement of these organs or absence of a transporter (Dr. C.

Maritz-Olivier, University of Pretoria, Department of Biochemistry, Personal communication, 2008).

A significant response was observed in the salivary glands , in terms of the ingestion of Gram-positive bacteria. In all cases a similar response was observed for the ingestion of a combination of Gram-positive and Gram-negative bacteria, however this may due to the ingestion of Gram-positive bacteria alone. The response to the ingestion of a combination of bacteria was pronounced in the midgut. It was corroborated by Matsuo *et al.* (2004), who have shown through the tracking of green fluorescent protein (GFP) expressing *E. coli* throughout the system of an injected argasid tick. It was found that *E. coli* are unable to traverse the midgut epithelium. It was found that a 24 day period was sufficient in allowing the complete eradication of the bacteria from the midgut. This would imply that the complete eradication of microorganisms would occur in the midgut which should theoretically correlate with the more potent response expected to be observed in the midgut.

Since this study represents the first known data generated from RNAi studies on argasid ticks, several technical details required optimization. In the ixodid tick species several attempts have been made at RNAi in these ticks and so the parameters used are known and in most cases, optimized. In the case of the argasid species, further work would involve a time course study of the response of the tick in terms of the expression of the transcript in response to the stimuli provided during the experiment. Additionally, an investigation of the regulation of the transcript in all tissues, as well as a suitable positive control and housekeeping gene will allow the positive identification of an associated phenotype related to successful silencing. Furthermore, the time of dissection following feeding as well as the probability of the injection of dsRNA into ticks following feeding requires investigation. Once these parameters have been established under normal physiological conditions, silencing of the transcripts may then be attempted with possible higher success rates due to the fact that more functional knowledge of the transcripts, as well as the intricate regulation has been obtained.

Optimization of the dose of dsRNA and response as well as the optimization of the injection volume for argasid ticks, needs to be performed. An investigation into the concentration of dsRNA injected relative to the body mass of ticks should be made. It may be possible that due to the larger body mass of argasid ticks, a higher concentration of dsRNA would be required. In this study, the possibility of a lack of specificity of the dsRNA produced for the target mRNA of interest was eliminated with the dsRNA designed in regions showing high

conservation between *O. moubata* and *O. savignyi* for both the defensin and lysozyme transcripts. Additionally, dsRNA is cleaved into approximately 21 nt fragments of siRNA which then target the mRNA of interest and it is unlikely that the mRNA of interest was incorrectly targeted. Alternatively it may have been possible that the dsRNA was unsuccessful in traversing the necessary barriers in order to reach the tissues and organs of interest. For this reason, an additional positive control (knockdown of an already established transcript of functional importance in argasid ticks) should be included into future experiments. There is currently no such control available with regards to argasid ticks.

Several other methods for the introduction of dsRNA into ticks are available. These include feeding of the dsRNA into ticks by means of a microcapillary. This method may prove problematic in argasid ticks due to the small concealed mouthparts. Alternatively, the method of soaking ticks where the first coxa has been severed, may prove useful. The presence of transport mechanisms as well as RNAi machinery should be investigated in order to confirm that internalization, processing and silencing are indeed possible.

The field of RNAi, however, is currently under intense investigation and research has shown that the abovementioned suggestions for optimization may not prove fruitful. Current literature shows the sensitivity of such experiments and the mass of considerations that need to be taken into account in order to perform a successful experiment.

dsRNA introduced into a cell, tissue or whole organism is seen to induce a toxic response. Reynolds *et al.,* 2006 and Federov *et al.,* 2006 have shown that this response has been is due to:
1. **the length of the dsRNA introduced:** it was found that the longer the nucleotide length of the duplex introduced, the higher the likelihood of the induction of an inflammatory/immune response. The ideal duplex length is approximated at 21-23 nt.
2. **delivery media:** the method as well as media used for delivery of the dsRNA may be toxic to cells and lead to a compromised experimental situation.

Once dsRNA is introduced into a cell, ideally, the antisense strand of the duplex should be taken up by the RISC complex. This is due to the fact that the sequence of the antisense strand exhibits complementarity to the target mRNA. With dsRNA produced in the laboratory, no modifications are made in order to ensure that the antisense strand only, is taken up into RISC (Brown & Samarsky, 2006). This means that the sense strand is fully

likely to be taken up by RISC and target a transcript not under investigation, leading decreased or no specificity of targeting of the antisense strand to the target of interest. Commercially available dsRNA molecules are synthesized (Dharmacon Inc. Lafayette) with this problem in mind. Once the duplex has been constructed, 2' O-methyl moieties are added to the strands. This leads to a lack of phosphorylation on the 5' end of the sense strand. Studies have shown that 5' phosphorylation is essential for RISC identification of the strand and uptake. This proprietary modification therefore ensures that only the antisense strand is taken up by RISC thereby eliminating the possibility of off-target effects arising from non-specific sense strand targeting (Jackson *et al.,* 2006).

Research has shown that the endogenous miRNA pathway also employs RISC for the mediation of binding of a miRNA to a complementary target mRNA leading to translational repression. Once the miRNA is removed from the target RNA, translation continues (Bartel, 2004). In the case of *Caenorhabditis elegans*, these "tiny RNAs" were seen to play a regulatory role in the developmental stages of the worm (Lau *et al.,* 2001). The same role was identified in Zebrafish (Wienholds *et al.,* 2005). Analysis of putative dsRNA sequences targeting mRNAs has shown that should the dsRNA contain mismatches when binding to the target mRNA, translational repression occurs, rather than mRNA degradation as expected with the use of dsRNA. In the majority of cases it was found that this is due to non specific binding of the dsRNA to the 3' UTRs of several other non-target mRNAs (Birmingham *et al.,* 2006). Theoretically, it may be possible that since RISC is already exploited in the endogenous miRNA pathway, the addition of dsRNA to a cell may shift the equilibrium between the number of free RISC molecules and those involved in the miRNA process. This may translate to a lower availability of RISC molecules to participate in the miRNA process, which in turn could lead to a detrimental effect in normal physiological functions of the cell or organism.

At present, miRNA in ticks is an unexplored territory. Investigations into this field will allow for insight into not only the roles of miRNA in specific pathways within an organism but also through the use of miRNA inhibitors which prevent binding of a miRNA to a target mRNA, identify potential effects of shifting the RISC equilibrium towards interactions with dsRNA rather than miRNA. It would be of particular interest should miRNAs be involved in immune related regulatory mechanisms in ticks which would then allow for a more strategic design of RNAi experiments with insight into false positive phenotypes occurring as a result of miRNA inhibition. Furthermore, the elucidation of complete tick genomes will allow for bioinformatic predictions of miRNA regions as well as the potential of a dsRNA to act as a miRNA.

At this point it may be concluded that the series of experiments presented in this chapter represent the first known attempt at RNAi in argasid ticks. As mentioned above, several different parameters require investigation as well as optimization. Taking these parameters into consideration, the ideal experimental setup should initially involve the use of cell cultures in order to implement more controlled delivery of dsRNA into cells and prevent whole organism false positive phenotypes upon success, this may then be expanded to whole tick investigations.

dsRNA used for experimentation should ideally be custom synthesized in order to ensure that the molecule is:

1. **21 - 23 nt long:** in order to prevent an inflammatory response from cells or ticks
2. **modified with a 2' O-methyl moiety:** in order to ensure that only the antisense strand is taken up by RISC
3. **analysed for seed region binding to the 3' UTR of non-target mRNAs:** in order to eliminate the possibility of sequence related off target effects
4. **highly functional:** in order to ensure that the dsRNA is not only 100% complementary to the target mRNA but also shows a high functionality in terms of silencing.

A suitable positive control, such as β-actin, GAPDH or other housekeeping genes should be used in order to confirm that the mechanism of RNAi processing in the cell is fully functional.

A non-targeting control dsRNA should be used in experimentation in order to confirm that dsRNA is internalized by the target cell or successfully administered to an organism. This control will also allow for the identification of any false phenotype which occurs not as a result of silencing but rather as a result of the introduction of foreign dsRNA into a cell/organism.

Furthermore, in the case of introduction of dsRNA into whole organisms, an effective delivery control should be used. This would allow for the identification of a phenotype which results due to injury or effects of the delivery media itself.

As mentioned above, the higher the number of nucleotides introduced (which includes a higher concentration of dsRNA) the higher the immune/inflammatory response. In order to circumvent this problem, a pool of several highly functional dsRNAs may be used. This will decrease the effective concentration of each dsRNA used and multiple dsRNAs destined for a

single mRNA target should theoretically have a higher potential for silencing with a decreased toxic effect.

Due to the complexity of RNAi experiments as well as several highly sensitive parameters for which optimization is essential, it may be concluded that the results of this chapter have therefore provided a starting block for future experimentation. As more knowledge of these parameters and pathways are determined in ticks, such experiments will be undoubtedly successful.

Chapter 5:

Concluding discussion

Since ticks are classified as obligate hematophagous ectoparasites, the primary feeding event involves a bloodmeal on a vertebrate host. Feeding is a non-sterile process and may facilitate the ingestion of several microorganisms of bacterial or fungal origin. The temperature, pH and nutrient medium of the tick midgut lumen following feeding provide optimal growth conditions for these ingested microorganisms (Sonenshine, 1993). For this reason, it is essential that ticks possess a well developed immune system. In the case of invertebrates, literature has shown that a well developed innate immune system exists in the absence of an adaptive immune system (Hoffmann *et al.,* 1995).

Innate immunity is classified as the first line of defense against an invading microorganism and involves an initial cellular response followed by the induction of a humoral immune response. Cellular immunity, in the case of ticks, is mediated by hemocytes produced by the mesodermally derived hematopoietic organ. Once mature, hemocytes may function in phagocytosis, nodulation or encapsulation of the invading microorganism. Further penetration by an invading microorganism leads to the induction of a humoral immune response which includes, among other responses, the induction of AMP synthesis.

Antimicrobial peptides are stimulus-induced peptides found in organisms ranging from plants, invertebrates and vertebrates including large mammals as well as man. A common feature of these peptides is their cationic nature and inherent low molecular weight (Marshall & Arenas, 2003). However, antimicrobial peptides lacking the characteristic cationic nature have also been found.

Microplusin is a 10 kDa cysteine-rich AMP found in the hard tick species, *R. (B.) microplus* (Fogaca *et al.*, 2004)*.* This AMP exhibits anti Gram-positive activity and is specifically bacteriostatic towards *Micrococcus luteus*. It was therefore suggested that an investigation into the mode of action of the AMP would provide insight into the mechanism of survival of the tick when challenged by microorganisms. Since the transcription of AMPs are induced by the detection of a foreign invader, as a response in the elicitation of the innate immune response,

129

an understanding of the mode of action of such an AMP or homolog thereof, should theoretically allow for the elucidation of a putative mechanism of survival of ticks following an immune challenge.

It was therefore hypothesized that a microplusin homolog would be found in the salivary gland of the argasid tick, *O. savignyi.* These experiments entailed attempts at PCR-mediated amplification of a microplusin homolog using degenerate and gene specific primers. It was reasoned that *R. (B.) microplus* tissue be used as a positive control. The internal positive control was β-actin. The results of the experiments revealed the absence of the microplusin transcript in *R. (B.) microplus* egg, mixed lifestages and whole adult tissues. The internal positive control was efficiently amplified in all experiments. The work of Nijhof (2008) on the fat body, ovaries, salivary glands, gut and malpighian tissues of *R. (B.) microplus* revealed that microplusin is expressed only in the fat body of fully fed, adult female ticks. This result then confirmed that the tissues used as a positive control were the wrong tissues. Furthermore, the ixodid fat body is a diffuse organ of small size. In argasid ticks, the fat body is distributed throughout the connective tissue of the body and so isolation during dissection is problematic. The fact that no microplusin homolog was identified in whole adult tissue used for the positive control confirms that not only is the transcript of interest of low abundance, but that the transcript was indeed diluted due to the diffuse nature of the fat body distributed throughout the connective tissue of the tick.

The identification of the transcript in adult tissue and not in egg tissue reveals a possible life stage specific regulation which may explain the lack of identification of the transcript when mixed life stages were used for the positive control. In order to successfully assess these findings further experimentation may be performed using isolated fat body from fully fed adult female ticks as the positive control. To elucidate the existence of life stage specific regulation wish to be elucidated, a range of tissues including the gut, salivary glands, ovaries, malpighian tubules and fat body of ticks of various life stages must be investigated.

The aim of the experiments performed in chapter 2 was the identification of an argasid microplusin homolog. It is clear that the mechanism of regulation as well as the stimuli of induction of synthesis of AMPs differs significantly between ixodid and argasid ticks. It is known that a microplusin homolog is present in the salivary glands of the argasid tick, *A. monolakensis.* It may be fruitful to use the salivary glands of this argasid tick as a positive control in future

experiments. Furthermore, an investigation into the tissue expression of this homolog in *A. monolakensis* as well as the stimulus of induction will provide a more specific life stage and time of induction of the transcript. This may provide a clearer idea of the situation in argasid ticks and reveal any differences in these parameters between argasid and ixodid ticks. The findings in *A. monolakensis* will allow for a safer extrapolation for a starting tissue, life stage and feeding or injury history for the elucidation of a microplusin homolog in *O. savignyi*.

From the work in chapter 2, ambiguity arises with regards to the presence of a microplusin homolog in the midgut of *O. savignyi*. Either no argasid homolog of microplusin exists or the reaction parameters were unfavourable therefore disallowing the identification of a microplusin homolog.

Lysozyme is classified as an enzyme catalyzing the cleavage of the β-1,4-glycosidic bond linking NAM and NAG in the peptidoglycan cell wall of bacteria, thereby eliciting antibacterial activity. Biochemical characterization of tick gut lysozyme (TGL) has shown that this molecule possesses an N-terminal amino acid sequence (K-V-Y-D-R-C-S-L-A-S-E-L-R) and shows high identity to vertebrate digestive lysozymes. Furthermore, the DRCSLA motif is found within *D. melanogaster* digestive lysozymes. For this reason, it has been postulated that lysozyme possesses a digestive as well as an immunoprotective role within ticks (Grunclova *et al.,* 2003). Since lysozyme is implicated in immunoprotective and/or digestive roles in several arthropod species, specifically the ixodid (*D. andersoni* and *D. variabilis*) and the argasid (*O. moubata*) ticks, it was hypothesized that a homologous lysozyme molecule would be present in the gut of the argasid tick, *O. savignyi.*

Since feeding in ticks is classified as non-sterile, the presence of lysozyme in the midgut provides antibacterial protection against any bacteria that may be ingested. In the ixodid ticks *D. andersoni* and *D. variabilis*, lysozyme was seen to be upregulated in response to challenge with Gram- negative *(E. coli)* bacteria (Simser *et al.*, 2004) while in the argasid tick *O. moubata*, lysozyme was upregulated in the midgut in response to feeding (Kopacek *et al.*, 1999). In *O. moubata*, the active site residues are classified as Glu[33] and Asp[51] while a His residue at position 52 replaces the Tyr residue at the corresponding position in hen egg white lysozyme. This allows for the classification of tick lysozyme into the H-branch of the family.

In chapter 3 the partial sequence of the *O. savignyi* lysozyme reveals 71% similarity and 65% identity to that of *O. moubata* indicating the presence of a homologous lysozyme molecule in these closely related species. Since the 5' sequence obtained does not maintain conservation of the typical eight cysteine residues, the characteristic DRCSLA motif of digestive lysozymes nor the correct position of cleavage of the signal peptide, it is concluded that the 5' sequence was not successfully identified. Further experimentation in this regard may include the use of overlapping primers in 5'-RACE. This may allow for the successful elucidation of the 5' sequence as this method proved successful for the 3' end.

The tissue expression profile of lysozyme showed constitutive expression of lysozyme in the midgut and ovaries and no statistically significant differences between fed (uninfected blood) and bacteria fed argasid ticks with regards to the fat body and hemolymph. In the case of salivary glands, the levels of expression decreased following feeding. Additionally, an increase in the levels of the transcript was observed in salivary glands in response to feeding on Gram-positive bacteria. These results are in direct contrast to the data published for ixodid ticks, where lysozyme expression is upregulated in response to Gram-negative bacteria suggesting that a possible synergism or transcriptional linkage occurs between an AMP targeting Gram-positive bacteria and lysozyme (Sonenshine & Hynes, 2008). This would theoretically translate to the fact that as the intracellular levels of this proposed AMP is increased, so too are the levels of lysozyme.

Alternatively, the data may suggest a differential mechanism of antibacterial activity elicited by lysozyme, contrary to the currently available knowledge on the topic. However, further investigations will be required in order to confirm such possibilities. This would include isolation of the *O. savignyi* lysozyme molecule, in the active state, and subsequent analysis of activity against Gram-positive and Gram-negative bacteria as well as fungi. This may be done through the use of traditional plate based radial immunodiffusion assays. In this assay, bacterial cells are cultured on agar plated. Punctures are made in the agar and inoculated with the AMPs under investigation. As the peptide diffuses through the plate, bacterial cell lysis is indicated by the development of clear zones.

Defensins are AMPs found in species ranging from vertebrates to invertebrates. In ticks, the major activity of defensins is against Gram-positive bacteria. It has been shown that the *O. moubata* defensin is able to disrupt the membrane potential of cells within a period of 30-60

minutes and this therefore leads to the slow killing effect that is observed (Nakajima *et al.*, 2002). It was hypothesized that silencing of the defensin or lysozyme individually, will hamper the survival of the tick dramatically following subsequent feeding and/or bacterial challenge. Furthermore, it is hypothesized that a combination silencing will have a greater effect as compared to individual silencing.

A tissue expression profile allowed for the assessment of the induction of transcription of defensins in response to a given stimulus. The tissue expression profile of defensin revealed that the transcript is primarily induced in salivary glands following ingestion of Gram-positive bacteria. Furthermore, in the hemolymph, defensin transcription is induced by feeding.

RNAi facilitates an *in vivo* functional analysis of genes within a system. In chapter 4 the defensin transcript as well as the lysozyme molecule of *O. savignyi* was analyzed for the respective functional role in digestion and/or immunoprotection of the tick following ingestion of Gram-positive bacteria or a combination of Gram-positive and Gram-negative bacteria.

The experiments were unsuccessful in producing statistically significant silencing. The effective injection concentration was calculated based on work performed in ixodid ticks. It may be possible that in order to successfully silence argasid transcripts, a significantly higher or lower number of molecules is required. Future experiments may therefore include experiments optimizing the effective injection concentration in argasid ticks. This may be done targeting a transcript which when silenced exhibits a detrimental phenotype.

Furthermore, a time course study of the response of the tick in terms of the expression of the transcript in response to the stimuli provided during the experiment is required and may reveal the time of dissection following feeding as well as the probability of the injection of dsRNA into ticks following feeding. Once these parameters have been established under normal physiological conditions, silencing of the transcripts may then be attempted with possible higher success rates due to the fact that more functional knowledge of the transcripts as well as the intricate regulation, has been obtained.

Alternatively, it may have been possible that the dsRNA was unsuccessful in traversing the necessary barriers in order to reach the tissues and organs of interest. For this reason, an additional positive control (knockdown of an already established transcript of functional

importance in argasid ticks) should be included into future experiments. However, this prospect is currently problematic since no such argasid control is available. Alternatively, currently establishaed cell cultures of argasid tick tissues which include salivary gland and ovaries, may be used. Silencing may then be performed and analysed using real time PCR. The advantage of this method would be the facilitation of antibody-mediated determination of lysozyme in non-silenced cells and comparison to protein levels in silenced cells. Problems which may arise will be the establishment of cultures of these sensitive cell lines as well as the unsuccessful uptake of dsRNA.

Unsuccessful uptake of dsRNA may be due to the absence of a Sid-1 transporter in ticks. A substantial point of research for all future work would be the identification of the argasid tick Sid-1 homolog, if present. This will therefore provide insight into the mechanism of uptake of dsRNA and should the transporter not be found, it may be possible that the transport method present in ticks, may employ a different method of uptake as expected. Elucidation of this mechanism, if present will yet again increase the success of RNAi experiments in argasid ticks.

At this point it may be concluded that this series of experiments represent the first known attempt at RNAi in argasid ticks. As mentioned in chapter 4, several different parameters require optimization and once optimized, it may be safely assumed that the success rates of such RNAi experiments in argasid ticks will indeed be increased.

Overall, the experimentation performed allowed for the molecular identification of the partial sequence of the *O. savignyi* lysozyme transcript . Despite the ambiguity that arose in terms of the elucidation of a microplusin homolog in the gut of *O. savignyi*, the tissue expression profiles that were generated for the lysozyme and defensin transcripts provide suggestive evidence of the putative functional role of these transcripts in immunoprotection following feeding due to the upregulation of transcript levels post bloodmeal. As discussed, future work facilitating the optimization of favourable reaction parameters for RNAi will allow for accurate determination of the *in vivo* functional roles of the abovemetioned transcripts.

References

Ambion TRI-Reagent Solution User manual 9738M, Revision B, August 10, 2007

Arrieta M.C., Leskiw B.K. and Kaufman W.R., 2006, Antimicrobial activity in the egg wax of the African cattle tick *Amblyomma hebreaum* (Acari: Ixodidae), Experimental and Applied Acarology

Bachali S., Jager M., Hassanin A., Schoentgen F., Jolles P., Fiala-Medioni A. and Deutsch J.S., 2002, Phylogenetic analysis of invertebrate lysozymes and the evolution of lysozyme function, Journal of Molecular Evolution, 54, 652-664

Bartel D., 2004, MicroRNAs: genomics, biogenesis, mechanism and function, Cell, 116, 281-297

Bechinger, B., 2004, Structure and Functions of lytic peptides, Critical Reviews in Plant Sciences 23, 271-292

Beutler B., 2004, Innate immunity: an overview, Molecular immunology, 40, 845-859

Birmingham A., Anderson E.M., Reynolds A., Ilsley-Tyree D., Leake D., Fedorov Y., Baskerville S., Maksimova E., Robinson K., Karpilow J., Marshall W.S. and Khvorova A., 2006, 3' UTR seed matches, but not overall identity, are associated with RNAi off-targets, Nature Methods, 3, 199-204

Botha M., 2008, Honours, Biochemistry, University of Pretoria

Brown K. and Samarsky D., 2006, RNAi off-targeting: Light at the end of the tunnel, Journal of RNAi and Gene silencing, 12, 175-177

Bulet, P., Hetru, C., Dimarcq, J., L., Hoffmann, D., 1999, Antimicrobial peptides in insects: structure and function, Developmental and Comparative Immunology 329-344

Bulet P., Stocklin R. and Menin L., 2004, Antimicrobial peptides: from invertebrates to vertebrates, Immunological reviews, 198, 169-184

Buresova V., Franta Z. and Kopacek P., 2006, A comparison of *Chryseobacterium indologenes* pathogenicity to the soft tick *Ornithodoros moubata* and hard tick *Ixodes ricinus,* Journal of Invertebrate Pathology, 93, 96-104

Ceraul S.M., Sonenshine D.E., Ratzlaff R.E. and Hynes W., 2003, An arthropod defensin expressed by the hemocytes of the American dog tick, *Dermacentor variabilis* (Acari: Ixodidae), Insect and molecular biology 33, 1099-1103

Charrel R.N., Fagbo S., Moureau G., Alqahtani H.M., Temman S. and de Lamballerie X., 2007, Alkhurma Hemorrhagic Fever virus in *Ornithodoros savignyi* ticks, Emerging Infectious Diseases, 13, 153-155

Clontech Super SMART™ PCR cDNA Synthesis Kit User Manual (2002)

Cooper E.L., Kauschke E and Cossarizza A., 2002, Digging for innate immunity since Darwin and Methcnikoff BioEssays, 24, 319-333

DeMar T., 2006, Innate immunity in ticks: A review, Journal of the Acarological Society of Japan, 15, 109-127

de la Fuente, J., Kocan, K.M., Almazan, C., Blouin, E. F., 2007, RNA interference for the study and genetic manipulation of ticks, Trends in Parasitology, 427-433

Federov Y., Anderson E.M., Birmingham A., Reynolds A.,Karpilow J., Robinson K., Leake D. and Marshall W.S., 2006, Off-targeting by siRNA can induce toxic phenotype, RNA, 12, 1188-1196

Fehlbaum P., Bulet P., Michaut L., Lagueux M., Broekaert W.F., Hetru C. and Hoffmann J.A., 1994, Insect Immunity: septic injury of *Drosophila* induces the synthesis of a potent antifungal peptide with sequence homology to plant antifungal peptides, Journal of Biological Chemistry, 269, 33159-33163

Fogaca A.C., Almeida I.C., Eberlin M.N., Tanaka A.S., Bulet P. and Daffre S., 2006, Ixodidin, a novel antimicrobial peptide from the hemocytes of the cattle tick *Boophilus microplus* with inhibitory activity against serine proteinases, Peptides, 27, 667-674

Fogaca A.C., Lorenzini D.M., Kaku L.M., Esteves E., Bulet P. and Daffre S., 2004, Cysteine-rich antimicrobial peptides of the cattle tick *Boophilus microplus:* isolation, structural characterization and tissue expression profile, Developmental and Comparitive Immunology, 28, 191-200

Ganz T. and Lehrer R.I., 1995, Defensins, Pharmacology and Therapeutics, 66, 191-205

Hara S. and Yamakawa M., 1995, A novel antibacterial peptide family isolated from the silkworm, *Bombyx mori*, Biochemical Journal, 310, 651-656

Herbeck J.T and Wall D.P., 2005, Converging on a general model of protein evolution, Trends in Biotechnology, 23, 485-487

Grunclova, L., Fouquier, H., Hypsa, V., Kopacek, P., 2003, Lysozyme from the gut of the soft tick *Ornithodoros moubata*: the sequence, phylogeny and post-feeding regulation, Developmental and Comparitive Immunology, 27, 651-660

Hancock R.E. and Chapple D.S., 1999, Peptide antibiotics, Antimicrobial Agents Chemotherapy, 43, 1317-1323

Hashimoto Y., Yamada K., Motoshima H., Tadahiro O., Yamada H., Yasukochi T., Miki T., Ueda T. and Imoto T., 1996, A mutation study of catalytic residue Asp 52 in Hen egg lysozyme, Journal of Biochemistry, 119, 145-150

Hoffmann J.A. and Reichhart J.M., 2002, *Drosophila* innate immunity: an evolutionary perspective, Nature, 3, 121-126

Hoffmann J.A., 1995, Innate immunity of insects, Current Biology, 7, 4-10

Hoffmann J.A., Kafaos F.C., Janeway Jr C.A. an Ezekowitz R.A.B., 1999, Phylogenetic perspectives in innate immunity, Science, 284, 1313-1318

Hynes W.L., Stokes M.M., Hensley S.M., Todd S.M. and Sonenshine D.E., 2008, Using RNA interference to determine the role of varisin in the innate immune system of the hard tick, *Dermacentor variabilis* (Acari: Ixodidae), Experimental and Applied Acarology 46, 7-15

Iwanaga S., 2002, The molecular basis of innate immunity in the horseshoe crab, Current Opinion in Immunology 14, 87-95

Jackson A.L., Burchard J., Leake D., Reynolds A., Schelter J., Guo J., Johnson M., Lim L. and Karpilow J., 2006, Position-specific chemical modification increases specificity of siRNA-mediated gene silencing, RNA, 12, 1197-1205

Jiggins F.M. and Kim K., 2005, The evolution of antifungal peptides in *Drosophila*, Genetics, 171, 1847-1859

Jiravanichpaisal P., Lee B.L. and Soderhall K., 2006, Cell mediated immunity in arthropods: Hematopoiesis, coagulation, melanization and opsonization, Immunobiology, 211, 216-236

Johns R., Sonenshine D.E. and Hynes W.L., 2001, Identification of a defensin from the hemolymph of the American dog tick, *Dermacentor variabilis*, Insect Biochemistry and Molecular Biology, 31, 857-865

Jolles J. and Jolles P., 1975, The lysozyme from *Asteria rubens,* European Journal of Biochemistry, 54, 19-23

Kadota K., Satoh E., Ochiai M., Inoue N., Tsuji N., Igarashi I., Nagasawa H., Mikami T., Claveria F.G. and Fujisaki K., 2002, Existence of phenol oxidase in the argasid tick *Ornithodoros savignyi*, Parasitology Research, 8, 781-784

Kavi, H.H. 2005, RNA silencing in Drosophila, FEBS Letters, 579, 5940-5949

Kelly S., Yamamoto H. and Robles L.J., 2008, Analysis of the 3' untranslated regions of α-tubulin and *S*-crystallin mRNA and the identification of CPEB in dark- and light-adapted octopus retinas, Molecular Vision, 14, 1446-1445

Kim D.H. and Ausubel F.M., 2005, Evolutionary perspectives on innate immunity from the study of *Caenorhabditis elegans*, Current opinion in immunology, 17, 4-10

Kim D.H., Feinbaum R., Alloing G., Emerson F.E., Garsin D.A., Inoue H., Tanaka-Hino M., Hisamoto N., Matsumoto K. and Tan M.W., 2005, A conserved p38 MAP kinase pathway in *Caenorhabditis elegans* innate immunity, Proceedings of the National Academy of Science, 101, 10990-10994

Kimbrell D.A. and Beutler B., 2001, The evolution and genetics of innate immunity, Nature Reviews, 2, 256-267

Kocan K.M., de la Fuente J., Manzano-Roman R., Naranjo V., Hynes W.L. and Sonenshine D.E., 2008, Silencing expression of the defensin, varisin in male *Dermacentor variabilis* by RNA interference results in reduced *Anaplasma marginale* infections, Experimental Applied Acarology, 46, 1-4

Kopacek, P., Vogt, R., Jindrak, L., Weise, C., Safarik, I., 1999, Purification and characterization of the lysozyme from the gut of the soft tick *Ornithodoros moubata*, Insect Biochemistry and Molecular Biology, 989-997

Kubista M., Andrade J.M., Bengtsson M., Forootan A., Jonak J., Link K., Sindelka R., Sjoback R., Sjogreen B., Strombom L., Stahlberg A. and Zoric N., 2006, The real-time polymerase chain reaction, Molecular Aspects of Medicine, 27, 95-125

Kurata S., Ariki S. and Kawabata S., 2006, Recognition of pathogens and activation of immune responses in *Drosophila* and horseshoe crab innate immunity, Immunobiology, 211, 237-249

Lai R., Takeuchi H., Lomas L.O., Jonczy J., Rigden D.J., Huw H.R and Turner P.C., 2004a, A new type of antimicrobial protein with multiple histidines from the hard tick, *Amblyomma hebreaum*, The FASEB Journal, 1-17

Lai, R., Lomas, L., O., Jonczy, J., Turner, P., C., Rees, H., H., 2004b, Two novel non-cationic defensin-like antimicrobial peptides hemolymph of the female tick, Amblyomma hebreaum, Biochemical Journal 379, 681-685

Lau N.C., Lim L.P.,Weinstein G. and Bartel D.P., 2001, An abundant class of tiny RNAs with probable regulatory roles in *Caenorhabditis elegans*, Science, 294, 858-862

Lavine M.D. and Strand M.R., 2002, Insect hemocytes and their role in immunity, Insect Biochemistry and Molecular Biology, 32, 1295-1309

Leclerc V. and Reichhart J.M., 2004, The immune response of *Drosophila melanogaster,* Immunological Reviews, 198, 59-71

Levashina E.A., Ohresser S., Bulet P., Reichart J.M., Hetru C. and Hoffmann J., 1995, Metchnikowin, a novel immune-inducible proline-rich peptide from *Drosophila* with antibacterial and antifungal properties, European Journal of Biochemistry, 233, 694-700

Liu M., Zhang S., Liu Z., Li H. and Xu A., 2006, Characterization, organization and expression of *AmphiLysC*, an acidic c-type lysozyme gene in amphioxus *Branchiostoma belcheri tsingtauense,* Gene, 367, 110-117

Lowenberger C., 2001, Innate immune response of *Aedes aegypti*, Insect Biochemistry and Molecular Biology, 31, 219-229

Mans B.J., Louw A.I. and Neitz A.W.H., 2003, The major tick salivary gland proteins and toxins from the soft tick *Ornithodoros savignyi*, are part of the tick lipocalin family: Implications for the origins of tick toxicoses, Molecular Biology and Evolution (20): 1158-1167

Mans B.J. and Neitz A.W.H., 2004, Adaptation of ticks to a blood-feeding environment: evolution from a functional perspective, Insect Biochemistry and Molecular Biology, 34, 1-17

Marshall S.H. and Arenas G., 2003, Antimicrobial peptides: a natural alternative to chemical antibiotics and a potential for applied Biotechnology, Electronic Journal of Biotechnology, 6, 271-284

Matsumoto T., Nakamura A.M. and Takahashi K.G., 2006, Cloning of cDNAs and hybridization analysis of lysozymes from two oyster species, *Crassostrea gigas* and *Ostrea edulis*, Comparative Biochemistry and Physiology, Part B 145, 325-330

Matsuo T., Okoda Y., Badgar B., Inoue N., Xuan X., Taylor D and Fujisaki K., 2004, Fate of GFP-expressing *Escherichia coli* in the midgut and response to ingestion in a tick, *Ornithodoros moubata* (Acari: Argasidae), Experimental Parasitology , 108, 67-73

Matsuzaki K., 2002, Why and how are peptide-lipid interactions used for self defence, Biochemical Society Transactions, 29, 598-601

Nakajima Y., van der Goes van Naters-Yasui A., Taylor D and Yamakawa M., 2001, Two isoforms of a member of the arthropod defensin family from the soft tick, *Ornithodoros moubata* (Acari: Argasidae), Insect Biochemistry and Molecular Biology

Nakajima, Y., Taylor, D., Yamakawa, M., 2002, Involvement of antibacterial peptide defensin in tick midgut defense, Experimental and Applied Acarology 28, 135-140

Nakajima, Y., Ishibashi, J., Yukuhiro, F., Asaoka, A., Taylor, D., Yamakawa, M., 2003, Antibacterial activity and mechanism of action of tick defensin against Gram-positive bacteria, Biochimica et Biophysica Acta, 125-130

Nilsen I.W. and Myrnes B., 2001, The gene of chlamysin, a marine invertebrate-type lysozyme, is organized similar to vertebrate but different from invertebrate chicken-type lysozyme genes, Gene, 269, 27-32

Nuttall, H., F., G., Warburton, C., Cooper, W., F., Robinson, L., E., Cambridge University Press, 1908

Olivier N.A., MSc thesis, Biochemistry, University of Pretoria

Olsen O.J., Nilsen I.W., Sletten K. and Myrnes B., 2003, Multiple invertebrate lysozymes in blue mussel *(Mytilus edulis)*, Comparative Biochemistry and Physiology, Part B 136, 107-115

Oppenheim J.., Biragyn A., Kwak L.W. and Yang D., 2003, Roles of antimicrobial peptides such as defensins in innate and adaptive immunity, Annals of the Rheumatic diseases, 62, 17-21

Phillips D.C., 1967, N.A.S. Symposium, 57, 485 (adapted from Canfield and Liu, 1965)

Promega Corporation DNA analysis notebook, Part # BR075B, 129 update

Rajput Z.I., Hu S., chen W., Arijo A.G. and Xiao C., 2006, Importance of ticks and their chemical and immunological control in livestock, Journal of Zhejiang University Science B (11): 912-921

Rees J.A., Miniatte M. and Bulet P., 1997, Novel antibacterial peptides isolated from a European bumblebee, *Bombus pascuorum* (Hymenoptera, Apoidea), Insect Biochemistry and Molecular Biology, 27, 413-422

Reynolds A., Anderson E.M., Vermeulen A., Fedorov Y., Robinson K., Leake D., Karpilow J. and Marshall W.S., 2006, Induction of the interferon response by siRNA is cell type and duplex length dependent, RNA, 12, 988-993

Ribiero J.M.C., 1988, The midgut hemolysin of *Ixodes dammini*, The Journal of Parasitology, 74, 532-537

Rodriguez de la Vega R.C and Possani L.D., 2005, On the evolution of invertebrate defensins, Trends in Genetics, 21, 330-332

Rudenko N., Golovchenko M. and Grubhoffer L., 2007, Gene organization of a novel defensin of *Ixodes ricinus:* first annotation of an intron/exon structure in a hard tick defensin gene and first evidence of the occurrence of two isoforms of one member of the arthropod defensin family, Insect molecular biology, 16, 501-507

Ruedisueli, F., L., Manship, B., University of Lincoln (2006), Available online at: http://webpages.lincoln.ac.uk/fruedisueli/FR-webpages/parasitology/Ticks/TIK/tick-key/softticks_adult.htm

Shai, Y., 2002, Mode of action of membrane active antimicrobial peptides, Peptide Science, 66, 236-248

Shai Y. and Jelinek R., 2002, Mode of action of membrane active antimicrobial peptides, European Journal of Biochemistry, 269, 3869-3880

Shanbaky N.M. and Helmy N., 2000, First record of natural infection with Borrelia in *Ornithodoros (Ornithodoros) savignyi*: Reservoir potential and specificity of the tick to Borrelia, Journal of the Egyptian Society of Parasitology (3): 765-780

Simser J.A., Macaluso K.R., Mulenga A. and Azad F, 2004, An immune responsive factor D-like serine proteinase homologue identified from the American dog tick *Dermacentor variabilis,* Insect Biochemistry and Molecular Biology, 13, 25-35

Simser J.A. Macaluso K.R., Mulenga A. and Azad F., 2004, Immune-responsive lysozymes from hemocytes of the American dog tick, *Dermacentro variabilis* and an embryonic cell line of the Rocky Mountain wood tick, *D. andersoni,* Insect Biochemistry and Molecular Biology, 34, 1235-1246

Sonenshine D.E., Biology of ticks, Volume 1, Oxford University Press, 1991

Sonenshine D.E., Biology of ticks, Volume 2, Oxford University Press, 1993

Sonenshine D.E., Ceraul S.M., Hynes W.E., Macaluso K.R. and Azad A., 2002, Expression of defensin-like peptides in tick hemolymph and midgut in response to challenge with *Borrelia burgdorferi, Escherichia coli* and *Bacillus subtilis*, Experimental and Applied Acarology, 28, 127-134

Sonenshine D.E. and Hynes W.L., 2008, Molecular characterization and related aspects of the innate immune response in ticks, Frontiers in Bioscience, 13, 7046-7063

Theiler G. and Hoogstraal H., 1955, The identity of *Ornithodoros savignyi* (Audouin, 1827) and *O. pavimentosus* Neumann, 1901 (Ixodoidea, Argasidae), Journal of Parasitology, 41, 245-247

Todd S.M., Sonenshine D.E. and Hynes W.L., 2007, Tissue and life-stage distribution of a defensin gene in the Lone Star tick, *Amblyomma americanum,* Veterinary and Medical Entomology, 21, 141-147

Tsuji N., Battsetseg B., Boldbaatar D., Miyoshi T., Xuan X., Oliver J.H. Jr. and Fukisaki K., 2007, Babesial vector tick defensin against *Babesia sp.* parasites, Infection and immunity, 75, 3633-3640

Tsuji N. and Fujisoki K., 2007, Longicin plays a crucial role in inhibiting the transmission of *Babesia* parasites in the vector tick, *Haemaphysalis longicornis*, Future Microbiology, 2, 575-578

Tzou P., de Gregorio E. And Lemaitre B., 2002, How *Drosophila* combats microbial infection: a model to study innate immunity and host pathogen interactions, Current Opinion in Molecular biology, 5, 102-110

Vizioli J. and Salzet M., 2002, Antimicrobial peptides from animals: focus on invertebrates, Trends in pharmacological Sciences, 23, 494-496

Voet D. and Voet J.G., Biochemistry 3rd edition, Wiley International Edition, Wiley, 2004, ISBN: 0-471-39223-5

Vredevoe L., University of California, Department of Entomology, 2006, Available online at: http://entomology.ucdavis.edu

Wienholds E., Kloosterman W.P., Miska E., Alvarez-Saavedra E., Berezikov E., de Bruijn E., Horvitz H.R., Kauppinen S. and Plasterk R.H.A., 2005, MicroRNA expression in Zebrafish embryonic development, Science, 309, 310-311

Wilson K and Walker J., Practical Biochemistry 5th edition, Cambridge Press, 2001, ISBN: 052165873X

Youheng W., Qianghai X., Ting Z., Zongchun M., Jia Y. and Wei-Jun M., 2009, Differential regulation of mRNA stability controls the transient expression of genes encoding *Drosophila* antimicrobial peptides with distinct immune response characteristics, Nucleic Acid Research, 37, 6550-6551

Yu D., Sheng Z., Xu X., Li J., Yang H., Liu A., Rees H.H. and Lai R., 2006, A novel antimicrobial peptide from salivary glands of thehard tick, *Ixodes sinensis*, Peptides, 27, 31-35

Zhou J.M., Ueda R., Umemiya H., Battssetseg D., Boldbaatar X., Xuan K. and Fujisaki, 2006, A secreted cystatin from the tick *Haemaphysalis longicornis* and its distinct expression patterns in relation to innate immunity, Insect Biochemistry and Molecular Biology, 36, 527-535

Zhou J., Liao M., Ueda M., Gong H., Xuan X. and Fujisaki K., 2007, Sequence characterization and expression patterns of two defensin like antimicrobial peptides from the tick *Haemaphysalis longicornis*, Peptides, 28, 1304-1310

Zhioua E., Yeh M.T. and LeBrun R.A., 1997, Assay for prophenoloxidase activity in *Amblyomma americanum, Dermacentor variabilis* and *Ixodes scapularis,* Journal of Parasitology, 3, 553-554

Appendix A:

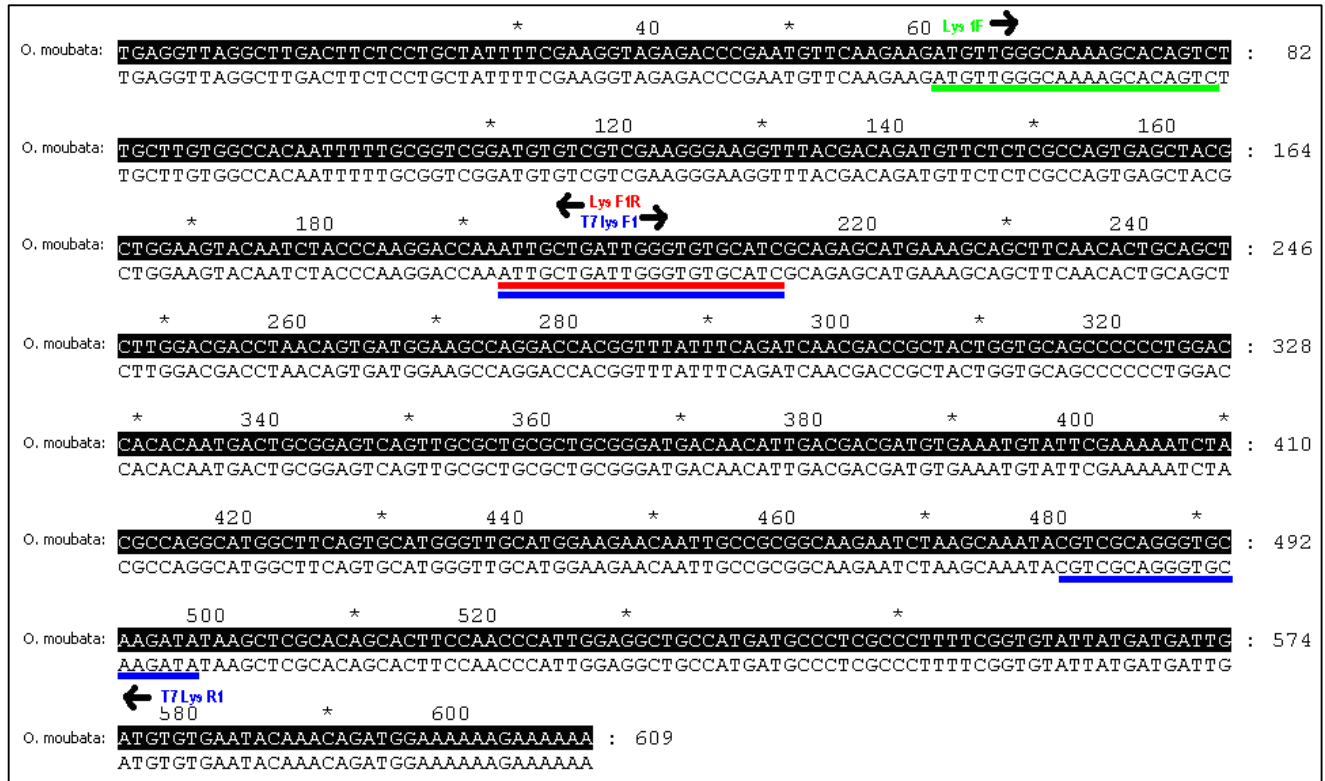# Supplementary information to Chapter 4

Figure 4.12: Annotated nucleotide sequence of the *O.moubata* lysozyme sequence: regions highlighted show the regions used for the design of the T7 primers as well as primers used for real time analysis

In vivo functional analysis of lysozyme and defensin in the soft tick, *O. savignyi*

Real time analysis was performed in order to assess the level of silencing of the defensin and lysozyme transcripts. Following injection, ticks were then fed on native blood, blood infected with Gram-positive bacteria or a combination of Gram-positive and Gram-negative bacteria. The individual groups were each injected with defensin dsRNA, lysozyme dsRNA or a combination of both defensin and lysozyme dsRNA. In all cases real time analysis was used in order to assess the levels of the both the defensin and lysozyme transcripts. The results presented in chapter 4 show only the levels of defensin in the control group and the defensin dsRNA injected ticks. In this case the ticks that were fed on native blood, blood infected with Gram-positive bacteria or blood infected with a combination of both Gram-positive and Gram-negative bacteria were analyzed. The same was done in the case of lysozyme. The bar graphs presented below show the full analysis of the individual groups including the combination silenced group. The combination group was excluded from chapter 4 since little overall significance was observed.
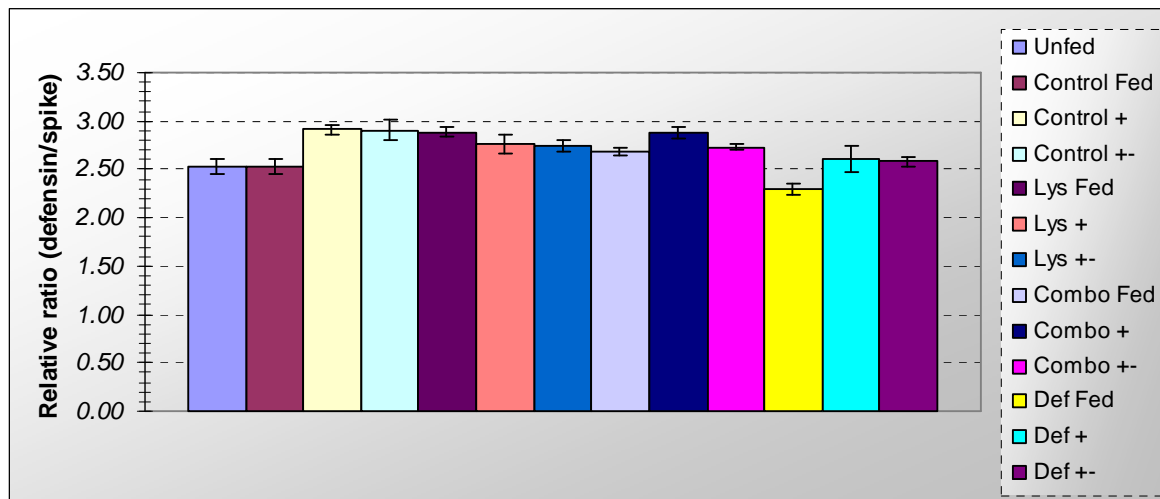

Figure 4.13: Bar graph representing the levels of the defensin transcript in the midgut: of control (DEPC-H$_2$O injected) experimental (lysozyme dsRNA, defensin dsRNA or combination dsRNA) injected ticks. Additionally, the results compare feeding of ticks on native (uninfected blood) and blood infected with Gram-positive bacteria as well as a combination of Gram-positive and Gram-negative bacteria
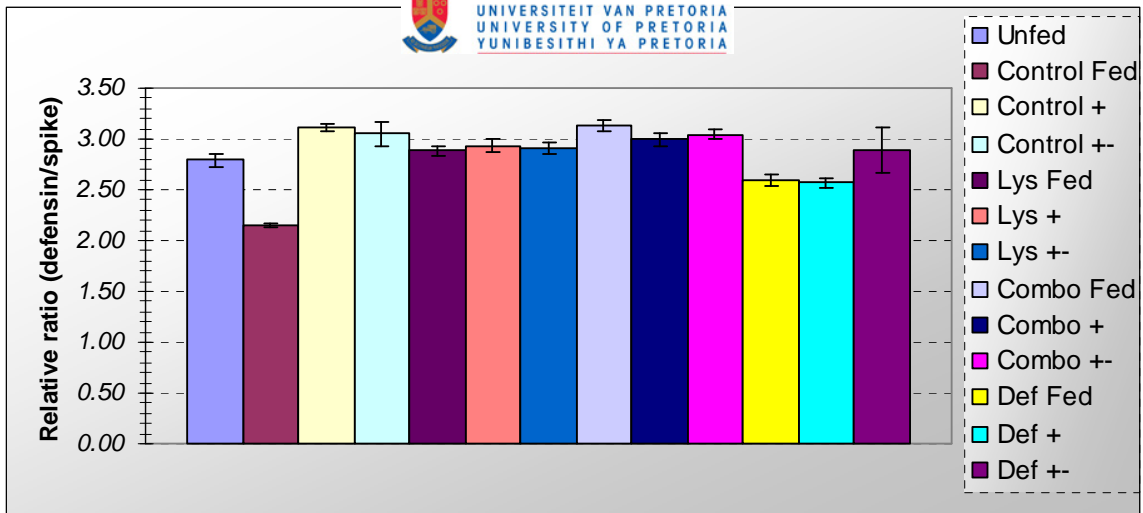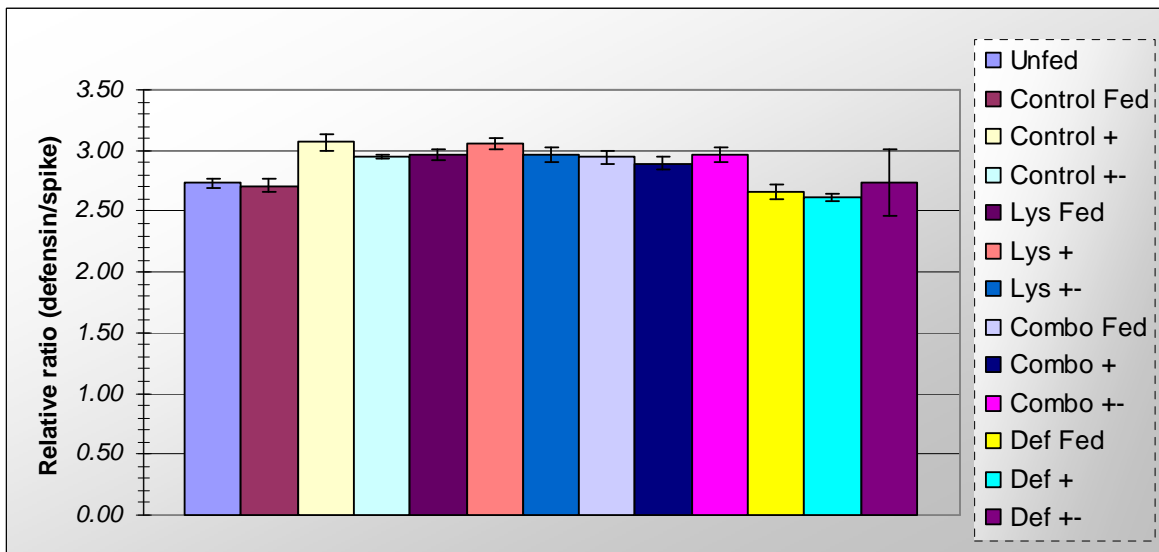
Figure 4.14: Bar graph representing the levels of the defensin transcript in the salivary glands: of control (DEPC-H$_2$O injected) experimental (lysozyme dsRNA, defensin dsRNA or combination dsRNA) injected ticks. Additionally, the results compare feeding of ticks on native (uninfected blood) and blood infected with Gram-positive bacteria as well as a combination of Gram-positive and Gram-negative bacteria
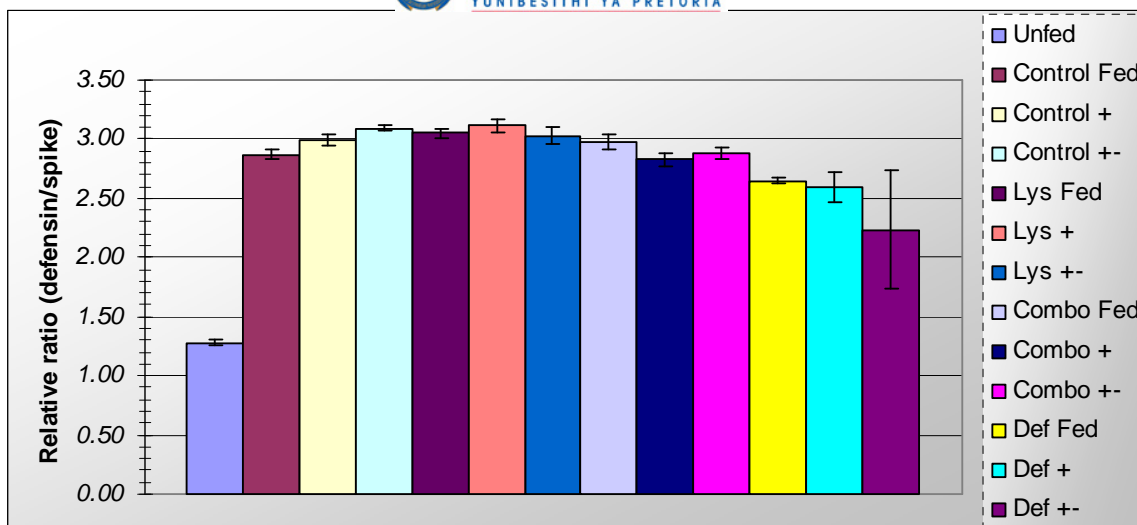

Figure 4.15: Bar graph representing the levels of the defensin transcript in the ovaries: of control (DEPC-H$_2$O injected) experimental (lysozyme dsRNA, defensin dsRNA or combination dsRNA) injected ticks. Additionally, the results compare feeding of ticks on native (uninfected blood) and blood infected with Gram-positive bacteria as well as a combination of Gram-positive and Gram-negative bacteria
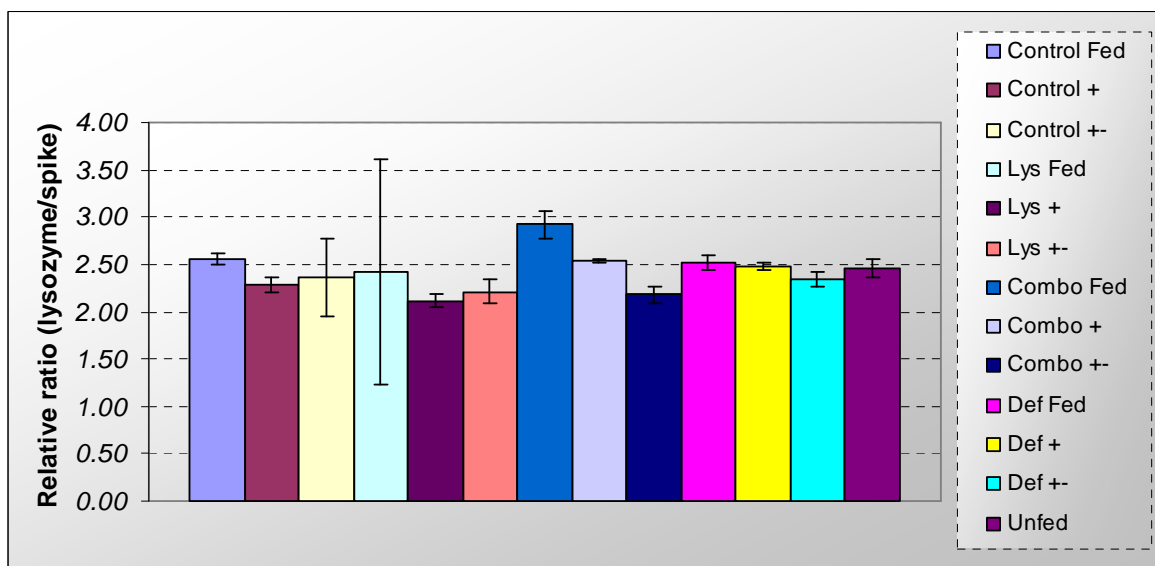
Figure 4.16: Bar graph representing the levels of the defensin transcript in the hemolymph:
of control (DEPC-H2O injected) experimental (lysozyme dsRNA, defensin dsRNA or combination dsRNA) injected ticks. Additionally, the results compare feeding of ticks on native (uninfected blood) and blood infected with Gram-positive bacteria as well as a combination of Gram-positive and Gram-negative bacteria
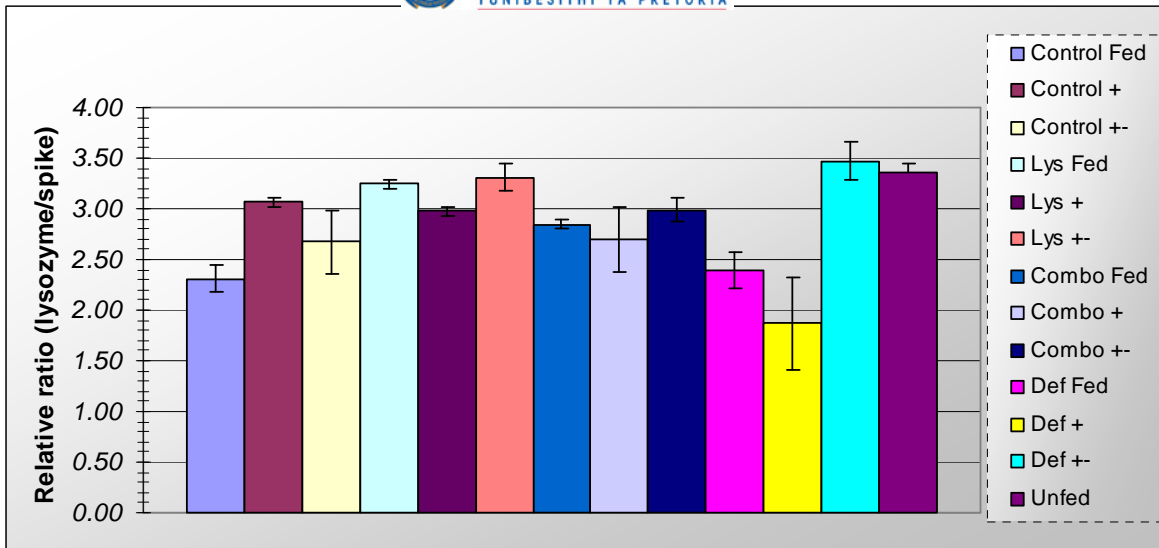

Figure 4.17: Bar graph representing the levels of the lysozyme transcript in the midgut: of control (DEPC-H2O injected) experimental (lysozyme dsRNA, defensin dsRNA or combination dsRNA) injected ticks. Additionally, the results compare feeding of ticks on native (uninfected blood) and blood infected with Gram-positive bacteria as well as a combination of Gram-positive and Gram-negative bacteria

Figure 4.18: Bar graph representing the levels of the lysozyme transcript in the salivary glands: of control (DEPC-H2O injected) experimental (lysozyme dsRNA, defensin dsRNA or combination dsRNA) injected ticks. Additionally, the results compare feeding of ticks on native (uninfected blood) and blood infected with Gram-positive bacteria as well as a combination of Gram-positive and Gram-negative bacteria
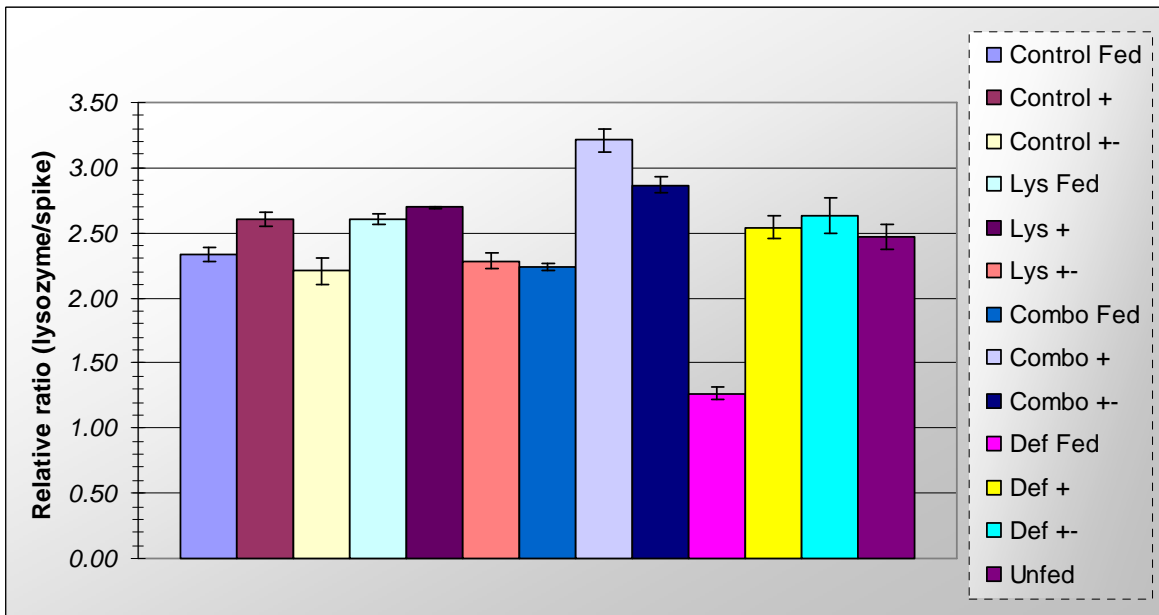

Figure 4.19: Bar graph representing the levels of the lysozyme transcript in the ovaries of: control (DEPC-H2O injected) experimental (lysozyme dsRNA, defensin dsRNA or combination dsRNA) injected ticks. Additionally, the results compare feeding of ticks on native (uninfected blood) and blood infected with Gram-positive bacteria as well as a combination of Gram-positive and Gram-negative bacteria
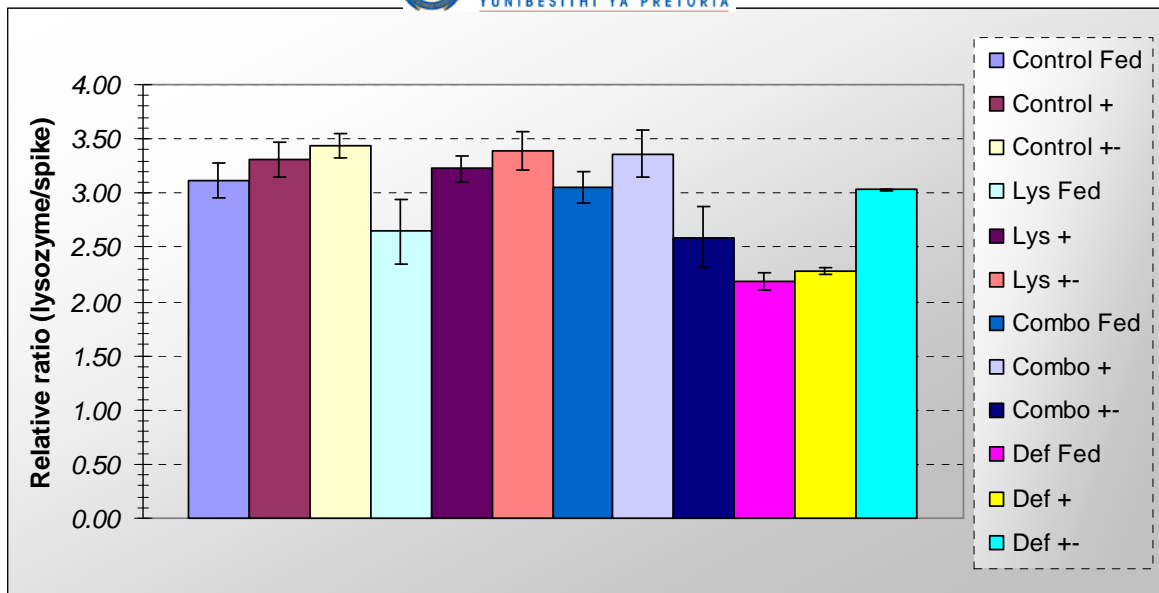
Figure 4.20: Bar graph representing the levels of the lysozyme transcript in the hemolymph of: control (DEPC-H2O injected) experimental (lysozyme dsRNA, defensin dsRNA or combination dsRNA) injected ticks. Additionally, the results compare feeding of ticks on native (uninfected blood) and blood infected with Gram-positive bacteria as well as a combination of Gram-positive and Gram-negative bacteria